Adiabatic quantum transport in multiply connected systems

J. E. Avron

Department of Physics, Technion, Haifa 32000, Israel
and Division of Physics, Mathematics, and Astronomy, California Institute of Technology, Pasadena, California 91125

A. Raveh and B. Zur

Department of Physics, Technion, Haifa 32000, Israel

The adiabatic quantum transport in multiply connected systems is examined. The systems considered have several holes, usually three or more, threaded by independent flux tubes, the transport properties of which are described by matrix-valued functions of the fluxes. The main theme is the differential-geometric interpretation of Kubo's formulas as curvatures. Because of this interpretation, and because flux space can be identified with the multitorus, the adiabatic conductances have topological significance, related to the first Chern character. In particular, they have quantized averages. The authors describe various classes of quantum Hamiltonians that describe multiply connected systems and investigate their basic properties. They concentrate on models that reduce to the study of finite-dimensional matrices. In particular, the reduction of the "free-electron" Schrödinger operator, on a network of thin wires, to a matrix problem is described in detail. The authors define "loop currents" and investigate their properties and their dependence on the choice of flux tubes. They introduce a method of topological classification of networks according to their transport. This leads to the analysis of level crossings and to the association of "charges" with crossing points. Networks made with three equilateral triangles are investigated and classified, both numerically and analytically. Many of these networks turn out to have nontrivial topological transport properties for both the free-electron and the tight-binding models. The authors conclude with some open problems and questions.

CONTENTS

LIST OF SYMBOLS

$\mathbf{A}$	vector potential
$\mathbf{A}(x,e)$	vector potential associated with an edge, Eq. (4.8)
C	closed two-surfaces, the set of cells of a graph
$\mathbb{C}$	the complex numbers
C_j	cuts in Ω
$D(P)$	the singularity set for the projection P
$D(a)$	the U(1) incidence matrix of a graph, Eq. (3.9)
E	the set of edges in a graph, energies
$E_j(\mathbf{A})$	the jth eigenvalue of $H(\mathbf{A})$
F	the faces of a graph, the vector in Eq. (4.36)
$G(V)$	point group acting on vertices of a graph
$G(E)$	point group acting on edges of a graph
$G(F)$	point group acting on faces of a graph
$H(\mathbf{A})$	Hamiltonian associated with the gauge field $\mathbf{A}$
$H_{\rm ad}$	adiabatic Hamiltonian, Eq. (6.1)
$H_2(S)$	the homology groups of S
I	inversion, Eq. (9.5)
$\vert\mathbb{I}\rangle$	the vector $(1,1,1,\ldots,1)$
$I(m,\psi)$	current around the mth hole at the state ψ, Eq. (5.4)
$\langle I(m,\psi)\rangle$	flux-averaged current around the mth hole at the state ψ, Eq. (5.5)
$I(e),I(f)$	edge and loop currents
$I(\psi)$	current one-form at the state ψ, Eq. (5.6a)
$\langle I(\psi)\rangle$	flux-averaged current one-form at the state ψ, Eq. (5.6b)
$I_{\rm Ad}(m,\psi)$	adiabatic current around the mth hole at the state ψ
L_{ij}	the inductance matrix of a network
$M(k)$	metric in $\mathbb{C}^{\vert V\vert}$, Eq. (4.40), induced from that in the Hilbert space
P	projector on a spectral subspace, Eq. (7.1)
P_j	projector on a spectrum below the jth gap
Q	$1-P$
$\mathbb{R}$	the reals
$S(k,v)$	scattering matrix for vertex v and wave number k
S_ϕ	a small two-sphere centered at ϕ
$\mathbb{T}^h$	the h-dimensional torus
$T(k)$	a linear map from $\mathbb{C}^2$ to the Hilbert space,

	Eq. (11.1)
$T_m(\Phi)$	a line in the torus passing through Φ
$T_{lm}(\Phi)$	a planar slice of the torus passing through Φ
U	unitary operator
U_{Ad}	the adiabatic evolution operator, Eq. (6.2)
$U(n)$	the space of unitary $n\times n$ matrices
V	the set of vertices in a graph
$\mathbf{V}, V_t, V_\Phi$	scalar potentials, Eq. (2.5)
$W(x)$	eigenvalue function of fast variables, (4.5)
$\mathbf{W}(x)$	renormalized eigenvalue function of fast variables
$\mathbb{Z}$	the integers
$\mathbf{a}(x,e)$	indefinite integral of vector potential associated with the edge e
$\mathbf{a}(e)$	definite integral of vector potential associated with the edge e
c	a cell in a graph
$\mathrm{ch}(P,C)$	first Chern number, Eq. (8.7)
d	exterior derivative with respect to Φ
$\mathbf{d}$	exterior derivative with respect to x
e	an edge in a graph, the charge of the electron
$\lvert e\rvert$	the length of an edge
f	face of a graph
$\lvert f\rvert$	the number of edges of f
g, g_{Ad}	the physical and adiabatic conductance
$g_{\mathrm{Ad}}(P)$	the adiabatic conductance at the state P
$[g_{\mathrm{Ad}}(P)]_{jm}$	the jm coefficient of the adiabatic conductance matrix at the state P
$\langle g_{\mathrm{Ad}}(P)\rangle$	the average conductance at the state P
$h(\Phi)$	a 2×2 Hermitian matrix function, Eq. (7.2)
$h(k,a)$	the de Gennes–Alexander matrix, Eq. (4.28)
$h_0(k,a)$	the de Gennes–Alexander matrix for a graph with unit edges, Eq. (4.30)
h	the number of holes
k	wave number
v	a vertex in a graph
$\lvert v\rvert$	the valence (coordination number) of a vertex
(v,u)	an edge directed from v to u
$[v,e]$	the vertex-edge incidence matrix, Eq. (3.2)
z	complex number
z_3	the cubic root of unity
$z_j^{(2)}$	an element of the basis for the second homology
α,β	complex numbers
Δ	the Laplacian of a graph Eq. (3.5)
∂	the boundary operator
∂_j	$\equiv\partial_{\Phi_j}$
$\hat{\epsilon}$	the unit vector for ϵ
$\epsilon_0,\boldsymbol{\epsilon}$	a real four-vector, Eq. (7.2)
η	wave function of the fast variable, Eq. (4.5)
Φ	the vector of fluxes
Φ_j	the jth entry in Φ
ϕ	flux values for level crossings
$\boldsymbol{\phi}$	a three-vector of fluxes where levels cross
γ_j	a closed contour
$\Gamma(A),\Gamma_t$	the adiabatic connection, Eq. (6.3)
κ	a vector in $\mathbb{C}^{\lvert V\rvert}$, Eq. (4.18)
$\lambda(v)$	vertex potential, Eq. (4.2)
Λ	real valued functions, gauge transformations
ψ_t	a time-dependent solution of the Schrödinger equation
ψ_{Ad}	a time-dependent solution of the adiabatic evolution equation
$\psi_j(A)$	the jth eigenfunction of $H(A)$
$\psi(v)$	wave function on the vertices
$\psi_{\mathrm{in/out}}$	incoming and outgoing waves toward a vertex, Eq. (4.14)
σ	the triplet of Pauli matrices
(θ,ρ)	cylindrical coordinates
$\theta(k,v)$	the angle associated with unitary point scatterers, Eq. (4.23)
$\omega,\omega[P]$	curvature two-form associated with the projection P, Eq. (6.7)
Ω	a multiply connected domain in coordinate space
χ	characters of groups, Eq. (7.12)
$\lvert\psi\rangle,\lvert\varphi\rangle$	a pair of degenerate eigenvectors
$\langle\cdot\rvert\cdot\rangle$	scalar product of fast variables, Eq. (3.9)
$\langle\cdot,\cdot\rangle$	scalar product in $\mathbb{C}^{\lvert V\rvert}$ induced from the Hilbert space
$(\cdot,\cdot)$	the ordinary scalar product in $\mathbb{C}^{\lvert V\rvert}$
$\lvert\cdot\rvert$	cardinality
$\#(i,j)$	number of common vertices of triangles i and j
$\otimes$	magnetic flux going into the plane
$\odot$	magnetic flux coming out of the plane

I. INTRODUCTION

In this work we study adiabatic transport in multiply connected systems. A typical system might be a mesoscopic piece of normal metal with several holes, shown schematically in Fig. 1(a), or the network shown in Fig. 1(b), which is made of thin, mesoscopic, normal-metal wires. Yet another setting is the array of Josephson junctions. Figure 1(b) is a degenerate version of Fig. 1(a) having the same topology.[1] In either case, the holes are threaded by flux tubes, carrying independent fluxes, which serve as drives and controls. The electrons (Cooper pairs) do not feel the magnetic fields associated with the fluxes; they feel only the vector potentials. This generalizes the setting in the original Bohm-Aharonov effect (Aharonov and Bohm, 1959, 1961) in two ways. First, we allow several, possibly many, holes. Second, we allow for time-dependent fluxes. In the Bohm-Aharonov effect there is one hole and the flux is fixed. The insistence on several holes turns out to be important in that the theory trivializes in the one-hole and two-hole situations. So,

[1]The two figures are of the same homotopy type.

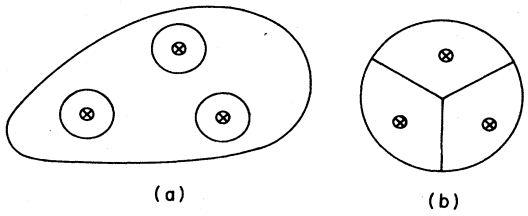

FIG. 1. A multiply connected domain Ω in $\mathbb{R}^2$: (a) with three-holes threaded by three flux tubes $\Phi_{1,2,3}$; (b) a degenerate version of (a) made of thin connecting wires.

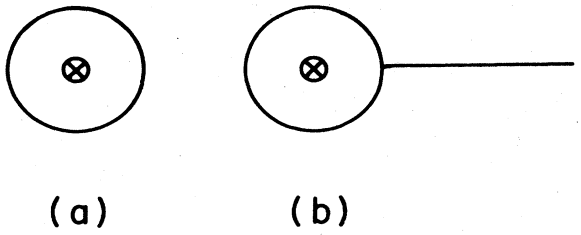

FIG. 2. Multiply connected domains with a single hole: (a) a ring; (b) a lasso.

for the most part, we shall consider systems with at least three holes. Time-dependent fluxes are used to drive the system by generating electromotive forces (emf's) around the respective holes.

By a general result (Byers and Yang, 1961), observables, in the time-independent case, depend on the flux periodically with period of one flux quantum. In emu and atomic units the flux quantum unit is 2π. Due to this periodicity, it turns out that for certain purposes the flux space may be identified with the multidimensional torus. This may be viewed as the basic reason for many of the interesting features of the Bohm-Aharonov effect and its multiflux generalizations. It turns out that, for certain purposes, flux space can also be viewed as a multitorus in time-dependent situations where the time dependence is adiabatic. This, more than the topology of the system in coordinate space, is the basic reason for the topological aspects of the adiabatic transport that we discuss.

As in the Bohm-Aharonov effect, the phenomena we study are a result of quantum coherence and so require that the wave function be coherent over the sample and "know" about the holes. Such rigidity is present in superconductors over macroscopic lengths and in normal metals under more stringent conditions on length and temperature scales. We shall return later to the setting of superconductivity. Let us first briefly review the normal-metal situation.

When the length scale of the system is mesoscopic (i.e., a few hundred angstroms) and the temperature is in the sub-Kelvin range, the electronic wave function is coherent over the entire system and quantum effects are important. Quantum conductance in mesoscopic systems at low temperatures is a rapidly developing subject, partly because of its obvious technological significance and partly because of the interest in quantum coherence. The reader may wish to consult the review of Imry (1986) on this burgeoning subject. A considerable amount of work has been devoted to multiply connected systems with a single hole, such as the ring and the lasso in Fig. 2 (see, for example, Umbach *et al.*, 1984). Periodicity of the *dissipative conductance* in the flux threading the hole, with the period 2π, has been observed in the thin rings (Chandrasekhar *et al.*, 1985; Webb *et al.*, 1985). In thick, dirty rings the period is halved to π (Alt'shuler *et al.*, 1981; Sharvin and Sharvin, 1981; Alt'shuler, 1985). It is also expected that rings have persistent currents that depend (periodically) on the fluxes and that flow even in the absence of driving emf's (Büttiker *et al.*, 1983). Another quantum aspect is nonlocality. For example, the (dissipative) conductance of the tail of the lasso in Fig. 2(b) depends (periodically) on the flux threading the ring. The conductances in mesoscopic systems can be sample specific (Gefen *et al.* 1984; Büttiker *et al.*, 1985), and Onsager relations can be subtle (Benoit *et al.*, 1986; Büttiker, 1986b). Gefen and Thouless (1987) looked at mechanisms that lead to dissipation in small rings and, in particular, at the role of quantum interference and localization.

When the geometry becomes more complicated, as in the case of multihole systems, the various issues discussed above become issues in the more complicated settings. However, new issues, that have no analog in the one-loop setting, also arise. Nondissipative quantum conductances that have topological significance is one. This is the subject of this work.[2]

In multiply connected systems with several holes, a matrix of transport coefficients relates the current around one hole to the emf around another. Although somewhat pedantic, it is useful to distinguish between charge transport and conductance: conductances are defined as the linear coefficients that relate currents to emf's in situations where the emf's are (asymptotically, in the distant future) constants or harmonic functions of time. Charge transports relate the charges transported around holes to the increase in some of the fluxes by a single quantum, where the fluxes are asymptotically (both in the distant past and distant future) time independent.[3] The adiabatic transport coefficients are defined by the limit where the fluxes change adiabatically (the time scale is determined by the minimal gap in the spectrum), so the emf's are all weak. By general principles, *for finite systems,* there is no

[2]In Yurke and Denker (1984), quantum network means the study of capacitors and inductors quantized by imposing the canonical commutation relations. This is a different problem.

[3]Due to persistent currents, the transport we consider is actually associated with the *excess* charge transported by the increase in flux.

dissipation in this limit.[4] In particular, in a single loop, the adiabatic transport is trivial. In multiloop systems there can be nontrivial, adiabatic, and nondissipative transport.

The Hall effect is an example of a case in which an emf in one loop transports charge around another loop, and the quantum Hall effect illustrates that this can be done with no dissipation.[5] Let us explain. The Hall effect is shown schematically in Fig. 3(a). The classical (ordinary) Hall effect (Hall, 1879) is basically a room-temperature phenomenon, and the (integer) quantum Hall effect (von Klitzing *et al.*, 1980; see also Prange and Girvin, 1987 for a collection of review articles) is a low-temperature phenomenon. Quantum mechanics turns out to be important already in the ordinary Hall effect, even though it is observable in macroscopic systems at elevated temperatures. Indeed, there is no classical explanation of the anomalous (holelike) Hall coefficients that occur in certain materials. The classical Hall transport is accompanied by some dissipation. In the quantum Hall effect, the transport is nondissipative (at least in the region of the plateaus).

The quantum Hall effect may be viewed as a quantum phenomenon associated with multiply connected systems. The multiple connectivity is, in fact, central in some theories.[6] Indeed, the original argument of Laughlin (1981) is a gauge argument applied to a geometry of a single loop. Subsequent theories (see below) that rely on the identification of the Hall conductance with a standard topological object actually need two loops (Avron and Seiler, 1985; Niu and Thouless, 1987). Since the topological view will be central to much of what follows, we recall the motivation for the two loops. It is presented in Fig. 3(b), where the battery in Fig. 3(a) has been replaced by a time-dependent flux tube, and the ammeter in Fig. 3(a) by a second, independent, flux tube. (We shall explain later precisely in what sense flux tubes play the role of batteries and ammeters.) This structure leads to the identification of the Hall conductance with the first Chern number. (We shall discuss below the differential geometric and topological significance of the first Chern numbers.)

The study of nondissipative conductances in networks is closely related to the topological-geometric view of the quantum Hall effect. In fact, we have chosen to study networks partly because it is a setting that is tailored to the theory and does not have some of the difficulties that the Hall effect presents. In the Hall effect, the multiconnectivity is not believed to be an essential feature of the actual systems; the wave function is probably not coherent in the leads and the electronic circuitry. In networks the wave function is assumed to be coherent throughout.

Networks differ from the Hall effect not only in setting but also in some of the basic properties of the transport. The Hall conductance is actually *a property of the sample,* and the connecting leads in Fig. 3 are not believed to be important for the actual value of the Hall conductance. (This is believed to be related to the fact that the samples are macroscopic.) In networks the conductance matrix

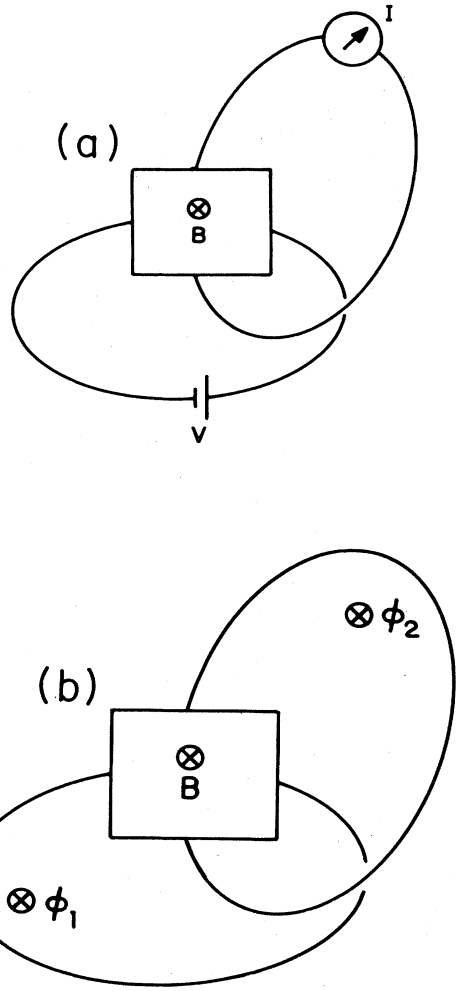

FIG. 3. The Hall effect. (a) The square represents the Hall probe acted on by a magnetic field. The system is driven by a battery V, and the Hall current I flows through the loop with the ammeter. (b) The Hall effect viewed as a two-loop system. The battery is replaced by a time-dependent flux tube, and the ampermeter by a time-independent flux tube.

[4]The convention we follow here is that the adiabatic limit is *not defined* when eigenvalues cross.

[5]Classical networks are another example in which emf's in one-loop transport charges around another loop. This phenomenon is, however, intrinsically related to dissipation: the associated transport matrix is symmetric. The nondissipative transport that we study below has an antisymmetric transport matrix. We thank S. Ruschin for a discussion on this point.

[6]The Born–von Karman periodic boundary conditions that are common in much of solid-state physics may also be viewed as a way of effectively making the system multiply connected.

reflects the multiconnectivity. In a sense, networks are like a quantum Hall effect without a magnetic field acting directly on the system and without a Hall probe.

There is actually a further and deeper connection with the integer quantum Hall effect. One of the interesting theoretical developments that followed the experimental work of von Klitzing has been the recognition that nondissipative Hall coefficients have geometric significance. The geometry that enters is related to the way (a family of) spectral subspaces curve inside the (infinite-dimensional, flat) Hilbert space. Kubo's formula for the Hall conductance is an expression for this curvature. The curvature is related to the Berry or holonomy phase (Simon, 1983; Berry, 1984). This fact[7] was noted by Thouless, Kohmoto, Nightingale, and den Nijs (1982) in a special case, and was later recognized to hold in great generality (Niu and Thouless, 1984; Avron and Seiler, 1985; Tao and Haldane, 1986). In particular, as we shall see, the geometric interpretation is not special to the Hall conductance and holds also for networks.

The classical Chern-Gauss-Bonnet-type formulas say that integrals of curvatures over closed surfaces are integers. The integers associated with integrals of the aforementioned curvature over closed two-dimensional manifolds are known as first Chern numbers (Chern, 1979; Choquet-Bruhat *et al.*, 1982). In the topological-geometrical view, the quantization of the Hall conductances observed by von Klitzing can be interpreted as a combination of the basic facts that nondissipative transports are curvatures and that flux space is a torus with Gauss-Bonnet-Chern theorem (Niu and Thouless, 1984; Avron and Seiler, 1985; Kohmoto, 1985; Niu, Thouless, and Wu, 1985; Avron, Seiler, and Shapiro, 1986; Tao and Haldane, 1986; Avron, Seiler, and Yaffe, 1987; Niu and Thouless, 1987). The precise statement is, in fact, that for general multiparticle Hamiltonians describing *finite systems,* the (adiabatic) Hall conductance, averaged over the threading flux in the current loop *at zero temperature,* is generically quantized to be integer multiples of $e^2/2\pi\hbar$ ($=1/2\pi$, in the present units). [Why the Hall experiments measure averages, and why the quantization is stable for finite temperatures, finite emf's, and macroscopic systems are questions outside the scope of this work and not yet fully understood in a general framework (Laughlin, 1981; Niu and Thouless, 1984; Avron, Seiler, and Shapiro, 1986; Kunz, 1987; Niu and Thouless, 1987).]

Multiply connected systems with many holes offer a rich setting, as there are many conductances related to curvatures. Such conductances have quantized averages. The averaging, even when the number of fluxes is large, is only over the *single* flux, distinguished by the current loop. The integers obtained are therefore functions of the remaining fluxes and are periodic with period of a flux unit. (The setting is also richer because it allows, in principle, for higher Chern numbers.)

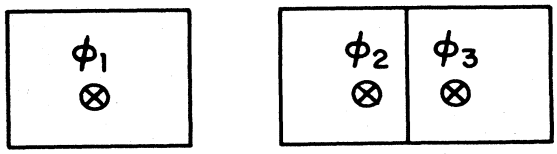

FIG. 4. A disconnected network with three loops that has trivial topological conductances.

As in the theory of the Berry phase, degeneracies (points of level crossings) play the role of sources for the Chern numbers and can be assigned integer "charges" (Herzberg and Longuet-Higgins, 1963; Longuet-Higgins, 1975; Alden Mead and Truhlar, 1979; Simon, 1983; Berry, 1984). Flux space, with points of charges removed, has an interesting second homology, which, together with a basic curvature (two-form), determines the Chern numbers. The case in which the charges are discrete is particularly simple, for then the information can be organized in a table. This is the generic situation for three-flux networks.

The adiabatic transport coefficients relate three distinct topological spaces: the physical network in three-dimensional space; the multidimensional punctured torus in flux space; and, finally, the bundle of spectral subspaces in the Hilbert space. The Chern numbers describe the twisting of these bundles and are related to the geometry of the network. For example, in a disconnected network, like Fig. 4, the transport coefficients associated with loops in distinct components are naturally expected to vanish. An outstanding problem is a deeper understanding of the ways the three topological spaces are related. It is interesting to recall that formulas that relate electric properties and topological properties of networks in ordinary three space have a distinguished predecessor, Ampere's law is related to the linking number and plays a role in knot theory (Flanders, 1963).

We say that a network is trivial if *all* its Chern numbers vanish (or are ill defined because of nongeneric crossings). We shall see that networks with one or two fluxes are trivial in this sense. This is not to say that the transport properties of one- and two-loop networks are trivial. In a trivial network there can still be a current flowing in one loop due to an emf in another. The (adiabatic) current is trivial only in the sense that its average over the flux in the current loop vanishes and that it lacks the topological significance of Chern character.[8] Nontriviality guarantees interesting *topological* transport

[7]The nontriviality of the bundle that arises in the study of Schrödinger operators with periodic structure and magnetic fields was first noted by several Soviet authors as early as 1980 (see Dubrovin and Novikov, 1980; Novikov, 1981; Lyskova, 1985, and references therein).

[8]In the case of nongeneric crossings, the adiabatic limit may become empty.

properties that are expected to have a certain robustness against sample specificity. We focus on nontrivial networks, and establish nontriviality by explicit model calculations. Results for tight-binding and one-dimensional network Hamiltonians, corresponding to various three-flux networks, are given. It turns out that nontrivial networks abound, and as a rule of thumb networks are nontrivial except for a reason. Because of the topological nature of the problem, at least the qualitative features of the results, and in particular the nontriviality, should survive for more realistic Hamiltonians.

The nontrivial three-flux networks that we shall describe below are a three-way quantum switch. By this we mean that depending on the value of the controlling flux in loop 1, say, the average current in loop 2, due to an emf in loop 3, will either flow, not flow, or flow in reverse. The switch is periodic in the controlling flux with period 2π. It is an honest three-state switch in the sense that the average current in loop 2 is a 1, 0, or -1 multiple of the emf. The switch is stable in the sense that each state is determined by an interval in the controlling flux. In fact, the controlling flux has to be varied on the order of a (fraction of a) flux unit to alter the state of the switch. Multistate switches, such as the five- and seven-state switches, where the currents are multiples of the emf's that are larger than unity, presumably arise in the study of multiloop networks. The nine networks that we have analyzed have only a few loops, and four of them turn out to be three-way switches for most states. Some of the networks turn out to be two-way switches in some states, that is, the averaged current can be made to change direction when the flux is reversed, but cannot be stopped. The other five networks are trivial.

II. SCHRÖDINGER OPERATORS FOR MULTIPLY CONNECTED DOMAINS

Consider a multiply connected domain Ω [see Fig. 1(a)] embedded in three- or two-dimensional Euclidean space. Suppose that Ω is a finite, smooth manifold and has smooth boundary $\partial\Omega$. Ω is threaded by h independent flux tubes. Φ_j is the flux in the jth tube, and Φ is the vector $(\Phi_1,\ldots,\Phi_h)$. Let $\mathbf{A}$ be the associated vector potential. We think of $\mathbf{A}$ as a one-form, or a vector field, as is convenient. $\mathbf{A}$ is closed on Ω, that is, the associated magnetic field $\mathbf{d}\mathbf{A}$ vanishes on Ω, expressing the fact that all the fluxes are outside Ω. $\mathbf{d}$ is the exterior derivative, and we use boldface to denote that the differentials are taken with respect to the coordinates in configuration space. We allow time-dependent fluxes so $\mathbf{A}$ may generate an electric field $-\partial_t\mathbf{A}$. The electric field need not vanish on Ω, since the emf's around the holes are $-\dot{\Phi}$. Φ are the periods of $\mathbf{A}$, that is,

$$\Phi_j=\int_{\gamma_j}\mathbf{A}\ , \tag{2.1}$$

where γ_j is a loop in Ω around the jth flux tube. Unless otherwise stated we shall always assume that a gauge has been chosen so that the fluxes are represented by a pure vector potential, that is, there is no Φ-dependent scalar potential. Also, it is convenient to choose the vector potential so that $\Phi=0$ corresponds to $\mathbf{A}=0$. Finally, the situations we have in mind are those in which the time dependence resides in the fluxes alone: we do not consider cases in which the flux tubes are, say, jiggled inside the holes. This means that we take $\mathbf{A}$ to be linear in Φ.

Given $\mathbf{A}$, we associate with it a Schrödinger operator $H(\mathbf{A})$ for electrons moving in Ω. In the single-particle case, with no background fields, the operator is (up to a factor $\frac{1}{2}$)

$$H(\mathbf{A})=\tfrac{1}{2}(-i\nabla-\mathbf{A})^2\ , \tag{2.2}$$

where $(-i\nabla-\mathbf{A})$ is the canonical velocity. Dirichlet boundary conditions are imposed on $\partial\Omega$. The general multiparticle case is more complicated only in that the operator is decorated by particle indices and interaction terms *that are* Φ *independent.* These complications do not affect the analysis below in any essential way, except for a messier notation. We stick with Eq. (2.2) for the sake of clarity.

$H(\mathbf{A})$ determines the dynamics according to the Schrödinger equation,

$$i\partial_t\psi_t=H(\mathbf{A})\psi_t\ . \tag{2.3}$$

In much of the following we shall be interested in the limit where the flux tubes, and therefore $\mathbf{A}$, change adiabatically. As is well known, the analysis of this limit reduces to the spectral study of the family of operators $H(\mathbf{A})$, i.e., time may be regarded as a parameter. We denote by $E_j(\mathbf{A})$ and $\psi_j(\mathbf{A})$ the eigenvalues and eigenfunctions of $H(\mathbf{A})$ for fixed fluxes, i.e.,

$$H(\mathbf{A})\psi_j(\mathbf{A})=E_j(\mathbf{A})\psi_j(\mathbf{A})\ . \tag{2.4}$$

By general principles (Kato, 1966; Reed and Simon, 1972–1978), $H(\mathbf{A})$ has a discrete spectrum in $[0,\infty)$, something borne out by the notation. Equation (2.4) does not determine $\psi_j(\mathbf{A})$ uniquely, as there is a phase ambiguity. A convenient choice will be singled out when needed.

Gauge transformations play an important, and occasionally confusing, role. A general gauge transformation may depend on the fluxes, and so is time dependent if the fluxes are, and may have an additional time dependence not coming from the fluxes. Let U be a multiplication unitary, that is, locally, $U=\exp(-i\Lambda)$, which is smooth in Φ and t and $x\in\Omega$ (x may be a local coordinate). The primed and unprimed systems, related (locally) by

$$\begin{aligned}&\psi'=U\psi\ ,\quad \mathbf{A}'=\mathbf{A}-\mathbf{d}\Lambda\ ,\\ &H'(\mathbf{A}')=UH(\mathbf{A})U^\dagger+V_t+\dot{\Phi}\cdot V_\Phi\ ,\\ &V_t\equiv-iU\partial_tU^\dagger=-\partial_t\Lambda,\quad V_\Phi\equiv-iU\,dU^\dagger\ ,\end{aligned} \tag{2.5}$$

have the same electric and magnetic fields acting *on* Ω and describe equivalent dynamics. Nonboldface d denotes the exterior derivative with respect to the fluxes.

$\dot{\Phi}\cdot V_\Phi$ is the canonical pairing between the vector $\dot{\Phi}$, describing the flow in flux space, and the one-form V_Φ.

$\mathbf{d}\Lambda$ has periods that are integral multiples of 2π:

$$\int_{\gamma_j} \mathbf{d}\Lambda = 2\pi n_j, \quad n_j \in \mathbb{Z} , \tag{2.6}$$

where, as before, γ_j is a loop in Ω around the jth hole. Such U's do not have a smooth continuation to the holes if the periods are nonzero, and this is why the fields in the holes can be different. Indeed, from Eqs. (2.1) and (2.5),

$$\Phi' = \Phi - 2\pi n , \tag{2.7}$$

where n is a vector with integer components n_j. It follows from Eq. (2.5) that if the fluxes are *time independent,* Hamiltonians with distinct fluxes that are related by Eq. (2.7) are unitarily equivalent and describe equivalent dynamics. So, for time-independent questions, flux space may be thought of as a multitorus. We shall refer to this as the Bohm-Aharonov periodicity. It is also known as the Byers-Yang theorem (Byers and Yang, 1961). As we shall see, this will also carry over to some time-dependent questions in the adiabatic limit.

The next question we want to consider is the relation between dynamics that have the same Ω, same fluxes, and same emf's, but different flux tubes. For example, consider two systems, identical except for the fact that some of the flux tubes have been moved about in their respective holes (see Fig. 5). In the time-dependent case, such systems have inequivalent dynamics. This is easy to understand in physical terms: different flux tubes, or flux tubes that are positioned in different places in the holes, have different $\mathbf{A}$'s acting on Ω, and induce different electric fields $-\partial_t \mathbf{A}$ on Ω. These electric fields are related only through the same emf's on each loop, but their local behavior is different. There is no reason for the dynamics in such cases to be equivalent. The corresponding Hamiltonians are not related by a gauge transformation.

Let us consider some concrete examples of flux tubes that illustrate the different fields and dynamics that can arise. One of the examples is a choice of flux tubes that make the Schrödinger operator periodic in the fluxes. The existence of such a choice will play a role in later sections.

Consider a planar Ω and let $x=(\rho_j,\theta_j)$ be cylindrical coordinates with origin in the jth hole. Let

$$\mathbf{A}(x) = \sum_{j=1}^{h} \Phi_j d(\theta_j) 2\pi \tag{2.8}$$

(away from $\theta=0$ and $\theta=2\pi$). This $\mathbf{A}$ is manifestly closed on Ω (it is locally exact) and satisfies Eq. (2.1). Suppose now that Φ is time dependent. Then there is a nonvanishing electric field acting on Ω given by

$$-\sum_{j=1}^{h} \dot{\Phi}_j \frac{\hat{\theta}_j}{2\pi\rho_j} . \tag{2.9}$$

The field clearly depends on the choice of origin of the coordinates, which is the position of the tube in the holes. For example, if Ω is a thin ring, the electric field is uniform only if the tube is placed at the center of the ring. There is no reason for the dynamics to be determined by Φ and $\dot{\Phi}$ alone; further details about the flux tubes matter.

As a second example for a choice of flux tubes or vector potentials, consider the *singular* gauge field

$$\mathbf{A}(x) = \sum_{j=1}^{h} \Phi_j \hat{n}(x) \delta(x - C_j) , \tag{2.10}$$

where C_j are cuts in Ω that make it simply connected (see Fig. 6) and $\hat{n}$ is a unit vector orthogonal to the cut. This $\mathbf{A}$ also satisfies Eq. (2.1). For fixed Φ, the Hamiltonians corresponding to various choices for the cuts C_j in Eq. (2.10) [or the tubes in Eq. (2.8)] are unitarily equivalent. However, if the Φ are time dependent, the dynamics are distinct. In fact, the electric field associated with Eq. (2.10) is zero everywhere except on the cuts and is given by

$$-\sum_{j=1}^{h} \dot{\Phi}_j \hat{n}(x) \delta(x - C_j) . \tag{2.11}$$

The choice of C_j clearly matters.

The Schrödinger operator associated with the flux tubes of Eq. (2.10) is $-\Delta$ on the cut domain, Fig. 6, with $\exp(i\Phi_j)$ boundary conditions across the cut C_j. The differential operator is thus independent of Φ, and the Φ dependence comes solely from the boundary condition, which is manifestly periodic in Φ. The nice thing about this choice of flux tubes is that they give a Hamiltonian that is manifestly periodic in Φ as well. For this choice, the time evolution is as if flux space were the h torus $\mathbb{T}^h$. And this holds even for time-dependent fluxes. For other choices of the flux tubes, say Eq. (2.8), this is not the case,

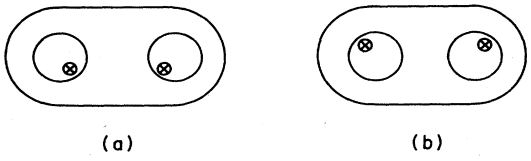

FIG. 5. Two identical systems, except that the flux tubes have been placed in different positions in the holes.

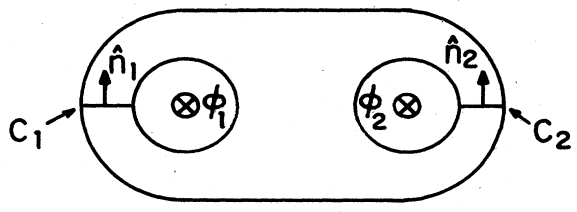

FIG. 6. Ω made simply connected by drawing appropriate cuts C_j. $\hat{n}$ is normal to the cut.

and flux space is better thought of as $\mathbb{R}^h$.

It is, of course, natural to ask what dynamical properties are independent of the choice of flux tubes and are functions of Φ and $-\dot{\Phi}$ alone. A related question is under what condition does the Bohm-Aharanov periodicity extend to time-dependent situations. It is, of course, reasonable to expect that in the adiabatic situation, some form of the Bohm-Aharonov periodicity should survive. However, it may survive for certain observables but not for others. Note that once certain properties are known to be functions of the fluxes and the emf's alone, one may choose the flux tubes to be those that make the Hamiltonian periodic in the fluxes. We shall use this to establish the Bohm-Aharonov periodicity of the averaged adiabatic transport coefficients.

A reader interested in the general structure and theory may want, at this point, to skip the next two sections and proceed with Sec. V on loop currents. The following two sections are devoted to the formulation of special classes of Hamiltonians for which the analysis reduces to the study of finite matrices. This simplification has no bearing on the general theory of adiabatic transport that we describe in Secs. V–XI, but it is of considerable use in the actual computation of the transport properties for specific networks, something we return to in Secs. XII and XIII.

III. TIGHT-BINDING HAMILTONIANS

From formal point of view, the Hamiltonians of the preceding section were distinguished by periodic dependence (up to unitary equivalence) on a set of parameters, i.e., fluxes. The simplest operators of this kind are, of course, periodic matrix functions. Finite matrices are especially useful when one is interested in concrete examples and in actual computations and not just in the general structure of the theory. Operators of the tight-binding type retain much of the structure of the original Schrödinger operator and lead to the study of finite matrices.

The tight-binding model arises from the Schrödinger equation in the limit of strongly attractive atomic potentials, hence the name. For a system made of N atoms, each contributing n atomic levels, the relevant Hilbert space, in the one-particle case, is $\mathbb{C}^{nN}$. The tight-binding Hamiltonian is the restriction of the appropriate Schrödinger operator to this subspace. We shall consider the case of $n=1$.

We choose to formulate them in a way that is natural from a graph-theoretic point of view. The reasons for doing so are partly that this is a nice mathematical formulation and partly that this brings out the possible relevance of the subject to areas outside solid-state physics. Similar operators arise in lattice gauge theories for different reasons (Wilson, 1974).

With the network Ω we associate a directed graph, Fig. 7, with vertices V, edges E, faces F, the cells C. There are, of course, no cells in planar graphs. A cautionary word about terminology in warranted. We used the term graph in a more restrictive sense than is usual in graph theory, as the graphs we consider have metric properties. For example, in Secs. XII and XIII we focus on graphs made of equilateral triangles. In graph theory edges have no lengths, so there is no notion of equilateral triangles. Consequently the notion of planarity is also distinct from that in (nonmetric) graph theory.

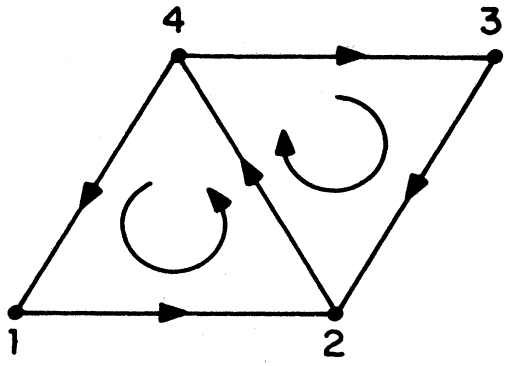

FIG. 7. A directed graph with four vertices, five edges, and two faces. The valence of vertex 2 is 3 and of vertex 1 is 2.

We denote by a lower-case letter an element of a set denoted by an upper-case letter, so v is a vertex in V. Moreover, $|\cdot|$ assigns to $\cdot$ a number. Thus $|V|$ and $|E|$ are the number of vertices and edges, etc. $|e|$ is the length of e and $|v|$ is the valence (coordination number) of the vertex v. We consider only simple graphs in which edges are uniquely specified by their vertices. $e=(v,u)$ is an edge directed from v to u. Figure 8 shows a graph that is not simple.[9]

We consider physical networks, embedded in Euclidean space. For connected networks the vertices, edges, etc., are related by the Euler characteristic,

$$|C|-|F|+|E|-|V|=-1\ . \tag{3.1}$$

The incidence matrix gives an algebraic description of the graph (Wilson, 1972; Biggs, 1974). $[v,e]$ denotes the vertex-edge incidence matrix, defined by

$$[v,(v_1,v_2)]=\delta(v,v_2)-\delta(v,v_1)\ . \tag{3.2}$$

The edge-face $[e,f]$ and face-cell $[f,c]$ incidence matrices are similarly defined. They obey the "boundary of the boundary is zero" rule (Patterson, 1969):

$$\sum_E [v,e][e,f]=0,\quad \sum_F [e,f][f,c]=0\ . \tag{3.3}$$

The Laplacian of a graph is the $|V|\times|V|$ matrix

[9]Nonsimple graphs are actually of interest, since nontrivial bundles appear in this case already for 2×2 matrices. For simple graphs, the lowest rank of matrices with nontrivial bundles is 4.

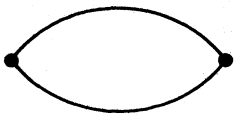

FIG. 8. A graph that is not simple. The two vertices do not determine a single edge.

$$[\Delta]_{uv} \equiv -\sum_{E} [u,e][v,e] \ . \tag{3.4}$$

For simple graphs,

$$[\Delta]_{uv} = \begin{cases} -|v| & \text{for } u=v \ , \\ +1 & \text{for } (u,v)\in E \ , \\ 0 & \text{otherwise} \ . \end{cases} \tag{3.5}$$

On a graph of a regular lattice, Δ is the discrete Laplacian. In particular, if ψ is a function on the vertices such that $\Delta\psi=0$, then ψ is harmonic in the usual sense that its value at a given vertex is the mean of its neighboring values. It is known that the spectral properties of Δ are related to the topology of the graph (Wilson, 1972; Biggs, 1974).

The operator in Eq. (3.5) describes a tight-binding model for a "molecule" made of atoms placed at the vertices of the graph, in the absence of magnetic fields. There is unit hopping between atoms connected by an edge, and the electrons experience an on-site interaction $|v|$. From a solid-state physics point of view, a simpler and more natural operator to study is one in which the diagonal in Eq. (3.5) is replaced by zero. (This is the case if the atoms at the vertices of the graph are identical.) We stick with the graph-theoretic choice (but the solid-state terminology).

The Laplacian carries no information on the fluxes threading the graph. From a graph-theoretic point of view, fluxes lead to the consideration of a "gauge incidence matrix" that is a U(1) generalization of Eq. (3.2).

Fluxes and gauge fields can be defined intrinsically on the graph. It is not necessary to think of them as embedded in Euclidean space. Fluxes $\Phi(f)$ are defined on the faces, and gauge fields $a(e)$ are defined on the edges. The fluxes are constrained by the zero divergence of the magnetic fields

$$\sum_{F} [f,c]\Phi(f)=0 \ , \tag{3.6}$$

and are related to the gauge fields by the discrete version of Eq. (2.1),

$$\Phi(f)=\sum_{E} [e,f]\mathbf{a}(e) \ . \tag{3.7}$$

By Eq. (3.3), such $\Phi(f)$'s automatically satisfy Eq. (3.6). Pure gauge fields are "gradients" of functions on the vertices,

$$\mathbf{a}_0(e)=\sum_{V} [v,e]\Lambda(v) \ , \tag{3.8}$$

with $\Phi(f)\equiv 0$ by Eq. (3.3). The space of nontrivial pure gauges is $|V|-1$ dimensional [since $\Lambda=$const has $\mathbf{a}_0(e)\equiv 0$]. The space of all gauge fields is $|E|$ dimensional and the space of admissible fluxes is $|F|-|C|$ dimensional, due to the constraint of Eq. (3.1). The number of flux tubes, or holes, is therefore $h=|F|-|C|$. From the Euler characteristic, Eq. (3.1), it follows that the flux tubes determine the gauge fields modulo pure gauges.

The gauge incidence matrix $D(\mathbf{a})$ is the linear map from $\mathbb{C}^{|V|}$ to $\mathbb{C}^{|E|}$ defined by

$$[D(\mathbf{a})]_{e,v} \equiv [v,e]\exp\{i[v,e]\mathbf{a}(e)/2\} \ . \tag{3.9}$$

The tight-binding Hamiltonian is, by analogy with Eq. (3.4),

$$H(\mathbf{a}) \equiv D^{\dagger}(\mathbf{a})D(\mathbf{a}) \ . \tag{3.10a}$$

Explicitly

$$[H(\mathbf{a})]_{uv} = \begin{cases} |v| & \text{for } u=v \ , \\ -\exp[i\mathbf{a}(e)] & \text{for } e=(u,v) \ , \\ 0 & \text{otherwise} \ . \end{cases} \tag{3.10b}$$

As a tight-binding model, $H(\mathbf{a})$ describes a "molecule" in a magnetic field so that the fluxes through the various faces are given by Φ. The magnetic fields modify the hopping terms to $\exp[i\mathbf{a}(e)]$. The graph-theoretic formulation leads to the on-site potential $|v|$, and, as discussed above, this is not a particularly natural choice in the tight-binding model. In tight binding it is more natural to let the on-site potential be a fixed constant, if all the atoms are identical. In the general case of distinct atoms, the on-site potential depends on the binding energy of the atom. Moreover, in the general case, the hopping need not have identical magnitudes.

We shall stick with Eq. (3.10) for the sake of concreteness. This choice does not affect the analysis, for we focus on stable (topological) properties. In particular, setting the diagonal to zero would not change the overall picture, but would modify details. For regular graphs, that is, graphs in which $|v|$ is the same for all vertices, like the tetrahedron, the two notions essentially coincide.

$H(\mathbf{a})$ is a $|V|\times|V|$ self-adjoint matrix that reduces to $-\Delta$ for $\mathbf{a}(e)=0$. We recall some of its basic properties. First, one has the (sharp) bounds

$$2\max_{v\in V}|v| \geq H(\mathbf{a}) \geq 0 \ . \tag{3.11}$$

The right-hand side of Eq. (3.11) follows directly from Eq. (3.10a). The left-hand side follows from consideration of the eigenvalue equation for the largest component of the eigenvector. Actually, $H(\mathbf{a})$ is strictly positive definite if $\Phi\neq 2\pi n$, $n\in\mathbb{Z}^h$, and has a one-dimensional kernel if $\Phi=2\pi n$. To see this, note that from

$$\langle\psi|H(\mathbf{a})|\psi\rangle = \|D(\mathbf{a})|\psi\rangle\|^2 \tag{3.12}$$

it follows that the kernel of $H(\mathbf{a})$ is the kernel of $D(\mathbf{a})$. The equation $D(\mathbf{a})\psi=0$ says that

$$\psi(u)=\exp[i\mathbf{a}(e)]\psi(v), \quad e=(u,v) . \tag{3.13}$$

This is consistent on the graph provided the periods of $\mathbf{a}(e)$ on the loops are integer multiples of 2π, that is, provided $\Phi=2\pi n$. In particular, for $\mathbf{a}(e)=0$, the ground state 0 has the eigenvector $(1,1,1,\ldots)$.[10]

Tight-binding Hamiltonians gauge transform in the usual way:

$$\begin{aligned} &H'(\mathbf{a})\equiv H(\mathbf{a}')+\partial_t\Lambda , \\ &\mathbf{a}'(e)\equiv\mathbf{a}(e)+\sum_V [v,e]\Lambda(v) . \end{aligned} \tag{3.14}$$

$H(\mathbf{a})$ and $H(\mathbf{a}')$ are unitarily equivalent and so have the same spectrum.

$H(\mathbf{a})$ is strictly periodic in the gauge fields:

$$H(\mathbf{a})=H(\mathbf{a}+2\pi n), \quad n\in\mathbb{Z}^{|E|} . \tag{3.15}$$

This relates Hamiltonians with different fluxes:

$$\Phi'(f)=\Phi(f)+2\pi\sum_E [e,f]n(e) . \tag{3.16}$$

For the applications that we consider in Secs. XII and XIII, this relation is enough to guarantee the existence of gauges in which the Hamiltonian is periodic in all the fluxes.

The space of gauge fields is $\mathbb{R}^{|E|}$, but because of Eq. (3.15) it may be thought of as $\mathbb{T}^{|E|}$. In $\mathbb{R}^{|E|}$ sits an $\mathbb{R}^{|V|-1}$ subspace of pure gauge transformations. The space of distinct gauge fields is therefore $\mathbb{R}^h$, where h is the number of holes:

$$h\equiv|F|-|C|=|E|-|V|+1 . \tag{3.17}$$

In view of Eq. (3.15), the gauge-distinct Hamiltonians are naturally defined on $\mathbb{T}^h$.

In conclusion, the simplest set of models with the structure of the general case discussed in Sec. II are periodic matrices of the tight-binding type. As we shall see, even for quite small matrices interesting things happen. An example with 4×4 matrices will be analyzed in detail in Sec. XII. This elementary aspect is one of the appeals of the theory.

[10] $H(\mathbf{a}=\pi)$ has top state with energy $2|v|$ for the same eigenvector if the graph is regular.

IV. SCHRÖDINGER OPERATORS FOR NETWORKS OF THIN WIRES

Networks of one-dimensional connecting wires are idealizations corresponding to physical networks in the limit that the widths of the wires are small relative to all other length scales in the problem. The corresponding Schrödinger operators have, of course, the basic features of the general case discussed in Sec. II, and like the tight-binding model offer some simplifications. The first and obvious simplification is that the partial differential operator of Sec. II is replaced by an ordinary differential operator. The second simplification is that, at least for the case of "free electrons," the problem can be further reduced to matrices. In fact, the matrices turn out to be close relatives of the tight-binding Hamiltonians.

There are several reasons for considering this subclass. First, it is a natural class to consider and it is a useful description of various physical settings. Second, to examine the stability of the transport properties of networks, it is useful to compare how sensitive they are to the dynamics. Free electrons are in some sense on the other end of the spectrum from those that are tightly bound, and so offer an interesting alternative dynamics.

The formulation of wave equations on networks of one-dimensional wires has a long history, partly because the setting arises in many areas of physics: single-mode acoustic and electromagnetic waveguide networks (Mittra and Lee, 1977; Ramo, Whinery, and van Duzer, 1984); organic molecules (Ruedenberg and Scherr, 1953; Platt, 1964); superconductivity in granular and artificial materials (deGennes, 1981; Alexander, 1983); and mesoscopic quantum systems (Imry, 1986). The construction of wave equations for such networks is a topic in its own right. Ruedenberg and Scherr, who were apparently among the first to address the problem, based their formulation on the analysis of the limit of wires of finite thickness. Alexander generalized this to networks in external magnetic fields. Recently, the problem came of age in a series of mathematical works by Exner and Šeba (1987), whose formulation is based on the von Neumann theory of self-adjoint extensions of formal differential operators.

Our aims in this section are, first, to formulate Schrödinger operators for one-dimensional networks; second, to motivate this formulation by showing the relation to the original partial differential operator; and finally, to describe the reduction to a matrix problem for "free electrons." This section contains a fair amount of known material and is of an expository nature. Readers familiar with Alexander's work may want to skip it.

In the limit of narrow wires, part of the geometric information in Ω is lost. Some of it translates to dynamical information in the one-dimensional wave operator in the form of various potentials. We shall first formulate, in an *ad hoc* way, the operator, and later make the connection with the limiting procedure. With the network we associate the following potentials: (1) the "vector" potentials $\mathbf{A}(x,e)$, which are roughly the tangential component of

$\mathbf{A}$ at the point x on the edge e; (2) scalar potentials $V(x,e)$; and (3) vertex potentials $\lambda(v)$, which are associated with the vertices. All these potentials are real.

The wave function ψ is a vector in $\bigoplus_E L^2(e)$, with components $\psi(x_i,e_i)$. The Schrödinger operator, acting on the edge e, is the ordinary differential operator

$$(H(\mathbf{A})\psi)(x,e)=([-i\partial_x-\mathbf{A}(x,e)]^2+V(x,e))\psi(x,e)\ . \tag{4.1}$$

ψ has a unique value at the vertices and satisfies the Sturm-Liouville type of boundary conditions,

$$\sum_E [v,e][(-i\partial_x-\mathbf{A}(x,e))\psi](x,e)\,|_v=-i\lambda(v)\psi(v)\ , \tag{4.2}$$

where $\psi(v)\equiv\psi(x,e)\,|_v$.

We first discuss Eq. (4.1) and examine the relation of the potentials to the magnetic and geometric information in the original multidimensional problem, and then we discuss Eq. (4.2).

Consider the eigenvalue problem

$$(-i\nabla-\mathbf{A})^2\Psi=E\Psi \tag{4.3}$$

in a striplike domain, Fig. 9, with Dirichlet boundary conditions. Note the absence of a scalar potential in Eq. (4.3). Ω is essentially straight, with x the coordinate along it and y that in the transverse direction. In the limit of small width, the y coordinate becomes[11] a "fast variable" relative to the "slow variable" x, so Ψ admits a Born-Oppenheimer decomposition (Born and Oppenheimer, 1927)

$$\Psi(x,y)\simeq\psi(x)\eta_x(y)\ , \tag{4.4}$$

where $\eta_x(y)$ is a normalized eigenstate of the transverse (fast) motion, i.e.,

$$(-i\partial_y-\mathbf{A}_y)^2\eta_x(y)=W(x)\eta_x(y)\ . \tag{4.5}$$

Write $\langle\mu\,|\,\eta\rangle$ for the scalar product in the y coordinates, i.e.,

$$\langle\mu\,|\,\eta\rangle(x)\equiv\int dy\,\mu_x^*(y)\eta_x(y)\ . \tag{4.6}$$

$\langle\eta\,|\,\eta\rangle(x)=1$ by normalization. With the ansatz Eq. (4.4), the slow variable $\psi(x)$ solves the ordinary differential equation

$$\{[-i\partial_x-\mathbf{A}_x(x)-i\langle\eta\,|\,\partial_x\eta\rangle(x)]^2+W(x)+\langle\eta\,|\,\partial_x\eta\rangle^2(x)+\langle\partial_x\eta\,|\,\partial_x\eta\rangle\}\psi(x)=E\psi(x)\ . \tag{4.7}$$

By the normalization of η, $i\langle\eta\,|\,\partial_x\eta\rangle(x)$ is a real-valued function. $\mathbf{A}_x(x)\equiv\langle\eta\,|\,\mathbf{A}_x\,|\,\eta\rangle(x)$. We see that the vector potential in Eq. (4.1) has the tangential component of the vector potential $\mathbf{A}$, corrected by gauge fields arising from the transverse motion:

$$\mathbf{A}(x,e)\equiv\langle\eta\,|\,\mathbf{A}_x\,|\,\eta\rangle(x)+i\langle\eta\,|\,\partial_x\eta\rangle(x)\ . \tag{4.8}$$

The emergence of gauge potentials in the slow dynamics whose origin is in the fast dynamics is a feature of the Born-Oppenheimer theory (Alden Mead and Truhlar, 1979; Combes, Duclos, and Seiler, 1981; Wilczeck and Zee, 1984; Alden Mead, 1987).

We now examine the scalar potentials. Since the original operator, Eq. (4.6), had no scalar potential, the scalar potentials in Eq. (4.7) have their origins in the geometry of Ω and the dynamics of the fast variables. As the width of Ω shrinks to zero, $W(x)$ is dominant and shoots to $+\infty$ as $(\text{width})^{-2}$ by the uncertainty principle. This makes E in Eq. (4.7) shoot to $+\infty$ as well. To obtain a finite limit, a simple renormalization is required, which is familiar from the study of points interactions (Albeverio *et al.*, 1988). Suppose that as the width shrinks to zero

$$W(x)-E\to W(x)-k^2\ , \tag{4.9}$$

where $\mathbf{W}(x)$ and k^2 are both finite. That is, we remove from $W(x)$ and E the same large constant (which may be identified with the constant attractive potential that keeps the electrons confined to Ω). This, together with the other two (subdominant) potential terms in Eq. (4.7), defines $V(x,e)$ in Eq. (4.1). It is instructive to note that for the limit Eq. (4.9) to exist, the wires must be of almost uniform width. Indeed, differentiating Eq. (4.9) gives

$$\partial_x W(x)=O(1)\ , \tag{4.10}$$

so $\partial_x(\text{width})$ is of order $(\text{width})^3$.

In the special case of uniform and straight wires we may choose

$$\eta_x(y)=\left[\exp\left[i\int^y \mathbf{A}_y(x,y')dy'\right]\right]\mu(y)\to\mu(y) \tag{4.11}$$

independent of x and $\mathbf{A}$. In this case $V(x,e)$ is constant (which one can take to be zero) and $\mathbf{A}(x,e)$ is the tangential component of the vector potential.[12]

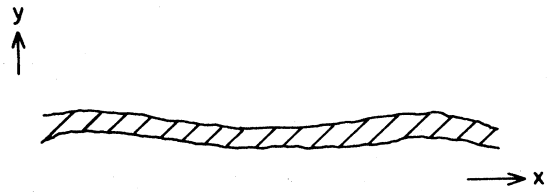

FIG. 9. A narrow striplike domain for which the study of the Laplacian reduces to the study of an ordinary differential equation in the Born-Oppenheimer approximation.

[11]By scaling the x and y coordinates to order unity, say, one finds that the x coordinate has a heavy mass associated with it while the y coordinate has a light mass.

[12]Twisting wires have additional geometric information that translates to dynamical information. In the case of the wave equation (without vector potential) this has been studied in Berry (1987), Haldane (1986), and Kugler and Shtrikman (1987).

In the following we restrict ourselves to networks of straight wires of uniform cross sections. We call these, for short, free electrons. The eigenfunctions of Eq. (4.1) are then

$$\psi(x,e)=\exp[i\mathbf{a}(x,e)][\psi_+(e)\exp(ikx) + \psi_-(e)\exp(-ikx)] , \quad (4.12)$$

where

$$a(x,e)\equiv\int_0^x \mathbf{A}(y,e)dy , \quad (4.13)$$

and ψ_+ and ψ_- are the amplitudes of the forward- and backward-moving waves on e.

We now want to "explain" the boundary condition (4.2). It was originally derived by Ruedenberg and Scherr (1953) by considering the zero-width limit of the multidimensional junction. Exner and Šeba show that such boundary conditions describe all the self-adjoint extensions of the operator (4.1). The scattering theory of junctions, an approach that has gained popularity in the quantum theory of complex systems (see, for example, Anderson *et al.*, 1980; Shapiro, 1983), gives some insight into Eq. (4.2).

Let $\psi_{\text{in/out}}(v)$ be the $|v|$-vector of incoming/outgoing amplitudes toward the junction v, with components $\psi_{\text{in/out}}(e,v)$ (where the edges e are incident on v):

$$\begin{aligned}\psi_{\text{in}}(e,v)&=\delta(1,[v,e])\psi_+(e)\exp\{i(k\,|e|+a(e))+\delta(-1,[v,e])\psi_-(e)\} ,\\ \psi_{\text{out}}(e,v)&=\delta(1,[v,e])\psi_-(e)\exp\{i(-k\,|e|+a(e))+\delta(-1,[v,e])\psi_+(e)\} ,\end{aligned} \quad (4.14)$$

where

$$\mathbf{a}(e)\equiv\mathbf{a}(|e|,e),\quad \mathbf{a}(-e)\equiv-\mathbf{a}(e) , \quad (4.15)$$

satisfy Eq. (3.7).

With each vertex v associate a scattering matrix $S(k,v)$, which is a unitary $|v|\times|v|$ matrix relating the incoming and outgoing amplitudes:

$$S(k,v)\psi_{\text{in}}(v)=\psi_{\text{out}}(v) . \quad (4.16)$$

The current flowing toward v on e is $k[|\psi_{\text{in}}(v,e)|^2-|\psi_{\text{out}}(v,e)|^2]$, so the total current flowing toward the vertex v satisfies Kirchoff's first law,

$$k\sum_e[|\psi_{\text{in}}(v,e)|^2-|\psi_{\text{out}}(v,e)|^2]=0 , \quad (4.17)$$

by the unitarity of S. Current is conserved at the vertices. Conversely, current conservation implies the unitarity of S.[13]

Define point junctions by the requirement that ψ has a unique continuation to the vertices, that is,

$$\psi_{\text{in}}(v,e)+\psi_{\text{out}}(v,e)=\langle\kappa(v)|\psi_{\text{in}}(v)\rangle , \quad (4.18)$$

where $\langle\kappa(v)|$ is a $|v|$-vector characterizing the vertex and the right-hand side is e independent. In vector notation, using Eq. (4.16),

$$[1+S(k,v)]|\psi_{\text{in}}\rangle=\langle\kappa(v)|\psi_{\text{in}}(v)\rangle|\mathbb{I}\rangle , \quad (4.19)$$

where $|\mathbb{I}\rangle$ is the $|v|$-vector

$$|\mathbb{I}\rangle\equiv(1,1,1,\ldots,) . \quad (4.20)$$

Equation (4.19) gives the operator relation

$$S(v)=-1+1|\mathbb{I}\rangle\langle\kappa(v)| . \quad (4.21)$$

Since S is unitary, the two equations, $S^\dagger S=1$ and $SS^\dagger=1$, lead to

$$\begin{aligned}&-|\mathbb{I}\rangle\langle\kappa(v)|-|\kappa(v)\rangle\langle\mathbb{I}|+|\kappa(v)\rangle|v|\langle\kappa(v)|=0 ,\\ &|\kappa(v)\rangle|v|\langle\kappa(v)|=|\mathbb{I}\rangle\langle\kappa(v)|\kappa(v)\rangle\langle\mathbb{I}| .\end{aligned} \quad (4.22)$$

The second equation says that $|\kappa(v)\rangle$ is proportional to $|\mathbb{I}\rangle$. The first constrains the proportionality constant to lie on a circle with radius $1/|v|$ in the complex plane, which is tangent to the imaginary axis:

$$S(k,v)=-1+(2/|v|)\cos[\theta(k,v)]\times\exp[i\theta(k,v)]|\mathbb{I}\rangle\langle\mathbb{I}| , \quad (4.23)$$

with $0\le\theta(k,v)\le\pi$. This singles out a circle in the $|v|^2$-dimensional space of unitary matrices.[14] Note that (in the spinless case considered here) $S(k,v)$ of a point junction is automatically time-reversal invariant: time reversal says that $(\psi_{\text{in}}(v))^*=\psi_{\text{out}}(v)$, from which it follows that $S=S^t$. Equation (4.23) is of this form.

To relate $\theta(k,v)$ of Eq. (4.23) and $\lambda(v)$ of Eq. (4.2), rewrite Eq. (4.2) as

$$k\langle\mathbb{I}|(\psi_{\text{in}}(v)-\psi_{\text{out}}(v))\rangle = -i\lambda(v)\langle\mathbb{I}|(\psi_{\text{in}}(v)+\psi_{\text{out}}(v))\rangle/|v| . \quad (4.24)$$

Substituting Eq. (4.23) in Eq. (4.16) and then in Eq. (4.24)

[13]Current conservation, Eq. (4.17), implies that $S^\dagger S$ must be a diagonal unitary and positivity implies that it is the identity. We are indebted to L. Sadun for pointing this out to us.

[14]After the completion of this work, we received JINR preprints (Exner and Šeba, 1987) in which Eq. (4.23) is derived. We thank F. Gesztesy for drawing our attention to these works.

gives

$$\lambda(v) = -|v| k \tan[\theta(k,v)] . \tag{4.25}$$

If $\lambda(v) \neq 0$, then, as the energy k^2 varies from 0 to ∞, the scattering matrix traverses the full circle of point scatterers in the space of unitaries.[15]

We conclude this section by describing a method, following Alexander (1983), that further reduces the study of the operators associated with one-dimensional networks to the study of finite matrices.[16] The wave function on the edge $\mathbf{e}=(v,u)$ can be written in terms of its values on the vertices, u and v:

$$\psi(x,e) = \exp[i\mathbf{a}(x,e)]\{\psi(u)\sin[k(|e|-x)] + \psi(v)\sin(kx)\exp[-i\mathbf{a}(e)]\}/\sin(k|e|) , \tag{4.26}$$

where $k \geq 0$. $\psi(x,e)$ has, by construction, a unique value on the vertices and satisfies the eigenvalue equation (4.1) with zero scalar potential. Substitution in the boundary conditions, Eq. (4.2), gives the matrix equation

$$h(k,\mathbf{a})\psi = 0 , \tag{4.27}$$

with ψ the $|V|$-vector on the vertices and $h(k,\mathbf{a})$ the $|V| \times |V|$ Alexander-de Gennes matrix:

$$[h(k,\Phi)]_{u,v} = \delta(u,v)\left[\sum_{E} |[e,v]| \cot(k|e|) - \lambda(v)/k\right] - \sum_{E} \delta([u,v],e)\frac{\exp[i\mathbf{a}(e)]}{\sin(k|e|)} . \tag{4.28}$$

The equation $\det[h(k,a)]=0$ determines the spectrum $\{k_j^2(\Phi) \mid j=0,1,\ldots,\Phi\in\mathbb{T}^h\}$ of the Schrödinger operator. This is an implicit-eigenvalue problem for the matrix $h(k,\Phi)$.

In the special case of no scattering potential at vertices, $\lambda(v)\equiv 0$, and edges of equal lengths, which one may then take to be unity with no loss of generality, Eq. (4.28) simplifies to

$$h_0(k,a)\psi = 0 , \tag{4.29}$$

where

$$[h_0(k,a)]_{uv} = \begin{cases} |v| \cos(k) & \text{for } u=v , \\ -\exp[i\mathbf{a}(e)] & \text{for } e=(u,v) , \\ 0 & \text{otherwise} . \end{cases} \tag{4.30}$$

Here $h_0(k,\mathbf{a})$ is periodic in $\mathbf{k}$ and $\mathbf{a}$ with period 2π. It is remarkable how close it is to the tight-binding Hamiltonians $H(\mathbf{a})$ of Sec. III. In fact, for a given graph,

$$h_0(0,\mathbf{a}) = H(\mathbf{a}) . \tag{4.31}$$

The Bohm-Aharnov periodicity and the gauge properties discussed in Sec. III transfer to this case as well. An interesting new ingredient is that the parameter space can now be thought of as the $(h+1)$-dimensional torus. The h torus is as in the tight-binding case. An extra period comes from k.

The map $k^2 \rightarrow \cos(k)$ maps the unbounded spectrum of the Schrödinger operator on a finite set. More explicitly, for fixed flux, the eigenstates are naturally paired (because of the symmetry of the cosine function), and each has two quantum numbers:

$$k_{+jn}(\Phi) = k_j(\Phi) + 2\pi n , \tag{4.32a}$$

$$k_{-jn}(\Phi) = [2\pi - k_j(\Phi)] + 2\pi n . \tag{4.32b}$$

Here $k_j(\Phi)$ is in $[0,\pi]$, and n natural. As we shall show, j runs over the finite set $1,\ldots,|V|$. [$k_{\pm jn}(\Phi)$ is constrained to be positive.]

In contrast with the situation in the tight-binding case, the Hilbert space can accommodate an infinite number of fermions. The n dependence is simple and explicit, and it is natural to expect that the problem can be fully analyzed by thinking of k as an angle and considering one period of $\cos(k)$.

Consider the set $\{(k,\Phi) \mid \Phi\in[-\pi,\pi]^h,\ k\in[0,2\pi], \det[h_0(k,a)]=0\}$. It may be thought of as the graph of "energy bands" over flux space restricted to its basic periods. Some of its basic properties are listed below.

(a) The bands are periodic in Φ (by Bohm-Aharonov periodicity); they are invariant under the reflection $\Phi \rightarrow -\Phi$ (by complex conjugating), and also under $k \rightarrow 2\pi - k$ [by the symmetry of $\cos(k)$].

(b) For fixed Φ there are $|V|$ bands, counting multiplicity, in the interval $k\in[0,\pi]$. [This follows from the self-adjointness of $h_0(k,a)$ and property (e) below.]

(c) The set of bands has a property that we shall call "π-shift" invariance, which is reminiscent of an electron-hole symmetry. By this we mean that the kernels of $h_0(k,a)$ and $h_0(k+\pi,\mathbf{a}+\pi)$ coincide. π is the vector $\pi(1,1,\ldots,1)$ in $\mathbb{R}^{|E|}$. This follows from

$$h_0(k,\mathbf{a}) = -h_0(k+\pi,\mathbf{a}+\pi) . \tag{4.33}$$

[15]This does not explain why λ is k independent. Formally, this can be related to the question of the choice of self-adjoint extension; see Exner and Šeba (1987).

[16]Some of the formulas that we shall write below do not make sense if $\sin(k|e|)=0$. These should be interpreted as the limit when k has a small imaginary part.

A shift of π of the gauge fields translates to the shift of the fluxes:

$$\Phi(f)\to\Phi(f)+\pi\sum_{E}[e,f]$$
$$=\Phi(f)+\pi\,|f|\,\mathrm{mod}(2\pi)\ . \tag{4.34}$$

$|f|$ is the number of edges of f. If $|f|$ is even, then Eq. (4.34) is the identity on the flux torus. If, however, $|f|$ is odd, Eq. (4.34) is a shift of π in the corresponding flux. We conclude that the spectrum is invariant under

$$(k,\Phi)\to(k+\pi,\Phi+\pi F)\ , \tag{4.35}$$

where F is the $|F|$-vector

$$F(f)=|f|\ . \tag{4.36}$$

This is a global property of the spectrum, not necessarily a property of any given band. This is illustrated in Fig. 10.

(d) The bands touch the plane $\cos(k)=1$ at the single point $\Phi=0$. This follows from Eq. (4.31) and the strict positivity of the tight-binding Hamiltonians, proven in Sec. III. When combined with Eq. (4.35) this also gives the result that the spectrum touches $\cos(k)=-1$ at the single point $F\pi$. Note that these are the points where Eq. (4.26) is ill defined.

(e) $h_0(k,\mathbf{a})>0$, as an operator identity, for $\cos(k)>1$, and similarly $h_0(k,\mathbf{a})<0$ for $\cos(k)<-1$. For $\cos(k)>1$, this is seen from the fact that $h_0(k,\mathbf{a})$ is an increasing function of $\cos(k)$, and from (d) above. Combining this with (c) above gives the result for $\cos(k)<1$.

For a given graph, the implicit eigenvalue problem associated with free electrons, Eq. (4.29), and the explicit eigenvalue problem associated with the tight-binding Hamiltonian describe rather different physics. Consequently it is remarkable that both lead to the reduction of a partial differential operator to related matrix problems. In fact, more is true. For *regular graphs* the eigenvalue problem (and, as we shall see below, also the topological conductances) turn out to be simply related:

$$\cos(k)=1-E/|v|\ , \tag{4.37}$$

where E is the eigenvalue for the graph-theoretic tight-binding model, and k^2 is the corresponding eigenvalue for free electrons. (A similar relation holds for the standard tight-binding model with zero on-site interaction, but again, only for regular graphs.)

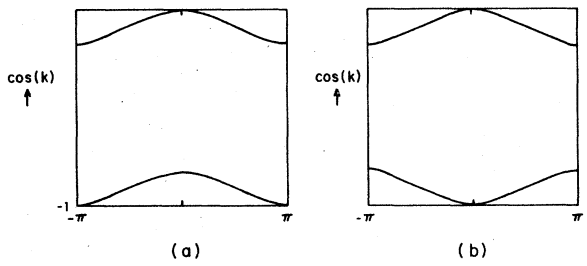

FIG. 10. Possible (schematic) spectra for $h_0(k,\Phi)$: (a) when the flux is through a face with an odd number of edges; (b) when the flux is through a face with an even number of edges.

The last point we discuss in this section is the normalization of the wave function. The length in the original Hilbert space induces a metric in the vector space $\mathbb{C}^{|V|}$. Writing $|\psi\rangle$ for the two-vector $(\psi(u),\psi(v))$ associated with the edge $e=(u,v)$ we find for the eigenstates

$$\|\psi(x,e)\|^2=\langle\psi\,|\,M(k;e)\,|\,\psi\rangle\ , \tag{4.38a}$$

where $M(k;e)$ is the 2×2 positive, Hermitian matrix

$$M(k;e)=\frac{1}{2\sin^2(k\,|\,e\,|\,)}\times\begin{bmatrix}\xi(k,e) & \exp[ia(e)]\eta(k,e)\\ \exp[-ia(e)]\eta(k,e) & \xi(k,e)\end{bmatrix},$$

with

$$\xi(k,e)\equiv|\,e\,|-\frac{\sin(2k\,|\,e\,|\,)}{2k} \tag{4.39}$$

and

$$\eta(k,e)\equiv\frac{\sin(2k\,|\,e\,|\,)}{2k}-|\,e\,|\cos(k\,|\,e\,|\,)\ .$$

As a consequence, eigenstates are normalized according to

$$\|\psi\|^2=\sum_{E}\|\psi(e,x)\|^2=\sum_{u,v\in V}\psi^*(u)[M(k)]_{uv}\psi(v)\ , \tag{4.38b}$$

where $M(k)$ is the $|V|\times|V|$ (positive) matrix

$$[M(k)]_{uv}=\begin{cases}\displaystyle\sum_{E}\frac{\xi(e,k)\,|\,[e,v]\,|}{2\sin^2(k\,|\,e\,|\,)} & \text{for } u=v\ ,\\ \dfrac{\exp[ia(e)]\eta(e,k)}{2\sin^2(k\,|\,e\,|\,)} & \text{for } e=(u,v)\ ,\\ 0 & \text{otherwise}\ .\end{cases} \tag{4.40}$$

For determining the spectrum, the correct normalization is not an issue. For most observables, however, it is. In particular, it is important for the calculation of the transport. We return to this in Secs. X and XI. As we shall see there, for the *averaged* transport coefficients, it turns out that because of the topological interpretation the normalization is, in fact, not an issue.

V. LOOP CURRENTS

In circuit theory, it is convenient to introduce loop currents so that Kirchhoff's first law of current conservation at each vertex is automatically satisfied. Let $I(f)$ be the loop current associated with the elementary face f and $I(e)$ be the current in the edge e. The two are related by

$$I(e)=\sum_{F}[e,f]I(f)\ . \tag{5.1}$$

Loop currents are the basic objects in quantum networks. In this section we define and examine the observables associated with them.

We motivate the definition by the following consideration: to "measure" the current flowing around the mth flux, consider a virtual change $\delta\Phi_m$. This creates a virtual emf around the mth loop, which does not affect the state of the system (this is what we mean by virtual), except that the current now goes through a potential drop. The virtual change in energy of the system is

$$\delta E = -I(m)\delta\Phi_m \ . \tag{5.2}$$

This suggests that $-\partial_m H(A)$ is the observable associated with the mth loop current. Here, and throughout, we use the convention $\partial_m \equiv \partial_{\Phi_m}$. For the Schrödinger operator of Sec. II,

$$-2\partial_m H(A) = (-i\nabla - A)\cdot(\partial_m A) + (\partial_m A)(-i\nabla - A) \ . \tag{5.3}$$

It is convenient to introduce form notation such that

$$I(\psi) \equiv \sum_{m=1}^{h} I(m,\psi)d\Phi_m \ , \tag{5.4a}$$

$$\langle I(\psi)\rangle \equiv \sum_{m=1}^{h} \langle I(m,\psi)\rangle d\Phi_m \ , \tag{5.4b}$$

$$dH \equiv \sum_{m=1}^{h} (\partial_m H)d\Phi_m \ , \tag{5.4c}$$

with the flux-averaged current defined by

$$\langle I(m,\psi)\rangle \equiv \frac{1}{2\pi}\int_0^{2\pi} d\Phi_m I(m,\psi) \ . \tag{5.5}$$

Equation (5.4) enables us to write some of the formulas without excessive indexing.

The loop current for a system at the state ψ is[17]

$$I(m,\psi) = -\langle \psi \mid \partial_m H \mid \psi\rangle \tag{5.6a}$$

in components and

$$I(\psi) = -\langle \psi \mid dH \mid \psi\rangle \tag{5.6b}$$

as a one-form.

Equation (2.5) can be used to define loop currents for different choices of gauge.

It is instructive to examine the relation of the loop-current operator with the conventional current-density operator, given by (up to factor $\frac{1}{2}$)[18]

$$(-i\nabla - \mathbf{A})\delta(x-y) + \delta(x-y)(-i\nabla - \mathbf{A}) \ . \tag{5.7}$$

In a single ring, loop and edge currents coincide, so we consider this case. Let $x=(\rho,\theta)$ be the canonical cylindrical coordinates with the z axis threading the ring. The current operator associated with a section of the ring with fixed azimuthal angle θ_0 is

$$\left[\frac{\delta(\theta-\theta_0)}{\rho(\theta_0)}v_\theta + v_\theta\frac{\delta(\theta-\theta_0)}{\rho(\theta_0)}\right] , \tag{5.8a}$$

where v_θ is the velocity operator in the θ direction. Equation (5.8a) follows from integrating the current density over the θ_0 sections of the ring. The average current (over θ) is therefore

$$\frac{1}{2\pi}\left[\frac{1}{\rho(\theta)}v_\theta + v_\theta\frac{1}{\rho(\theta)}\right] . \tag{5.8b}$$

Suppose now that the ring is threaded by a flux tube, so that the electric field associated with it is azimuthally oriented. The vector potential describing the most general flux tube is

$$\mathbf{A}(x) = \Phi\, d\Lambda(x) \ , \tag{5.9}$$

where

$$\Lambda(\theta+2\pi) = \Lambda(\theta)+1 \ . \tag{5.10}$$

The loop-current operator is

$$\frac{(\partial_\theta\Lambda)}{\rho(\theta)}v_\theta + v_\theta\frac{(\partial_\theta\Lambda)}{\rho(\theta)} \ . \tag{5.11}$$

Comparing Eqs. (5.8) and (5.11), we see that the normalized weight $\delta(\theta-\theta_0)$ in Eq. (5.8a) is replaced by the normalized weight $1/(2\pi)$ in Eq. (5.8b), and by a general normalized weight $(\partial_\theta\Lambda)$. The weight (which need not be positive) in Eq. (5.11) characterizes the flux tube. For example, the flux tube of Eq. (2.10), associated with a singular gauge field, that is supported on a half-line along the radial direction, has all the potential drop at θ_0. The associated Λ is a staircase function of the azimuthal angle, i.e., the integral part of $\Phi(\theta-\theta_0)/2\pi$. The corresponding loop current coincides with the current (5.8a). If, on the other hand, the tube is that of Eq. (2.8) and generates uniform fields $\Lambda(\theta)=(\Phi/2\pi)\theta$, the loop coincides with the average edge current, Eq. (5.8b). In steady state, current is conserved and is independent of the choice of Λ. The loop current (5.11) and the edge currents (5.8) coincide.

The basic definition of loop currents says that we may interpret the fluxes threading the loops as "ammeters" of loop currents.[19] The examples discussed above show that

[17]For the corresponding thermodynamic identity, see, for example, Byers and Yang (1961).

[18]The following is meaningful for the Schrödinger operators of Secs. II and IV. For tight-binding Hamiltonians, one has to use the virtual work argument of Eq. (5.2).

[19]One way to actually measure the loop currents is to observe the change in the fluxes resulting from induction. This is distinct from what is meant here by the statement that fluxtubes are ammeters. The theoretical framework neglects all induction effects. Induction is briefly discussed in Sec. XIV.

different ammeters, i.e., different flux tubes, measure distinct, although related, currents that coincide in steady states. The situation is like that in Sec. II, where different driving flux tubes gave distinct dynamics even though the fluxes and emf's were the same. Clearly, a particularly natural and convenient set of observables to focus on are those that are independent of the flux tubes and depend only on the fluxes Φ and emf's $-\Phi$. This corresponds to our desire to define the transport coefficients as ratios of currents to voltages, paying no regard to how the electric field and currents are distributed. As we shall see in Secs. VI and VIII, if the transport coefficients are defined via flux averaging, they have this property: the same (averaged) loop currents are measured by all "ammeters" and "batteries."

Suppose now that $H(\mathbf{A})$ is time dependent, because some of the fluxes are. Let $|\psi_t\rangle$ solve the time-dependent Schrödinger equation. Then, using the chain rule, Eq. (5.4), we can rewrite the mth loop current as

$$I(m,\psi_t)=-i\partial_t\langle\psi_t|\partial_m\psi_t\rangle\ , \tag{5.12a}$$

which, in form notation, is

$$I(\psi_t)=-i\partial_t\langle\psi_t|d\psi_t\rangle\ . \tag{5.12b}$$

Equations (5.4) and (5.12) are the basic equations of "loop transport." In the next section we shall see that, in the adiabatic limit, the loop currents are related to geometrical properties of the bundle of spectral subspaces of the Hamiltonians.

VI. ADIABATIC EVOLUTION AND TRANSPORT

When the fluxes generating $\mathbf{A}$ vary slowly in time, the evolution generated by $H(\mathbf{A})$ respects the spectral structure. This is the content of the adiabatic theorem. Namely, let $P(\mathbf{A})$ be a spectral projection for $H(\mathbf{A})$. Then states in $P(\mathbf{A})$ at time 0 evolve to states in $P(\mathbf{A})$ at time t, up to a small error term. Technical conditions aside, the theorem holds provided $P(\mathbf{A})$ is separated by gaps from the rest of the spectrum. We make this assumption throughout.

A convenient way to study the evolution in the adiabatic limit is to introduce an *adiabatic Hamiltonian,* an idea that goes back to Kato (1950). It generates an evolution that respects the adiabatic theorem with no error. As we shall see below, there is a choice to be made. One choice is to require that the evolution approximate the physical evolution the best it can. This leads to the following choice of generator (Avron, Seiler, and Yaffe, 1987):

$$\begin{aligned} &H_{\mathrm{Ad}}(\mathbf{A},P)\equiv H(\mathbf{A})+\Gamma_t(\mathbf{A})\ ,\\ &\Gamma_t(\mathbf{A})\equiv i[\partial_t P,P]\ . \end{aligned} \tag{6.1a}$$

Another choice, the one originally picked by Kato, is to take as generator

$$H_{\mathrm{K}}(\mathbf{A},P)\equiv\Gamma_t(\mathbf{A})\ . \tag{6.1b}$$

Although Eq. (6.1b) appears to be less motivated, it is, in certain ways, a more convenient choice for our purposes. In either case, the evolutions U_{Ad} have the property

$$U_{\mathrm{Ad}}(t)P(\mathbf{A}(0))=P(\mathbf{A}(t))U_{\mathrm{Ad}}(t)\ . \tag{6.2}$$

This is the precise meaning of the statement that the evolution respects the spectral structure of the Hamiltonian. Because of this, U_{Ad} has geometric significance as it defines transport of states in the bundle of spectral subspaces associated with the projection $P(\mathbf{A})$.

It is convenient to use form notation:

$$\Gamma(\mathbf{A})\equiv i[dP,P],\quad dP\equiv\sum_k(\partial_k P)d\Phi_k\ . \tag{6.3}$$

Equation (6.1b) can be rewritten as

$$H_{\mathrm{K}}(\mathbf{A},P)=\partial_t\Phi\cdot\Gamma(\mathbf{A})\ , \tag{6.4}$$

where the vector $\partial_t\Phi$ gives the flow in flux space. A centered dot denotes the pairing of vectors and forms, so, for example, $\partial_j\cdot d\Phi_k=\delta_{jk}$. $\Gamma(\mathbf{A})$, being a one-form, has a natural interpretation as the connection on the bundle of projections.

U_{Ad} parallel transports vectors in $P(\mathbf{A})$, and so is useful in the study of the geometry of the spectral subspace. Curvature is related to the noncommutativity of transport in different directions (Arnol'd, 1978), so parallel transport around a closed loop in flux space need not be the identity but rather a general unitary in $U(n)$, $n=\dim(P)$. The jk component of the curvature is

$$\omega_{jk}=\frac{U(\text{infinitesimal loop in } jk \text{ plane})-1}{|\text{ area of loop }|}\ . \tag{6.5}$$

From the evolution equation, the curvature associated with the projection P, for a small square loop in flux space, is given by[20]

$$\omega_{jk}=P[\partial_j P,\partial_k P]P\ . \tag{6.6}$$

In a component-free notation, ω is the curvature two-form:

$$\omega=P(dP)\wedge(dP)P\ . \tag{6.7}$$

It is imaginary as

$$\omega^\dagger=-\omega\ . \tag{6.8}$$

We now proceed to show that the components of ω are the matrix elements of the conductance.

The adiabatic current in the mth loop, $I_{\mathrm{Ad}}(m,\psi)$, is the obvious analog of Eq. (5.12), where ψ now solves the adi-

[20]Up to factors of i this is essentially the standard formula that says that the curvature is $dA-iAA$, where A is the connection one-form. For the generator in Eq. (6.1a) the curvature is $-iTP(\partial_j H-\partial_k H)P+P[\partial_j P,\partial_k P]P$, where T is the period associated with the loop. The first term in this expression is the "dynamical phase" and has vanishing periods. The second is the same as in Eq. (6.7).

abatic evolution. Let $P_j(\mathbf{A})$ be the one-dimensional projection $P_j(\mathbf{A})\equiv|\psi_j(\mathbf{A})\rangle\langle\psi_j(\mathbf{A})|$ associated with an isolated eigenvalue $E_j(\Phi)$. We may, and do, choose $\psi_j(\mathbf{A})$ according to the adiabatic evolution along the path shown in Fig. 11. This determines $\psi_j(\mathbf{A})$ with no ambiguity up to an overall constant phase on $\Phi\in\mathbb{R}^h$. Undoing the calculation leading to Eq. (5.12) [which turns out to be the same as replacing H in Eq. (5.6) by the adiabatic generator Eq. (6.1a)], one finds

$$I_{\mathrm{Ad}}(m,\psi_j)=-\partial_m E_j(\Phi) -i\{\langle\partial_m\psi_j(\mathbf{A})|\partial_t\psi_j(\mathbf{A})\rangle -\langle\partial_t\psi_j(\mathbf{A})|\partial_m\psi_j(\mathbf{A})\rangle\}\ . \quad (6.9)$$

By assumption, no levels cross, so the derivatives are well defined (see Sec. VII). Using the Schrödinger equation for the adiabatic evolution, Eq. (6.1a),

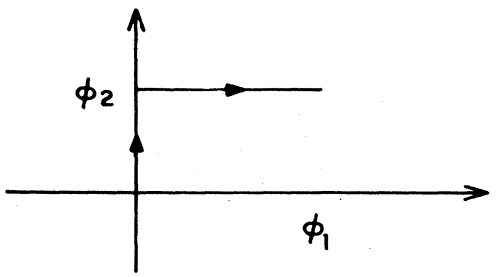

FIG. 11. A choice of paths for the adiabatic phase factors.

$$i\partial_t\psi_j=i\dot{\Phi}\cdot d\psi_j=H_{\mathrm{Ad}}(\mathbf{A})\psi_j\ , \quad (6.10)$$

and the fact that

$$\langle\psi_j|H_{\mathrm{Ad}}(\mathbf{A})|\psi_j\rangle=E_j(\Phi) \quad (6.11)$$

gives

$$I_{\mathrm{Ad}}(m,\psi_j)=-\partial_m E_j(\Phi)-i\sum_k\dot{\Phi}_k(t)(\langle\partial_m\psi_j(\mathbf{A})|\partial_k\psi_j(\mathbf{A})\rangle-\langle\partial_k\psi_j(\mathbf{A})|\partial_m\psi_j(\mathbf{A})\rangle)\ . \quad (6.12)$$

In index-free notation,

$$I_{\mathrm{Ad}}(P_j)=-dE_j-i\langle d\psi_j(\mathbf{A})|d\psi_j(\mathbf{A})\rangle\cdot\dot{\Phi}(t)=-dE_j-i\,\mathrm{Tr}[\omega(P_j)]\cdot\dot{\Phi}(t)\ . \quad (6.13)$$

This equation is the basic equation of adiabatic transport and plays a central role in all that follows. The transport matrix $i\,\mathrm{Tr}[\omega(P_j)]$ in Eq. (6.13) is, in view of Eq. (6.7), the curvature two-form. Written in longhand, $i\,\mathrm{Tr}[\omega(P)]$ is an $h\times h$ matrix with loop indices.

The current in Eq. (6.12) or Eq. (6.13) is affine in the emf's: in the absence of emf's there are persistent currents given by $-dE_j$. Persistent currents are common in atomic physics and manifest themselves in diamagnetism. Persistent currents also occur in macroscopic systems with macroscopic coherence, such as superconducting rings. Büttiker, Imry, and Landauer (1983) have suggested that persistent currents also occur in mesoscopic normal-metal rings, but this has not yet been observed. Another remarkable feature of Eq. (6.13) is that the currents at time t are determined by the emf's at the same time: the adiabatic transport has no memory. This implies that the adiabatic ac conductance is frequency independent (being the Fourier transform of a delta function in time).[21] Finally, there are no power-law correction terms in the adiabatic transport (Klein and Seiler, 1988).

The adiabatic transport coefficients $i\,\mathrm{Tr}[\omega_j(P)]$ depend on the flux tubes, i.e., depend on a choice of vector potential $\mathbf{A}$, for P depends on $\mathbf{A}$. This is as one expects from the discussion in the previous sections. Distinct flux tubes drive the system differently and measure its response differently. When we consider the transport of current *averages,* two nice things happen. First, the transport coefficients become independent of the flux tubes and become a property of the fluxes alone. Second, the persistent currents disappear, and one gets the usual linear response.

The average mth loop current is, by Eq. (5.5),

$$\langle I_{\mathrm{Ad}}(m,P_j)\rangle=-\frac{i}{2\pi}\int_0^{2\pi}d\Phi_m\{\langle\partial_m\psi_j(\mathbf{A})|\partial_t\psi_j(\mathbf{A})\rangle-\langle\partial_t\psi_j(\mathbf{A})|\partial_m\psi_j(\mathbf{A})\rangle\}=\frac{i}{2\pi}\int_{T_m(\Phi)}\mathrm{Tr}[\omega(P_j)]\cdot\dot{\Phi}\ . \quad (6.14a)$$

$T_m(\Phi)$ is the line $\Phi+\lambda\partial_m$, λ going from 0 to 2π. The persistent currents, being complete derivatives, have vanishing averages and drop from (6.14). The average transport coefficients, defined as the Fourier transform of the kernel in Eq. (6.13), written out as a matrix, are

$$2\pi[\langle g_{\mathrm{Ad}}\rangle(P_j)]_{km}=\frac{i}{2\pi}\int_0^{2\pi}d\Phi_k\int_0^{2\pi}d\Phi_m\{\langle\partial_m\psi_j(\mathbf{A})|\partial_k\psi_j(\mathbf{A})\rangle-\langle\partial_k\psi_j(\mathbf{A})|\partial_m\psi_j(\mathbf{A})\rangle\}$$
$$=\frac{i}{2\pi}\int_{T_{km}(\Phi)}\langle d\psi_j(\mathbf{A})|d\psi_j(\mathbf{A})\rangle=\frac{i}{2\pi}\int_{T_{km}(\Phi)}\mathrm{Tr}[\omega(P_j)]\ . \quad (6.14b)$$

[21]For the quantum Hall effect there is experimental support for the quantization of the ac conductance (Kuchar *et al.*, 1987).

$T_{km}(\Phi)$ denotes the $2\pi\times 2\pi$ square slice in flux space, passing through Φ. Properties of the transport that follow from Eq. (6.14) will be discussed in Sec. VIII.

The adiabatic response is strictly linear and has no memory. The physical response presumably has both nonlinear corrections and memory. This raises the issue, how good is the adiabatic approximation? A study of the nonlinear corrections to linear response in the context of the Hall effect has been made by Thouless and Niu (1984). However, there appears to be no understanding of these issues from a general mathematical point of view. For questions about tunneling, the adiabatic limit is known to be very good in the sense that corrections are often exponentially small in the time scale. Tunneling is, however, only one of the issues. And, although it is natural to expect that $g_{\rm Ad}$ and $\langle g_{\rm Ad}\rangle$ approximate the physical transport g and $\langle g\rangle$, this has not been shown in any great generality. Avron, Seiler, and Yaffe (1987) have shown that $\langle g_{\rm Ad}\rangle$ and $\langle g\rangle$ are close if interpreted as charge transport (with error that is polynomial in the inverse time scale), and suggest that $g_{\rm Ad}$ and g, without averaging, may actually *not* be close to each other. The case of constant and harmonic emf's appears to be largely open, at least from a rigorous mathematical point of view.

VII. LEVEL CROSSINGS

The assumption that $E_j(\Phi)$ is an isolated eigenvalue entered in several places in the previous section. First, the adiabatic theorem requires no level crossings; second, dP_j and dE_j may not exist at crossing; and, finally, the zero average of the persistent current relies on $E_j(\Phi)$'s being smooth and periodic. So points in flux space where levels cross are where the theory in the previous section breaks down. In an almost dialectic fashion, these points are also the source of nontrivial transport. If no levels cross anywhere in flux space, $\langle g_{\rm Ad}\rangle(P)$ vanishes identically. If levels do cross, the adiabatic transport is not defined at crossings, but is defined away from crossings and may be nontrivial. This says that crossings are where the "sources" of the transport are located. For this reason, getting a handle on crossings is a key issue in understanding the transport.

There are three questions that we address in this section: (1) What is the local behavior of P near level crossings? (2) How big is the set of crossing points in the generic case? and (3) What can one say about crossings when the network has symmetries? This is a "service section," where relevant information that is needed later is collected. Many of the results are standard. [For a general overview on level crossings see Berry (1983).]

The Hamiltonians introduced in Secs. II, III, and IV are all entire functions of the fluxes. The projection $P_j(\Phi)$ is given by

$$P_j(\Phi)=\frac{1}{2\pi i}\int_{\gamma_j}\frac{dz}{H(\Phi)-z}\ , \tag{7.1}$$

where γ_j is a contour surrounding the jth piece in the spectrum, Fig. 12. For convenience of notation we suppress henceforth the index j. $P(\Phi)$ inherits the smoothness of $H(\Phi)$ as long as γ stays outside the spectrum. If $H(\Phi)$ is periodic, or periodic up to unitary equivalence, then $P(\Phi)$ inherits that too. Finally, if $P(\Phi)$ is a finite-dimensional projection, then $\mathrm{Tr}(H^k(\Phi)P(\Phi))$ is smooth in Φ for all k. In particular, isolated energy bands are smooth. However, when gaps in the spectrum close, so that γ is pinched, smoothness may be lost. Let $D(P)$ be the set of points in flux space where P is not smooth. Points in $D(P)$ must be points of level crossings. Because of Eqs. (2.5)–(2.7), if $\phi\in D(P)$ then $\phi+2\pi k\in D(P)$. So if we think of flux space as $\mathbb{R}^h$, $D(P)$ is periodic there. It is, however, better to think of flux space as $\mathbb{T}^h$.

Consider the local behavior of $E_j(\Phi)$ and $P_j(\Phi)$ near a two-level crossing at ϕ. Restricting the Hamiltonian to the degenerate subspace at ϕ gives a 2×2 Hermitian matrix function

$$h(\Phi)\equiv\begin{bmatrix}\langle\psi|H(\mathbf{A}|\psi\rangle\langle\psi|H(\mathbf{A})|\varphi\rangle\\ \langle\varphi|H(\mathbf{A})|\psi\rangle\langle\varphi|H(\mathbf{A})|\varphi\rangle\end{bmatrix}$$
$$\equiv\epsilon_0(\Phi)1+\boldsymbol{\epsilon}(\Phi)\cdot\boldsymbol{\sigma}\ , \tag{7.2a}$$

where $|\psi\rangle$ and $|\varphi\rangle$ are the two independent eigenvectors of $H(\mathbf{A})$ at ϕ. Here $\boldsymbol{\epsilon}(\Phi)$ is a *real* three-vector valued function, and $\boldsymbol{\sigma}$ is the triplet of Pauli matrices. The two eigenvalues of Eq. (7.2a) are

$$E_\pm(\Phi)=\epsilon_0(\Phi)\pm|\boldsymbol{\epsilon}(\Phi)|\ , \tag{7.3a}$$

from which it follows that $\boldsymbol{\epsilon}(\phi)=0$. The eigenprojections are

$$P_\pm(\Phi)=[1\pm\hat{\boldsymbol{\epsilon}}(\Phi)\cdot\boldsymbol{\sigma}]/2\ . \tag{7.4}$$

$\hat{\boldsymbol{\epsilon}}$ is the unit vector associated with $\boldsymbol{\epsilon}$. Because of the absolute value in Eq. (7.3a) and the normalization to unit vectors in Eq. (7.4), neither $E_\pm(\Phi)$ nor $P_\pm(\Phi)$ need be smooth at ϕ. In $\boldsymbol{\epsilon}$ space, Eq. (7.3a) describes a *conic,* Fig. 13. Berry and Wilkinson (1984) call such points *diabolic.* The eigenvalues are continuous in $\boldsymbol{\epsilon}$ but not smooth, and the projections are not even continuous near $\boldsymbol{\epsilon}=0$. [The fact, as well as the example, are classical results due to Rellich (1969).]

The behavior in Φ space can be more complicated, and things depend on the way Φ space is mapped on $\boldsymbol{\epsilon}$ space. The simplest case is when the map is characterized by its linear piece. Because we are interested mostly in three-flux networks, we restrict ourselves to the case in which

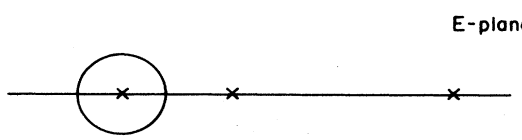

FIG. 12. A contour in the complex plane associated with a spectral projection.

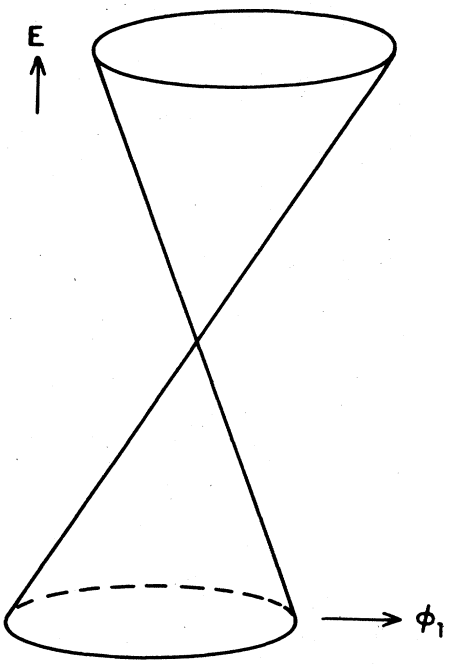

FIG. 13. A conic singularity.

Φ space is three dimensional. This is a particularly simple situation. Since ϵ is entire in Φ,

$$\epsilon(\Phi)\sim\sum_{m=1}^{3}(\partial_m\epsilon)\,|_\phi(d\Phi_m)\ . \tag{7.5}$$

We denote the linearized map from Φ to ϵ by $\nabla\otimes\epsilon$, that is,

$$[\nabla\otimes\epsilon]_{jk}\equiv\partial_j\epsilon_k\ . \tag{7.6a}$$

Now, if the linearized map is of rank 3, then the description of the singularity as conic holds in the Φ variables as well. In particular, in three-flux networks, diabolic points are those where

$$\det[\nabla\otimes\epsilon]\,|_\phi\neq 0\ . \tag{7.6b}$$

For the tight-binding Hamiltonians, the linearized map, Eq. (7.6b), can be written down by inspecting the graph. This is especially useful if one wants to compute the charges "by hand." Let us briefly describe this.

Let $e=(u,v)$ be an edge and $\mathbf{a}(e)$ the associated vector potential. For the tight-binding Hamiltonian $H(\mathbf{a})$ one has

$$\left\langle\psi\left|\frac{\partial H}{\partial\mathbf{a}(e)}\right|\varphi\right\rangle=i[-\psi^*(u)\varphi(v)e^{i\mathbf{a}(e)}+\psi^*(v)\varphi(u)e^{-i\mathbf{a}(e)}]\ . \tag{7.7}$$

For the sake of simplicity suppose that a gauge has been chosen so that $\mathbf{a}(e)=\Phi(e)$ for h of the edges, and $\mathbf{a}(e)=0$ for all other edges. (All the examples we consider in Secs. XII and XIII are of this form.) Suppose that ψ and φ span the degenerate subspace. Then from Eqs. (7.7) and (7.2a) one finds for the derivative of the map

$$\frac{\partial(\epsilon_2+i\epsilon_1)}{\partial\Phi(e)}=\psi^*(u)\varphi(v)e^{i\Phi(e)}-\psi^*(v)\varphi(u)e^{-i\Phi(e)}\ ,$$
$$\frac{\partial\epsilon_3}{\partial\Phi(e)}=\mathrm{Im}[\psi^*(u)\psi(v)e^{i\Phi(e)}-\varphi^*(u)\varphi(v)e^{i\Phi(e)}]\ . \tag{7.8}$$

Similar analysis can be made for two-level crossings in the de Gennes–Alexander problem, Eq. (4.29). Let $|\psi\rangle$ and $|\varphi\rangle$ be two degenerate eigenvectors of $h_0(k_0,\phi)$, with eigenvalue zero. Construct the 2×2 Hermitian matrix function of Φ and k,

$$\epsilon_0(k,\Phi)+\boldsymbol{\epsilon}(k,\Phi)\cdot\boldsymbol{\sigma}\equiv\begin{bmatrix}\langle\psi\,|\,h_0(k,\Phi)\,|\,\psi\rangle & \langle\psi\,|\,h_0(k,\Phi)\,|\,\varphi\rangle\\ \langle\varphi\,|\,h_0(k,\Phi)\,|\,\psi\rangle & \langle\varphi\,|\,h_0(k,\Phi)\,|\,\varphi\rangle\end{bmatrix}\ . \tag{7.2b}$$

This defines a map from (k,Φ) space to the $(\epsilon_0,\boldsymbol{\epsilon})$ space. The energy bands near (k_0,ϕ) are given by the vanishing of the determinant,

$$\epsilon_0^2(k,\Phi)-\boldsymbol{\epsilon}^2(k,\Phi)=0\ . \tag{7.3b}$$

This is a conic in $(\epsilon_0,\boldsymbol{\epsilon})$. If the Jacobian of the map is nonvanishing, it is also a conic in (k,Φ). The assumption that the degeneracy is isolated translates to $\boldsymbol{\epsilon}(k,\Phi)\neq0$ for (k,Φ) on a small three-sphere centered at (k_0,ϕ).

We now turn to the second question, how big is $D(P)$? This question was first posed by von Neumann and Wigner (1929), who also proposed a counting rule that gives the answer. A somewhat more precise formulation of the question is, in the space of "all" Hamiltonians what is the dimension of the space of Hamiltonians with degenerate eigenvalues? This, of course, depends on what one means by "all." The convention in the statistical theory of spectra (Dyson, 1964; Porter, 1965) is that for problems with magnetic fields, with or without spin, "all" means complex Hermitian matrices.

The space of Hermitian $n\times n$ matrices is an n^2-dimensional vector space. To illustrate the von Neumann–Wigner strategy we start with a warmup and show that the space of nondegenerate Hermitian matrices is of full dimension.

The unitary that diagonalizes a given Hermitian matrix with fixed nondegenerate spectrum,

$$E_1<E_2<\cdots<E_n\ , \tag{7.9a}$$

is determined up to a diagonal unitary matrix. So there is a one-to-one correspondence between nondegenerate Hermitian matrices with fixed spectrum and elements of

$$\mathrm{U}(n)/[\mathrm{U}(1)]^n\ . \tag{7.10a}$$

Since $\dim[\mathrm{U}(n)]=n^2$, the space in Eq. (7.10a) is $n(n-1)$ dimensional, which together with the n dimensions associated with varying E_j gives n^2, the full dimension.

Now consider the Hermitian matrices with, say, a degenerate ground state. Equation (7.7) is replaced by

$$E_1=E_2<\cdots<E_n\ . \tag{7.9b}$$

The corresponding diagonalizing unitaries are identified with elements of

$$\mathrm{U}(n)/[\mathrm{U}(1)]^{n-2}\times\mathrm{U}(2)]\ . \tag{7.10b}$$

This space is $n(n-1)-2$ dimensional. The dimension of the space associated with varying E_j is $n-1$ so, altogether, the space with a twofold ground-state degeneracy is of dimension n^2-3. The codimension is 3 and is independent of n. [For an alternative derivation, see Avron and Simon (1978).] It has $n-1$ components. More generally, the space of Hermitian matrices with m-fold degeneracy has $n-m+1$ components with codimension given by[22]

$$(m-1)+\dim \mathrm{U}(m)-m\dim \mathrm{U}(1)=m^2-1\ . \tag{7.11}$$

Thus the $n-1$ components with twofold degeneracy are connected by "filaments" of codimension 8, with triplet degeneracies. The codimensions are independent of the size of the matrices and hold for operators that are limits of matrices and have *discrete* spectra. [For recent interesting mathematical developments on the crossing rule see Friedland *et al.* (1984).]

The von Neumann–Wigner theorem suggests that a family of operators depending on n parameters has eigenvalue crossings on a set of codimension 3 in parameter space. This is an ansatz. It is not a theorem, because the n-parameter family may be embedded in a special way in the space of all Hermitian matrices. In fact, when taken too literally, the ansatz has easy counterexamples.[23] The ansatz says that $D(P)$ is of codimension 3 and is a set of points in a three-flux network, lines in four-flux network, etc. We find that the ansatz holds for many networks, and when it fails, it does so for an identifiable and often interesting reason.

We have already mentioned the fact that $D(P)$ acts as a source of transport and that getting a handle on $D(P)$ is the major step in the calculation of $\langle g_{\mathrm{Ad}}\rangle(P)$. It is therefore natural to consider symmetric networks in which group-theoretic methods can be used to give information on $D(P)$ and P. Symmetric networks have a point symmetry group G associated with the graph. G induces representations on the vertices, edges, and faces, which we denote by $G(V)$, $G(E)$, and $G(F)$, respectively. $D(P)$ is invariant under $G(F)$. Points in the flux space that are invariant under a (nontrivial) subgroup of $G(F)$ are points of symmetry. Group theory can sometimes say something about crossings at symmetry points. Unfortunately, there is no guarantee that $D(P)$ is contained in the set of points of symmetry, as there may be accidental degeneracies.

As an illustration, consider the tetrahedral network. It is associated with the tetrahedral graph shown in Fig. 14. G is the tetrahedral group T_d, and its character table is given in Table I taken from Landau and Lifshitz (1977). $|V|=|F|=4$, $|E|=6$. The tight-binding Hamiltonian and the Alexander–de Gennes matrix with $\Phi\equiv 0$, or $\Phi=(\pi,\pi,\pi)$, are invariant under $T_d(V)$. [Take $\mathbf{a}(e)=\Phi$ for all edges.] Because the graph has fixed valence $|v|=3$, the eigenvalue problem for the tight-binding and the de Gennes–Alexander cases are related by Eq. (4.37).

By inspection one sees that the four-dimensional representation associated with the vertices has

$$\chi(C_2)=0,\quad \chi(C_3)=1,\quad \chi(E)=4\ ,$$
$$\chi(S_4)=0,\quad \chi(\sigma_d)=2\ . \tag{7.12}$$

So the four-dimensional Hilbert space decomposes according to

$$A_1+T_2\ . \tag{7.13}$$

This says that $\Phi=0$ and $\Phi=(\pi,\pi,\pi)$ have points of triple degeneracy. For $\Phi=0$ the nondegenerate subspace is $\lambda(1,1,1,1)$, $\lambda\in\mathbb{C}$ and is associated with the eigenvalue zero for the tight-binding Hamiltonian, and $\cos(k\,|\,e\,|\,)=1$ for the de Gennes–Alexander matrix. The triple degeneracy lies in the orthogonal complement to (1,1,1,1), with eigenvalue 4 in the tight-binding case and $\cos(k\,|\,e\,|\,)=-\frac{1}{3}$ for the de Gennes–Alexander case. At $\Phi=(\pi,\pi,\pi)$, in the gauge where all bonds are -1, the same vector is the top state, with eigenvalue 6 for the tight-binding case and $\cos(k\,|\,e\,|\,)=-1$ in the de Gennes–Alexander case. The triply degenerate state has eigenenergy 2 in the tight-binding case and $\cos(k\,|\,e\,|\,)=\frac{1}{3}$ in the de Gennes–Alexander case [cf. Eq. (4.35)].

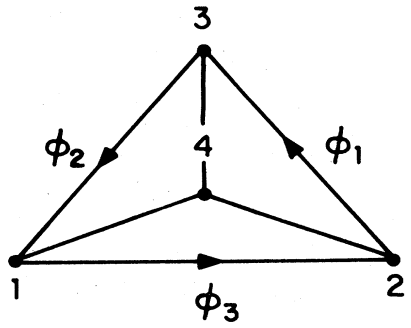

FIG. 14. The tetrahedral graph.

[22]In the case of real symmetric matrices the U(m) and U(1) in Eq. (7.11) are replaced by $O(m)$ and $O(1)$, respectively. This corresponds to the spin-zero, time-reversal-invariant situation. In the spin-$\frac{1}{2}$ time-reversal-invariant situation, Sp(m) and Sp(1) replace U(m) and U(1). This will be discussed in a forthcoming work of one of us (J.E.A.) with R. Seiler and B. Simon.

[23]Consider the Schrödinger equation on the line with potential $V(x;\phi)$, depending on n parameters ϕ so $V\to\infty$ at $|x|\to\infty$. The von Neumann–Wigner ansatz gives codimension 2 in this (real) case and clearly fails arbitrarily badly as the spectrum is simple for all ϕ due to a Wronskian identity.

TABLE I. Character table for the tetrahedral group.

T_d	E	$8C_3$	$3C_2$	$6\sigma_d$	$6S_4$
A_1	1	1	1	1	1
A_2	1	1	1	−1	−1
E	2	−1	2	0	0
T_1	3	0	−1	−1	1
T_2	3	0	−1	1	−1

Methods of group theory can also be used to reduce the matrix problem to smaller invariant spaces along symmetry lines. This can sometimes be used to compute explicitly the band functions along such symmetry directions. We shall see several applications of this in Secs. XII and XIII that permit analytic calculations of the crossing points as solutions to quadratic equations.

Finally, we want to recall that methods originally developed in the context of the Bloch theory of solids (Herring, 1937) can be used to tell when time reversal together with other symmetries implies level crossings.

Points of level crossings contain global spectral information. It turns out that for the tetrahedron they occur at symmetry points, so the global character of the problem is taken care of by symmetry. The global aspect of the problem is also the hard part of the analysis. Networks with no symmetry can therefore only be analyzed numerically. Even for networks with symmetry, where group-theoretic methods give some crossing points, there appears to be no way, except brute (numerical) force, to show that there are no other "accidental" points of level crossings. It would be useful to have "sum rules" that would indicate whether a set of crossings is complete or not. One set of such rules will be described in Sec. X.

VIII. GEOMETRY AND THE FORM CALCULUS FOR PROJECTIONS

We want to examine properties of the adiabatic transport $i\,\mathrm{Tr}[\omega(P)]$ of Eq. (6.13). The calculus involved is that of forms of projections. As pointed out by Bellissard (1986a), there is a relation to noncommutative geometry (Connes, 1969; Witten, 1986).

One important question that we have already raised in Sec. V, and that we address here is what transport properties depend only on the emf's and fluxes but not on other details about the flux tubes. From a mathematical point of view the answer turns out to be quite simple: transport is described by a closed two-form. A natural equivalence is to identify closed two-forms that differ by an exact form. This is the cohomology associated with the two-form, and, as we shall explain, it has the desired properties. In particular, it implies that the flux-averaged transport has this property. These, as well as related issues, are the subject of this section.

$i\,\mathrm{Tr}[\omega(P)]$ is a closed two-form. To see this, note that $P^2=P$ gives

$$P(dP)+(dP)P=dP,\quad P(dP)P=Q(dP)Q=0\ , \tag{8.1}$$

where $Q\equiv 1-P$. It follows that

$$\begin{aligned} &P(dP)^j=P(dP)^jQ,\quad j\ \text{odd}\ ,\\ &P(dP)^j=P(dP)^jP,\quad j\ \text{even}\ . \end{aligned} \tag{8.2}$$

Now, since $P^2=P$ and $d^2=0$, forms that are constructed from P and (dP) have the property that odd forms map P to Q and Q to P. In particular, the trace of any odd form vanishes. Since ω is an even form, $d\omega$ is an odd form, and so $d\,\mathrm{Tr}[\omega(P)]=0$.

Another interesting property of $\mathrm{Tr}[\omega(P)]$ is linearity. That is, if P_1 and P_2, as functions of the fluxes Φ, are mutually orthogonal, then

$$\mathrm{Tr}(\omega(P_1+P_2))=\mathrm{Tr}(\omega(P_1))+\mathrm{Tr}(\omega(P_2))\ . \tag{8.3}$$

This is remarkable because $\omega(P)$ is cubic in P. In view of Eq. (6.13), Eq. (8.3) may be interpreted as the additivity of the conductance for noninteracting fermions.

We want to consider different flux tubes, that carry the same fluxes, in the same basket. The Hamiltonians $H(\mathbf{A})$ and $H(\mathbf{A}')$ are unitarily equivalent, and so the corresponding projections are related by unitaries $U(\Phi)$. For the applications in Sec. XI we do not wish to exploit the full unitarity of U, and instead consider the more general setting where $P'\equiv UPU^\dagger$ and

$$U^\dagger U=1\ . \tag{8.4}$$

(We do not need to assume $UU^\dagger=1$ for the following calculation.) P' is a projection if P is. By explicit, tedious calculation,

$$\omega(P')=UP(\omega(P)+id\,(PVP)-(PVP)^2)PU^\dagger\ , \tag{8.5}$$

where, as before [cf. Eq. (2.5)], $V\equiv -iU^\dagger dU$. As a consequence

$$\mathrm{Tr}(\omega(P'))=\mathrm{Tr}(\omega(P))+id\,\mathrm{Tr}(PVP)\ . \tag{8.6}$$

$\mathrm{Tr}(\omega(P'))$ and $\mathrm{Tr}(\omega(P))$ differ by an exact form: a cohomology class is singled out. So, if we consider the transport two-form, $i\,\mathrm{Tr}(\omega(P))$, modulo exact forms, we get a transport property that is common to all flux tubes and depends only on the fluxes. We shall return presently to the question of what it means in practice to look at transport in cohomology. Before doing that, however, let us consider another important consequence of Eq. (8.6).

The gauge fields $\mathbf{A}$ and $\mathbf{A}'$ are linear in Φ. Therefore (locally) $U(\Phi)=\exp(i\Phi\Lambda)$, and $V=\Lambda\,d\Phi$ is a one-form that is independent of Φ. So, the Φ dependence of $(PVP)(\Phi)$ is determined by P. Now, from Sec. II we know that there are choices of flux tubes that make P periodic in flux space with a period of one flux unit. Any other choice of flux tubes is related to this one by an appropriate $U(\Phi)$. For this choice, each of the two terms on the right-hand side of Eq. (8.6) is periodic in Φ and so is the left-hand side. We conclude that the adiabatic transport $i\,\mathrm{Tr}(\omega(P))$ is periodic for all flux tubes [even those for which the Hamiltonian is not periodic, like Eq. (2.7)]. This establishes the fact that, for the adiabatic transport, flux space may be identified with the torus $\mathbb{T}^h$.

This may be viewed as a generalization of the Bohm-Aharonov periodicity, i.e., the Byers-Yang theorem, to a class of time-dependent problems.

How does one measure a cohomology class? The answer to this is suggested by de Rham theory (Flanders, 1963), which says that the study of periods is a way to study the cohomology. Consider a closed, two-dimensional surface C in that portion of flux space where P is smooth, i.e., in $\mathbb{T}^h/D(P)$. The Chern number associated with the projection P and the surface C is

$$\mathrm{ch}(P,C)\equiv\frac{1}{2\pi}\int_C i\,\mathrm{Tr}(\omega(P))\ . \tag{8.7}$$

By Stokes-Poincaré theorem (Arnol'd, 1978) this is an invariant in cohomology, i.e.,

$$\mathrm{ch}(P,C)=\mathrm{ch}(P',C)\ , \tag{8.8}$$

where $P'=UPU^\dagger$ and is real by Eq. (6.8). (It is actually an integer by a more complicated argument.) Also, if C is homologous to C' in $\mathbb{T}^h/D(P)$, then, by the closedness of ω (and Stokes-Poincaré theorem again)

$$\mathrm{ch}(P,C)=\mathrm{ch}(P,C')\ . \tag{8.9}$$

Of particular interest are two-dimensional sections of the torus $T_{kl}(\Phi)$ that do not intersect $D(P)$. Combining the definition of Eq. (8.7) with the basic formulas for the average transport, Eq. (6.15), we have

$$[\langle g_{\mathrm{Ad}}\rangle(P_j)]_{kl}=\mathrm{ch}(P_j,T_{kl}(\Phi))\ . \tag{8.10}$$

We see that the *average adiabatic transports* are properties of the cohomology class. They depend on the fluxes and emf's and are independent of the detailed fields generating them. We note, also, that from the periodicity in flux space the kl transport coefficient in Eq. (8.10) is a function of all Φ but Φ_k and Φ_l. So, in a two-flux network, the averaged transport coefficient is an antisymmetric 2×2 matrix of numbers (it is actually the zero matrix, as we shall see later), and in a three-flux network it is a 3×3 antisymmetric matrix whose entries are functions of one variable, etc.

$\mathrm{ch}(P,C)$ are topological invariants in the sense that they are independent of the details of the flux tubes and depend only on the fluxes. Actually, they are invariants in a stronger sense of deformations of the network Hamiltonian H. To see this, note that a general (self-adjoint) deformation of H can be decomposed into three "transversal" pieces: (1) deformations of the set of level crossings $D(P)$; (2) deformations of the spectrum that keep the spectral subspaces invariant; and (3) isospectral deformations, i.e., deformations of the spectral subspaces that keep the spectrum invariant. $\mathrm{ch}(P,C)$ is invariant under (1), for if C does not intersect $D(P)$, it also does not intersect a deformation of $D(P)$. $\mathrm{ch}(P,C)$ is invariant under (2), for $\omega(P)$ is invariant (it depends only on the projection P, not the energies E). Finally, isospectral deformations are given by unitaries and the invariance of $\mathrm{ch}(P,C)$ under these follows from Eq. (8.6).

We now recall the proof that $\mathrm{ch}(P,C)$ is an integer if P is one dimensional. [By Eq. (8.3) this extends to finite-dimensional P's that are deformations of sums of one-dimensional ones.] Let $C=C_1+C_2$, with $C_{1,2}$ contractible and $\gamma=\partial C_1=-\partial C_2$ (see Fig. 15). Since C_1 is contractible there is a choice of smooth phase for ψ_1 so that $P=|\psi_1\rangle\langle\psi_1|$. Then

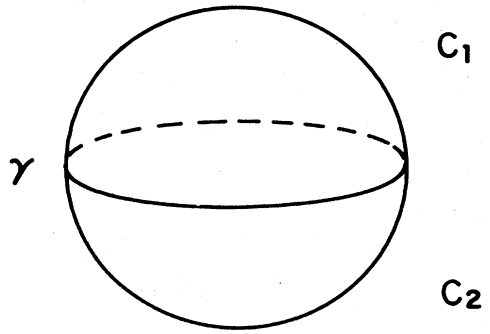

FIG. 15. A covering of a closed surface S^2 by two contractible surfaces with a common boundary γ.

$$i\int_{C_1}\mathrm{Tr}(\omega(P))=i\int_\gamma\langle\psi_1|\,d\psi_1\rangle\ . \tag{8.11}$$

The left-hand side is independent of the choice of (phase for) ψ_1 [see Eq. (7.1)]. The right-hand side is Berry's phase (Berry, 1984), associated with the parallel transport along the curve γ. Since the adiabatic evolution along γ is unique and is independent of whether we think of γ as the boundary of C_1 or of C_2, it must be that

$$\int_\gamma\langle\psi_1|\,d\psi_1\rangle=\int_\gamma\langle\psi_2|\,d\psi_2\rangle+2\pi i n\ , \tag{8.12}$$

with n integer. It follows that

$$\begin{aligned}\int_C\mathrm{Tr}(\omega(P))&=\int_{C_1}\mathrm{Tr}(\omega(P))+\int_{C_2}\mathrm{Tr}(\omega(P))\\&=2\pi i n\ ,\end{aligned} \tag{8.13}$$

proving the integrality.

We conclude by noting the physically obvious fact that there is no transport between the disconnected pieces of a network. Namely, if the loops l and m belong to disconnected pieces in the network, then $[\langle g_{\mathrm{Ad}}\rangle(P)]_{lm}=0$. To see this, choose a representation in which the Hamiltonian factorizes as

$$H_1(\Phi_1)\otimes1+1\otimes H_2(\Phi_2),\quad \Phi\equiv(\Phi_1,\Phi_2)\ . \tag{8.14}$$

This relation carries over to the projections and it makes $\omega(P(\Phi))$ vanish identically on any two-surface made of fluxes in disconnected components.

IX. TIME REVERSAL

Time reversal is the single most powerful tool in the analysis of networks. For Schrödinger operators, time reversal is the statement

$$H(\Phi)=U_0H^*(-\Phi)U_0^\dagger\ , \tag{9.1}$$

where U_0 is a fixed (Φ-independent) unitary. For spinless electrons, in a gauge where $H(\Phi=0)$ is real, and in the "coordinate representation," $U_0=1$. For spin-$\frac{1}{2}$ electrons in the same gauge and representation, $U_0=i\sigma_y$. It follows that

$$P(\Phi)=U_0P^*(-\Phi)U_0^\dagger\ , \tag{9.2}$$

and so

$$i\ \mathrm{Tr}(\omega(\Phi))=-i\ \mathrm{Tr}(\omega(-\Phi))\ . \tag{9.3}$$

We write $\omega(\Phi)$ for $\omega(P(\Phi))$. Equation (9.3) is Onsager's relation (Onsager, 1931).[24] It also follows from Eq. (9.2) that $D(P)$ is invariant under inversion:

$$D(P)=I[D(P)]\ , \tag{9.4}$$

where

$$I(\Phi)=-\Phi\ , \tag{9.5}$$

if one thinks of flux space as $\mathbb{R}^h$. If one thinks of flux space as $\mathbb{T}^h$, then Eq. (9.5) is interpreted modulo 2π.

From Eq. (9.3) we get

$$\mathrm{ch}(P_j,C)=-\mathrm{ch}(P_j,I[C])\ . \tag{9.6}$$

Let $T_{lm}(\Phi)$ be the lm slice of the torus in flux space passing through Φ. Then

$$I[T_{lm}(\Phi)]=T_{lm}(-\Phi)\ ; \tag{9.7}$$

see Fig. 16. Combining Eq. (8.10) with Eqs. (9.6) and (9.7) gives the antisymmetry of transport in the fluxes:

$$\langle g_{\mathrm{Ad}}\rangle(\Phi)=-\langle g_{\mathrm{Ad}}\rangle(-\Phi)\ . \tag{9.8}$$

This is a weaker version of Onsager's relation. (It is a statement about averages only.) In particular, in a network with only two fluxes, $\langle g_{\mathrm{Ad}}\rangle$ is a 2×2 matrix of numbers, and so zero. (Zero is the only antisymmetric number.)

Equation (9.8) makes certain periods vanish. Suppose that T_{lm} is a section that is invariant under inversion, e.g., the planes $\Phi_k=0$ ($\Phi_k=\pi$), $k\neq l,m$. If T_{lm} does not intersect $D(P)$ then, from Eq. (9.8),

$$\mathrm{ch}(P,T_{lm})=0,\quad T_{lm}=I[T_{lm}]\ . \tag{9.9}$$

If the two-torus T_{lm} intersects $D(P)$, the period is not defined. However, as we shall see, something can be said about this case as well.

We have already mentioned the fact that $D(P)$ acts as the source of charge transport. In a three-flux network $D(P)$ is, generically, a discrete set, and the "charge" of the point $\phi\in D(P)$ is defined by $\mathrm{ch}(P,S^2_\phi)$ where S^2_ϕ is a small two-sphere centered at ϕ (with outward drawn normal). Now, if $\phi\in D(P)$, $-\phi\in D(P)$ by Eq. (9.4), and[25]

$$I[S^2_\phi]=-S^2_{-\phi} \tag{9.10}$$

(see Fig. 17). Note the difference in the way inversion acts on the orientation of two-tori and two-spheres. Combining Eqs. (9.10) and (9.6),

$$\mathrm{ch}(P,S^2_\phi)=\mathrm{ch}(P,S^2_{-\phi})\ . \tag{9.11}$$

Degeneracies that are images of each other under inversion have *the same* charge.

We now return to sections of the torus that are invariant under inversion, $T_{lm}(\Phi)=I[T_{lm}(\Phi)]$, and intersect $D(P)$. Let $\hat n$ be the normal to the section. Then $I[T_{lm}(\Phi+\hat n\epsilon)]=T_{lm}(\Phi-\hat n\epsilon)$, and the translated sections will not intersect $D(P)$ for ϵ small. Therefore, their periods are well defined. From the closedness of $\omega(P)$ and Eq. (9.8) we obtain

$$\begin{aligned}\mathrm{charge}(T_{lm}(\Phi))&=(\mathrm{ch}(P,T_{lm}(\Phi+\hat n\epsilon))\\&\quad-\mathrm{ch}(P,T_{lm}(\Phi-\hat n\epsilon))\\&=2\,\mathrm{ch}(P,T_{lm}(\Phi+\hat n\epsilon))\ .\end{aligned} \tag{9.12}$$

Thus such planes are evenly charged. We learn that in either case, whether the invariant planes are charged or not, the periods of their ϵ translates are determined by the charges on the invariant planes. We shall make use

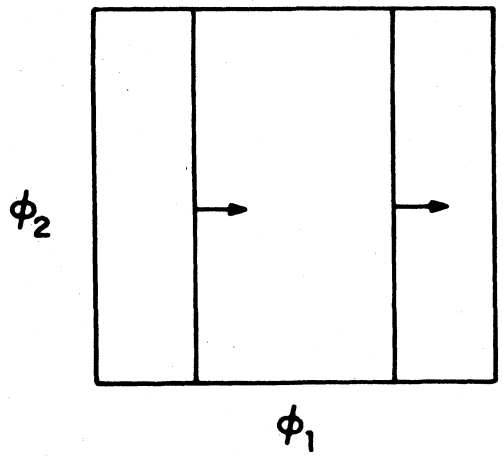

FIG. 16. The inversion of the section $T_{lm}(\Phi)$, with, say, $l=2$, $m=3$, is the lm section though $-\Phi$ with the same orientation, i.e., $T_{lm}(-\Phi)$.

[24]Strictly speaking, Eq. (9.3) is only a statement about the *adiabatic transport*, defined in Sec. VI. Whether it also applies to the physical transport depends on how well the two approximate each other. See the discussion in Sec. VI.

[25]To see why Eq. (9.9) holds, recall that the area form of the n-sphere is

$$\sum_j(-)^{j+1}\frac{x_j}{|x|}dx_0\wedge\cdots\wedge dx_{j-1}\wedge dx_{j+1}\wedge\cdots\wedge dx_n\ .$$

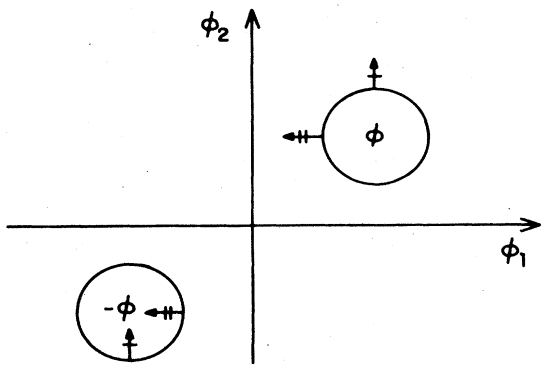

FIG. 17. The inversion on an even sphere at ϕ is a sphere at $-\phi$ but with reversed orientation.

of this fact in the next section.

Here we have considered the action of time reversal alone. Of course, time reversal is more powerful when combined with other symmetries (Herring, 1937).

X. CLASSIFICATION OF THREE-FLUX NETWORKS

The transport properties of three-flux networks with discrete $D(P_j)$'s are determined by the charges $\mathrm{ch}(P_j,S^2_\phi)$, $\phi\in D(P_j)$. This information can be arranged in tables that list the coordinates of the various charges. The corresponding matrix of average transport functions $\langle g_{\mathrm{Ad}}\rangle(P_j)$ can then be read directly from the table, as we shall proceed to explain. Toward the end of this section we introduce various notions of stability of the topological conductance and define n-type and p-type networks.

The set of Chern numbers $\{\mathrm{ch}(P,C)\}$ for all spectral projections P and all closed two surfaces C has a linear structure, so it is enough to have the periods for bases of the projections and bases, in the sense of homology, for surfaces in $\mathbb{T}^3/D(P)$. We first discuss the choice of a basis for the spectral projections. The point we want to make is that the first natural choice is actually not the best. That is, taking P_j to be the projection on the jth eigenvalue, so that j is an energy label, is bad because it contains redundant information: $D(P_j)$, $D(P_{j+1})$, and $D(P_{j-1})$ are not independent. A better choice is to take P_j to be the projection on the spectrum for all energies below the jth gap. $D(P_j)$ is then related to the set where the jth gap closes and is independent of $D(P_k)$, $k\neq j$. In other words, it is better to take j to be a gap label rather than an energy label. This choice also turns out to be the right choice in other contexts (Johnson and Moser, 1982; Thouless, 1983; Dana, Avron, and Zak, 1985; Avron and Yaffe, 1986; Bellissard, 1986b; Kunz, 1986]. By Eq. (8.3), this choice makes $\mathrm{ch}(P_j,T_{jk}(\Phi))$ the matrix of average transport in the *ground state of the j-electron system.*

In the general case, j runs over the naturals. In the special case of tight-binding models, the Hilbert space is $\mathbb{C}^{|V|}$, so j runs on $1,\ldots,|V|$. In this case $P_{|V|}=1$, and the associated curvature vanishes identically. For this reason, in tight-binding models, it is enough to consider j in $1,\ldots,|V|-1$. A similar thing occurs for free electrons, as we shall explain below.

Now we come to picking a basis for the two-chains. If we let $z^{(2)}_j$ be the basis of the second homology of the torus in flux space with $D(P_j)$ removed, then, clearly, every closed two-chain $z^{(2)}$ can be written as a linear combination with integer coefficients

$$z^{(2)}=\sum_k n_k z^{(2)}_k \ , \tag{10.1}$$

up to homology, so the basic periods $\mathrm{ch}(P_j,z^{(2)}_k)$ determine all periods:

$$\mathrm{ch}(P_j,z^{(2)})=\sum_k n_k \mathrm{ch}(P_j,z^{(2)}_k) \ . \tag{10.2}$$

$H_2(T^3/D(P))$ is clearly spanned by three basic sections made of two-tori, T_{lm}, $l,m=1,2,3$, and $|D(P_j)|$ spheres S^2_ϕ that surround the points ϕ in $D(P_j)$. This seems to suggest that, given j, one needs $|D(P_j)|+3$ periods. Actually, time reversal leads to relations between the periods, so only the "charges" are needed. In fact, not even all the charges are needed, as it is enough to have those in the half-torus, as we proceed to explain.

The three periods associated with slicing the torus can be disposed of. Choose a slice that is invariant under inversion, e.g., take the slice through 0 or π. If this slice happens to intersect $D(P)$, the relevant period is that of an ϵ-translate which does not intersect $D(P)$. Then, as discussed in Sec. IX, the period is half the charge on the invariant slice. In particular, it is zero if the invariant slice does not intersect $D(P)$, so the charges determine the periods of three basic sections of the torus.

The adiabatic transport $\langle g_{\mathrm{Ad}}\rangle(P_j)$ is now determined, for all Φ, by translating the above planar slices, picking up the charges swept in this process. We conclude that the charges determine the transport.

Not all the charges are, however, independent. By Eq. (9.11), the periods of S^2_ϕ and $S^2_{-\phi}$ are the same, so it is enough to know the periods in half of the torus, say, $0\leq\Phi_1<\pi$. Finally, even the charges in half the torus are not completely independent, for their total charge is zero. To see this, observe that the charge of half the torus is half the charge of the full torus, by Eq. (9.11). The charge in the total torus is, however, easily seen to be zero from the periodicity of $\langle g_{\mathrm{Ad}}\rangle$.

The charges provide an efficient way of displaying the transport properties. More interesting is that the charges "localize" the problem: the charge at ϕ is a local property of the bundle associated with P and can be computed from properties of the Hamiltonian near ϕ by methods of perturbation theory. In practice this means that it is only necessary to diagonalize the Hamiltonian at the point ϕ itself. This is an improvement over Eq. (6.14), which requires diagonalizing the Hamiltonian on a planar section of the torus, and so requires global information on the bundle. (Of course, one still needs to know

where the eigenvalues cross, and this involves global information.)

We illustrate this with an example. Consider an isolated two-level crossing, and let $h(\Phi)$ be as in Eq. (7.2a). The map from the space of 2×2 self-adjoint matrices to $\mathbb{R}^3$ given by

$$\epsilon(\Phi)=\tfrac{1}{2}\,\mathrm{Tr}(h(\Phi)\sigma) \tag{10.3}$$

has $\epsilon(\phi)=0$, but $\epsilon(\Phi)\neq 0$ for Φ on a small sphere surrounding ϕ. This is a consequence of the assumption that ϕ is an isolated degeneracy [see Eq. (7.3a)]. Equation (10.3) defines a continuous map from the two-sphere S^2_ϕ to $\mathbb{R}^3/0\sim S^2$. (Here $\sim$ denotes equivalence in homotopy.) Such maps are characterized by their degree (Dubrovin *et al.*, 1984), and, as we shall now show, the degree is $-(charge)$.

From Eq. (7.4) the projection P_- associated with the gap is

$$P_-(\Phi)=\tfrac{1}{2}[(1-\hat{\epsilon}(\Phi)\cdot\sigma)]\ , \tag{10.4}$$

and by Eq. (6.7) the curvature is

$$\begin{aligned}\omega(P_-)&=\mathrm{Tr}[P_-(dP_-)(dP_-)P_-]\\&=-\tfrac{1}{8}\,\mathrm{Tr}[\sigma\cdot\hat{\epsilon}(\sigma\cdot d\hat{\epsilon})(\sigma\cdot d\hat{\epsilon})]\\&=-\frac{i}{4}\hat{\epsilon}\times d\hat{\epsilon}\cdot d\hat{\epsilon}\ .\end{aligned} \tag{10.5}$$

In the second step we used $\mathrm{Tr}(dP\,dP)=d\,\mathrm{Tr}(P\,dP)=d\,\mathrm{Tr}(P\,dP\,P)=0$. Therefore the charge is

$$\begin{aligned}\mathrm{ch}(P_-,S^2_\phi)&=\frac{1}{2\pi i}\int_{S^2_\phi}\omega(P_-)\\&=-\frac{1}{8\pi}\int_{S^2_\phi}\hat{\epsilon}\times d\hat{\epsilon}\cdot d\hat{\epsilon}\ .\end{aligned} \tag{10.6}$$

The right-hand side is $-(degree)$ of the map from the two-sphere S^2_ϕ, to the two-sphere $\hat{\epsilon}(\Phi)$.

In this way, the averaged conductances can be computed by diagonalizing the Hamiltonian for a discrete set of points $D(P)$. Equation (10.6), however, still involves integration. In numerical calculations integrals may be tedious, so it is nice that, in the generic situation, calculating the degree actually reduces to computing the determinant of a single 3×3 matrix. This observation, made in a related context, is due to Simon (1983). Consider the linearized map of Eq. (7.6). Its determinant is the Jacobian of the transformation from Φ space to ϵ. The degree is the sign of the Jacobian. It follows that

$$\mathrm{ch}(P_j,S^2_\phi)=-\mathrm{sgn}\det(\nabla\otimes\epsilon)\ . \tag{10.7}$$

This formula holds only if $\det(\nabla\otimes\epsilon)\neq 0$. If the determinant vanishes, the degree is not determined by the linearized map and could be *any* integer: $0, \pm 1, \pm 2$, etc. It would be useful to have formulas that would cover some of the cases in which the degree is not determined by the linearized map.

The bundles that arise in the study of the reduced free-electron problem admit a similar analysis, but turn out to have more structure. We recall that the relevant line bundle $\psi_j(\Phi)$ satisfies Eq. (4.29) for an appropriate $\cos[k_j(\Phi)]$.

By analogy with the previous case, let $\nabla\otimes\epsilon$ denote the linearized map from (k,Φ) to (ϵ_0,ϵ) in Eq. (7.2b). If this map is of full rank, the analog of Eq. (10.7) is

$$\mathrm{charge}(k_0,\phi)=-\mathrm{sgn}\det(\nabla\otimes\epsilon)\ . \tag{10.8}$$

The bands of the tight-binding model with *zero on-site potential* have an analog of the "π-shift" invariance discussed in Eq. (4.35). It says that if (E,Φ) is in the spectrum, so is $(-E,\Phi+\pi F)$, and both have the same eigenvectors. As a consequence,

$$\mathrm{charge}(E,\phi)=-\mathrm{charge}(-E,\phi+\pi F)\ . \tag{10.9a}$$

The reason for the minus sign is that the "π shift" flips the sign of the energy, and this flips the "projection below" to a "projection above." The graph-theoretic tight-binding models do not have this invariance, except in the case of regular graphs, for which similar considerations give

$$\mathrm{charge}(E,\phi)=-\mathrm{charge}(-E+2\,|\,v\,|,\phi+\pi F)\ . \tag{10.9b}$$

The band spectrum of the free-electron model also has the "π-shift" invariance, as discussed in Sec. IV, for both regular and irregular graphs. It says that $h_0(k,\phi)$ and $h_0(k+\pi,\phi+\pi\,|\,f\,|\,)$ have the same kernel. As a consequence,

$$\mathrm{charge}(k,\phi)=\mathrm{charge}(k+\pi,\phi+\pi F)\ . \tag{10.9c}$$

There is no sign change, in this case, for the ordering of energies is preserved by the map. Similarly, $h_0(k,\phi)$ and $h_0(2\pi-k,\phi)$ have the same kernel. This gives yet another relation for the charges:

$$\mathrm{charge}(k,\phi)=-\mathrm{charge}(2\pi-k,\phi)\ . \tag{10.9d}$$

As a consequence of Eqs. (10.9c) and (10.9d) it is clearly sufficient to list the charges with $k\in[0,\pi]$, rather than $[0,2\pi]$, and in this interval one has

$$\mathrm{charge}(k,\phi)=-\mathrm{charge}(\pi-k,\phi+\pi F)\ . \tag{10.9e}$$

The topological conductances of free electrons on a network with $|V|$ vertices, and edges of equal lengths, are periodic functions of the number of electrons with period $2|V|$ (and are antiperiodic with period $|V|$). This is a consequence of the reduction to a $|V|\times|V|$ matrix problem, which makes the eigenvectors independent of the quantum number n in Eq. (4.32). [Since the metric in Eq. (4.39) is not periodic in k, there is a gap in this argument that will be patched in the next section.] The $|V|$-electron system, like the no-electron system, has trivial transport. For the classification problem this means that the charge tables have to cover band indices $j\in 1,\ldots,|V|-1$.

This periodicity is interesting from another point of view. In networks with few loops and few electrons, one

may expect the topological conductances to be relatively simple functions, with few jumps from one integer to another, and of order unity. This should be the case, for there is no large number in the problem. However, in mesoscopic systems with few loops, the number of electrons can be quite large, and this could make the topological conductances complicated. In particular, large values and wild oscillations cannot be excluded *a priori*. For noninteracting electrons, we see that this is not the case, as the number of electrons is counted modulo $|V|$ and so is kept small. This suggests that the conductances should be "relatively simple."

Finally, we note that regular graphs have equivalent transport properties for the three models we have considered: the graph-theoretic tight-binding, the tight-binding with zero on-site potential, and the de Gennes–Alexander model. This follows from the fact that regular graphs, by definition, are such that $|v|$ is the same for all vertices. The two tight-binding models then differ by a constant, and the implicit and explicit eigenvalue problems are related by Eq. (4.37). Since the eigenvectors in the three dynamics are the same, the only distinction comes from the scalar product, which is different in the tight-binding and the free-electron cases. However, modulo a technical point that will be discussed in the next section, it is a basic feature of the Chern character that it is independent of the differential structure (i.e., the scalar product). This leads to the identity of the charges.[26]

An interesting aspect of the topological conductance concerns the issue of electrons and holes. In the Hall effect, electrons and holes are distinguished by comparing the direction of the actual current with the naive expectation that comes from analyzing the motion in crossed electric and magnetic fields. In networks there is also the possibility for both signs (the Chern number is not constrained to be of definite sign), and it is natural to try to classify networks by types as well, as a kind of generalization of the electron-hole concept (Avron, Seiler, and Shapiro, 1986). To do so, one has first to decide on a "naive expectation" and then to call the conductance electronlike if it agrees with that and holelike if it does not. In contrast with the Hall effect situation, where the "naive expectation" does not require any nontrivial quantum-mechanical calculation, in networks there appears to be no "naive expectation" in this sense.[27] It is natural to take the free-electron model for the network as a benchmark and call the conductances electronlike or holelike if they agree/disagree with the free-electron prediction. This definition, however, is conditioned on the stability and simplicity of the topological conductance, as we proceed to explain.

The free-electron model could, in principle, have complicated conductance functions as in Fig. 18(a), and the tight-binding model for the same graph could be as in Fig. 18(b). In such a case the tight-binding model is neither *n*-type nor *p*-type. The type is well defined if the graph of the topological conductance does not change signs too often. Simplicity of the graph is related to notions of stability that we proceed to formulate for three-flux networks.

We say that the *i-j* conductance is *flux stable* if it is of fixed sign for $\Phi_k \in (0,\pi)$. A network is *flux stable* if all pairs of the conductances are. If the free-electron network is nontrivial and flux stable, and if some other dynamics associated with the same graph is also flux stable and nontrivial, its type is well defined. If the dynamics leads to trivial transport, we say that it is insulating. (This definition fails in the case where the free-electron dynamics give zero topological conductance, and some other dynamics does not.)

Another stronger notion of stability is related to the stability of types when the number of particles is not fixed. We say that the *i-j* conductance is μ *stable* if it is flux stable and the sign is independent of the number of electrons.

A natural set of questions is the following.

(a) When are networks flux stable? General networks are expected not to be flux stable. However, as we shall see, all the nontrivial networks made of three equilateral triangles turn out to be flux stable.

(b) Are there simple rules for determining when a given dynamics leads to electronlike or holelike behavior?

(c) When are networks μ stable? Again, *a priori*, one expects that the sign of the conductance could depend on the number of electrons. As we shall see, eight out of nine three-flux networks turn out to be μ stable in the tight-binding dynamics. For such networks, the type is not affected by coupling to a bath with fixed chemical potential.

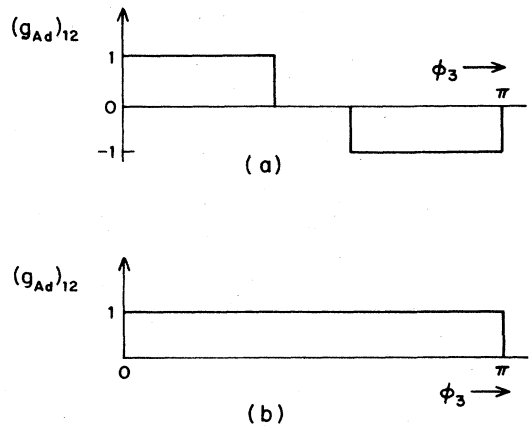

FIG. 18 The putative graphs of the topological conductances: (a) for the free-electron model; (b) for the tight-binding model. There is no natural way to decide whether the tight-binding model is *n*-type or *p*-type.

[26]We thank B. Simon for this observation.

[27]The "naive expectation" for a network made of ordinary resistors cannot be used to define types, for this gives a symmetric, instead of antisymmetric, matrix.

XI. CHERN NUMBERS: REDUCTION TO A MATRIX PROBLEM

One of the interesting aspects of the average conductances is that an object that arises in the study of certain partial differential operators can be computed reliably by studying finite matrices. In Sec. IV the partial differential Schrödinger equation was reduced to an ordinary differential equation in the limit of thin wires. For most questions the ordinary differential equation is only an approximation. The average conductances, being topological invariants, are insensitive to deformations, so the ordinary differential equation result is exact if the wires are sufficiently thin and one is not too close to level crossings.[28] A further reduction, from the ordinary differential equation to a matrix problem on the vertices, involves no further approximation. Since a wave function on the vertices determines the wave function on the edges, it is clear that computing the conductances of the network is a matrix problem.

Our purpose here is twofold. First, we want to describe explicit formulas for the *unaveraged* conductances that apply directly to the matrix problem. This requires the right Riemann metric (i.e., scalar product) in the matrix space, which is induced from the Hilbert space metric. Second, we want to close a gap in an argument made in the last section, that is, to complete the proof that the averaged conductances, i.e., the Chern numbers, can be computed directly from the matrix problem without regard to the "right" metric, using, for example, the usual "flat" scalar product.

Let $e=(u,v)$ be an edge with vertices u and v. Let ψ be the wave function on the vertices with components $\psi(v)$. Fix the edge e. Define a linear map $T(k)$ from $\mathbb{C}^{|V|}$ to $\oplus L^2(e)$ by

$$(T(k)\psi)(x,e)\equiv\frac{\exp[i\mathbf{a}(e,x)]}{\sin(k\,|e|)}\{\psi(u)\sin[k(|e|-x)]+\psi(v)\exp[-i\mathbf{a}(e)]\sin(kx)\}\ . \tag{11.1}$$

Using this map one can write the curvature two-form in Eq. (6.12) in terms of the de Gennes–Alexander $|V|$ vector. This yields direct, although somewhat longish, formulas for the curvature in terms of these $|V|$ vectors.

$T^\dagger(k)$, the adjoint of $T(k)$, is a linear operator from the range of $T(k)$ to $\mathbb{C}^{|V|}$ such that

$$T^\dagger(k)T(k)=1\ . \tag{11.2}$$

$TT^\dagger$ is not the identity, but because of Eq. (11.2) it is a projection. We apply Eq. (8.6) with

$$\begin{aligned}&P'\equiv T(k)PT^\dagger(k),\quad V\equiv -iT^\dagger(k)dT(k)\ ,\\ &\mathrm{Tr}(\omega(P'))=\mathrm{Tr}(\omega(P))+d\,\mathrm{Tr}(PV)\ .\end{aligned} \tag{11.3}$$

Equation (11.3) says that the curvature associated with the $|V|\times|V|$ projection matrix and the curvature associated with the projection in the $\oplus_E L^2(e)$ Hilbert space differ by an exact form in flux space $\mathbb{R}^h/D(P)$. In particular, to compute the *unaveraged conductance directly*, one may use Eq. (11.3) together with the $|V|\times|V|$ projection matrix $P(\Phi)$ of the Alexander–de Gennes problem. Because of the metric $M(k)$ of Eq. (4.40), P is related to the normalized eigenvector with eigenvalue 0 by

$$[P(\Phi)]_{uv}=\psi(u)\sum_{v'}\psi^*(v')[M(k)]_{v'u}\ . \tag{11.4}$$

Because of the metric $M(k)$, the actual computations are, of course, more involved. Similarly, one can write formulas in terms of eigenfunctions rather than projections.

For the computation of Chern numbers, however, one may use the flat metric. The issue at stake is whether (PV) in Eq. (11.3) is periodic in flux space. If so, the periods over the torus for the matrix, and the Hilbert space problem, are the same. The period for the matrix problem is a Chern number and by deformation argument it is independent of the metric, so it remains to show that PV in Eq. (11.3) is periodic.

From Eq. (11.1) it follows that

$$dT=i(d\mathbf{a}(x,e))(T\sigma_z)-|e|\,dk\cot(k\,|e|)T+dk\,T\begin{bmatrix}(|e|-x)\cot[k(|e|-x)] & 0\\ 0 & x\cot(kx)\end{bmatrix}, \tag{11.5}$$

from which we get

$$\int_e dx[T\psi]^*(x)[(dT)\varphi](x)=(\psi,[T^\dagger dT]\varphi)\ , \tag{11.6}$$

where $[T^\dagger dT]$ is a 2×2 Hermitian matrix with entries

[28] The same argument can be made about the tight-binding limit.

$$\sin^2(k\,|\,e\,|\,)(T^\dagger dT)_{11}=\int_e dx\,\sin^2[k(\,|\,e\,|\,-x)][\,i\,d\mathbf{a}(x,e)-|\,e\,|\,dk\,\cot(k\,|\,e\,|\,)+(\,|\,e\,|\,x)dk\,\cot(k\,|\,e\,|\,-x)]\,,$$

$$\sin^2(k\,|\,e\,|\,)(T^\dagger dT)_{12}=\int_e dx\,\sin^2[k(\,|\,e\,|\,-x)]\sin(kx)\exp[-i\mathbf{a}(e)]\times[-i\,d\mathbf{a}(x,e)-|\,e\,|\,dk\,\cot(k\,|\,e\,|\,)+x\,dk\,\cot(kx)]\,, \tag{11.7}$$

$$\sin^2(k\,|\,e\,|\,)(T^\dagger dT)_{22}=\int_e dx\,\sin^2(kx)[-i\,d\mathbf{a}(x,e)-|\,e\,|\,dk\,\cot(k\,|\,e\,|\,)-x\,dk\,\cot(kx)]\,.$$

The Φ dependence comes from the Φ dependence of k, dk, $d\mathbf{a}$, and $\exp(-i\mathbf{a})$. The first two are periodic in Φ by the noncrossing. The third is Φ independent, and the fourth is periodic, at least for the applications in Secs. XII and XIII. It follows that $[T^\dagger dT]$ is periodic. It is also smooth in Φ provided $\sin(k\,|\,e\,|\,)\neq 0$.

XII. NONTRIVIALITY: THE HOLES EFFECT

The general structure in the preceding sections is consistent with $\langle g_{\rm Ad}\rangle=0$ identically. A basic question, therefore, is whether there are nontrivial networks. Our original interest in networks came from our interest in the Hall effect and so did much of our early intuition about what one should expect. The first networks we looked at were two-flux networks, because they are the simplest, and because the Hall effect also has two loops. Not surprisingly they were all found to be trivial for the same reason that there is no Hall conductance in zero magnetic field, namely, time reversal. One needs a third loop and a third flux to play the roles of the crystal and magnetic field. Next, we looked at three-flux networks. The first was that of Fig. 19, which looks like the Hall effect expect that a hole replaces the Hall sample and Φ_3 replaces the magnetic field B. This graph is nonplanar and the associated tight-binding model was indeed found to be nontrivial. However, as we subsequently realized, nonplanarity is not essential for nontriviality, and neither is the close correspondence with the Hall effect. In fact, nontrivial networks appear to be "generic." Here we focus on one particular planar network that is a close relative of Fig. 19 and that is shown in Fig. 20. We dub it the holes graph. We present the analysis of the tight-binding and the free-electron models for this graph.

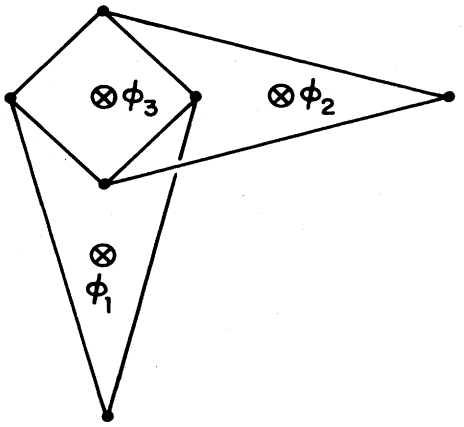

FIG. 19. A three-loop graph that mimics the Hall effect and whose corresponding tight-binding model is not trivial.

One reason for singling out the holes graph is historical: this was the first graph we analyzed in detail. From a textbook, didactic point of view this is an unfortunate choice for, as it turns out, this is a complicated model. The tetrahedron and the gasket of the next section are symmetric graphs, and this simplifies the analysis. So the holes graph is actually a typical representative of the harder, low-symmetry, models. A reader who would rather first study a model that can be analyzed in a few lines of calculation is referred to the subsection on the tetrahedron in the next section. With the graph we associate two dynamics: the (graph-theoretic) tight-binding and the free-electron dynamics. Since the graph is not regular, there is no reason why the dynamics should coincide, and a meaningful comparison of the transport properties can be made. In particular, as we shall see, both lead to nontrivial (topological) transport.

We shall first describe the numerical and analytical methods involved and the way the results will be presented. The same methods and conventions hold in the next section, where results for a whole batch of graphs are given.

As we have explained in Sec. X, the hard part of the problem is the global piece of isolating level crossings.

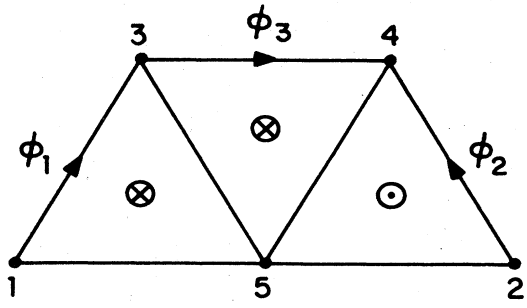

FIG. 20. The graph of the holes effect. ⊗ and ⊙ denote fluxes going into and out of the plane. The gauge field is chosen so that a phase Φ_1 is associated with the edge (1,3), Φ_2 with the edge (2,4), and Φ_3 with the edge (3,4). The graph has five vertices, seven edges, and three loops.

The two main tools are numerical method and the application of symmetry principles. The numerical method is, of course, quite powerful as it applies to general graphs, and is easily adaptable from one network to another. We have used the two methods in tandem, in the sense that the numerical results often suggested analytic derivations. Let us first describe the main features of the numerical analysis of networks.

Isolating the points of degeneracies is not trivial from a numerical point of view, because the finite numerical accuracy may blur a true degeneracy with near avoided crossing. One way to test for degeneracies is to compute the Chern number associated with small spheres or cubes. This is the complex version of an idea proposed many years ago by Herzberg and Longuet-Higgins (1963) and Longuet-Higgins (1975) in the real case. (In the real case the sphere is replaced by a circle, and the two-form by a one-form associated with adiabatic transport.) If the charge is nonzero, there is at least one degeneracy there; if it vanishes, no firm conclusion can be made. So, in principle, it is possible to divide the unit cell in flux space into small cubes and compute the charge of each cube by an appropriate surface integral. In practice this method is very expensive in computer time, for the unit cell has to be divided into many cubes if the degeneracy is to be identified with some precision. Further, each of the small cubes has to be wrapped by a fine mesh for the surface integrals. The mesh has to be fine enough so that the surface integral is close to an unambiguous integer. And finally, the integrand requires diagonalization of the Hamiltonian at every point of the mesh. A typical CPU time for such an integral, for a five-vertex network on an IBM 3081D, is on the order of 1000 sec. Instead of this systematic but time-consuming procedure we have used a simpler method that suggests where points of level crossings may lie. Once these were isolated, their charges were computed by surface integrals. We then checked that we did not miss charges by computing Chern numbers for many planar slices of the unit cell.

We looked for degeneracies by directly examining the smoothness of the projection. If we divide the cube with a mesh of size ϵ, then normalized eigenvectors away from a degeneracy satisfy

$$|\langle\psi_j(\Phi)|\psi_j(\Phi+\epsilon)\rangle| = 1-O(\epsilon^2)\ . \tag{12.1a}$$

Near a degeneracy the projection need not be close to 1. For example, if a diabolic crossing is midway between Φ and $\Phi+\epsilon$, then [see Eq. (7.4)] $\langle\psi_j(\Phi)|\psi_j(\Phi+\epsilon)\rangle = O(\epsilon^2)$. In general one has

$$|\langle\psi_j(\Phi)|\psi_j(\Phi')\rangle| = \tfrac{1}{2}[1+\hat{e}(\Phi)\cdot\hat{e}(\Phi')]\ , \tag{12.1b}$$

with a "typical value" of order $\frac{1}{2}$. We chose a sequence of $\epsilon_j = 2\pi/(3\times 2^j)$, $j=1,\ldots,10$ and computed the overlap in Eq. (12.1) for successive ϵ_j if the overlap was not close enough to 1. Once a small cube with a possible degeneracy was identified, its charge was used to decide on crossing.

The charges have been computed numerically as a surface integral using a formula that is equivalent to Eq. (8.7). [Since standard programs for diagonalization of matrices yield eigenvectors rather than projections, it proved convenient to write the analog of Eq. (8.7) in terms of eigenfunctions.]

The symmetry principles can be applied only on a case-by-case basis. For the holes graph the permutation of the vertices

$$U=(12)(34)(5)\ , \tag{12.2a}$$

implementable as a unitary transformation on the Hamiltonian, is equivalent to

$$(\Phi_1,\Phi_2,\Phi_3)\rightarrow(\Phi_2,\Phi_1,-\Phi_3)\ . \tag{12.2b}$$

The set of points in flux space that are left invariant under the combined action of U and time reversal defines "symmetry" points. They lie on two planes, which turn out to play a special role. The planes are

$$(\Phi_1,-\Phi_1,\Phi_3),\quad(\pi-\Phi_1,\pi+\Phi_1,\Phi_3)\ . \tag{12.3}$$

Another set of symmetry points are those that are left invariant under the action of U alone. These lie on two lines, and these lines also play a special role. The lines are given by

$$(\Phi,\Phi,0),\quad(\Phi,\Phi,\pi)\ . \tag{12.4}$$

As we shall see, the symmetry points turn out to be the loci of level crossings in both the tight-binding and the free-electron models. Moreover, the symmetry can be used to reduce the Hamiltonian to invariant subspaces,

TABLE II. The charges for the tight-binding model corresponding to Fig. 20, the holes effect. Only the charges in the half-cube of flux space with ϕ_3 in $[0,\pi]$ are listed. They have identical inversion images. $\cos(\pi\alpha)\equiv\frac{1}{2}-\sqrt{2}$ or $\alpha\sim 0.867$.

No.	ϕ/π	E	Gap	Charge	Multiplicity
1	$(\frac{2}{3},-\frac{2}{3},\frac{1}{3})$	1	1	−1	2
2	$(\frac{2}{3},\frac{2}{3},1)$	1	1	1	2
3	$(\alpha,-\alpha,\alpha/2)$	$3-\sqrt{2}$	2	1	2
4	$(\alpha,\alpha,0)$	$3-\sqrt{2}$	2	−1	2
5	$(-\frac{2}{3},\frac{2}{3},\frac{2}{3})$	3	3	−1	2
6	$(\frac{2}{3},\frac{2}{3},1)$	3	3	1	2

where the eigenvalue equations can be solved analytically, as we shall see below.

Following the classification scheme described in Sec. X, we collected the results in a single table. Table II describes the results for the tight-binding dynamics and Table III those for the free-electron dynamics. The tables are organized as follows. The coordinates of the crossings are listed under ϕ. E is the corresponding degenerate energy. The gap that closes at this degeneracy is listed under "gap." Gap 2 means that the second and third levels cross at that point. Gap index j describes the transport properties of the j-electron system in the ground state. By general principles (see Sec. X), it is sufficient to consider $j=1,\ldots,|V|-1$.

With each point listed in the table one can associate a cluster of points by symmetry operations. For the holes graph there is a quadruplet associated with U and time reversal. All the points in such a cluster have identical charges. In the tables, we denote by *multiplicity* the number of *distinct* points in the torus obtained by applying these symmetry operations. The numbering in the first column is arbitrary, but we have grouped crossings according to their gap index.

The data in the tables are a mixture of numerical results and analytic calculations in the following sense. The coordinates of degeneracies (and sometimes the charges, too) are analytic statements. However, the claim that there are no other degeneracies is based on numerical evidence.

The (graph-theoretic) tight-binding Hamiltonian corresponding to the graph of Fig. 20 is

$$H(\Phi)=\begin{bmatrix} 2 & 0 & -e^{i\Phi_1} & 0 & -1 \\ 0 & 2 & 0 & -e^{i\Phi_2} & -1 \\ -e^{-i\Phi_1} & 0 & 3 & -e^{i\Phi_3} & -1 \\ 0 & -e^{-i\Phi_2} & -e^{-i\Phi_3} & 3 & -1 \\ -1 & -1 & -1 & -1 & 4 \end{bmatrix} . \tag{12.5}$$

Because the Hamiltonian is 5×5, the eigenvalue equation, $\det[H(\Phi)-E]=0$, can be written out analytically with a finite amount of human effort. Although this computation can be done "by hand" it is actually easier, and possibly safer, to compute it mechanically using one of several available formal manipulation programs. (We have used REDUCE.) The result is

$$\begin{aligned}\det[H(\Phi)-E]=&-E^5+14E^4-70E^3+152E^2-137E+38-2((2-E)(3-E)-1)[\cos(\Phi_1)+\cos(\Phi_2)]\\&-2(2-E)^2\cos(\Phi_3)-2(2-E)(\cos(\Phi_1+\Phi_3)+\cos(\Phi_2-\Phi_3))-2\cos(\Phi_1-\Phi_2+\Phi_3) .\end{aligned} \tag{12.6a}$$

Points of (double) degeneracy are the simultaneous zeros of this and

$$\begin{aligned}&\frac{d}{dE}\det[H(\Phi)-E]=0 ,\\ &\frac{d}{dE}\det[H(\Phi)-E]=-5E^4+56E^3-210E^2+304E-137+2(5-2E)(\cos(\Phi_1)+\cos(\Phi_2))\\&\qquad+4(2-E)\cos(\Phi_3)+2(\cos(\Phi_1+\Phi_3)+\cos(\Phi_2-\Phi_3)) .\end{aligned} \tag{12.6b}$$

TABLE III. The charges for the free-electron model associated with Fig. 20, the holes effect. Only the charges in the sections ϕ_3 and k in $[0,\pi]$ are listed. There are identical charges at flux-inverted points, and opposite ones at $2\pi-k$. $\phi_1/\pi\sim0.6824$, $\phi_2/\pi\sim0.4299$, $\phi_3/\pi\sim1.6618$, $\phi_4/\pi\sim0.051$.

No.	ϕ	$\cos(k)$	Gap	Charge	Multiplicity
1	$(\pi-\phi_1,\pi-\phi_1,0)$	$\frac{-1-\sqrt{7}}{6}$	1	1	2
2	$(\pi-\phi_1,-\pi+\phi_1,\pi-\phi_2)$	$\frac{-1-\sqrt{7}}{6}$	1	−1	2
3	(ϕ_3,ϕ_3,π)	$\frac{1-\sqrt{7}}{6}$	2	−1	2
4	$(\phi_3,-\phi_3,\phi_4)$	$\frac{1-\sqrt{7}}{6}$	2	1	2
5	$(\pi-\phi_3,-\pi+\phi_3,\pi-\phi_4)$	$\frac{-1+\sqrt{7}}{6}$	3	−1	2
6	$(\pi-\phi_3,\pi-\phi_3,0)$	$\frac{-1+\sqrt{7}}{6}$	3	1	2
7	$(\phi_1,-\phi_1,\phi_2)$	$\frac{1+\sqrt{7}}{6}$	4	1	2
8	(ϕ_1,ϕ_1,π)	$\frac{1+\sqrt{7}}{6}$	4	−1	2

Equations (12.6a) and (12.6b) for the degeneracies have the following obvious symmetries. If $(\boldsymbol{\phi}_j, E_j)$ is a solution, so is $(-\boldsymbol{\phi}_j, E_j)$, and if $(\phi_1, \phi_2, \phi_3, E_j)$ is a solution, so is $(\phi_2, \phi_1, -\phi_3, E_j)$.

The advantage of having explicit formulas like Eqs. (12.6a) and (12.6b) is not so much for finding the solutions, since, in general, this can be done only numerically. Originally, the entries in the table were derived by combining the numerical results with guesswork, which was then verified by substitution in Eq. (12.6). With reasonable numerical accuracy, the coordinates and energy of the crossings at points 1, 2, 5, and 6 suggest a natural guess. For points 3 and 4 the key turned out to be the guess for the energy. Equation (12.6b) then gives a linear equation for one unknown, $\cos\pi\alpha$.

As we subsequently realized, much of the guesswork can be replaced by group theory. This approach also revealed a remarkable property of the band functions, namely, that there are "flat bands" on the symmetry lines, Eq. (12.4), whose energy is independent of Φ. The energy values for these flat bands are given by the solution of quadratic equations. The crossing points can then be computed from Eq. (12.6b). In this way one gets the entries in the table, as we now proceed to explain.

Consider the symmetry lines in Eq. (12.4). The invariant subspaces under U are

$$\begin{aligned} &\text{I:}\ (\alpha_1, \alpha_1, \alpha_2, \alpha_2, \alpha_3)\ , \\ &\text{II:}\ (\alpha_1, -\alpha_1, \alpha_2, -\alpha_2, 0)\ . \end{aligned} \tag{12.7}$$

$\alpha_{1,2,3} \in \mathbb{C}$. I is a three (complex) dimensional space and II is two dimensional. Reducing the Hamiltonian of Eq. (12.5) to II gives a 2×2 eigenvalue problem, and the band functions on the symmetry lines of Eq. (12.4) are given as the solution of quadratic equations. The result is four flat bands:

$$E_{\rm II}(\Phi,\Phi,0) = 3 \pm \sqrt{2}, \quad E_{\rm II}(\Phi,\Phi,\pi) = 2 \pm 1\ . \tag{12.8}$$

The other three bands along these lines are given by a solution of a cubic equation. We do not know what the reason is for flat bands in this problem, but because of this the energies at crossings are known for three of the six points in the table. From Eq. (12.6a) the coordinates of points 2, 4, and 6 are given by a linear equation in $\cos(\Phi)$.

Some of the properties of Table II worth noting are as follows.

(1) In agreement with the von Neumann–Wigner ansatz one finds that the simultaneous solutions of Eq. (12.6a) and Eq. (12.6b) are a discrete set $\{(\boldsymbol{\phi}_j, E_j)\}$. $D(P)$ is then the union over j of $\{\boldsymbol{\phi}_j\}$.

(2) For each gap index, the total charge, counting multiplicity, is zero. This is the neutrality of the cube in flux space proven in Sec. X. It gives $|V| - 1$ sum rules that check for the completeness of the set of crossings.

(3) For each gap index, planes with constant Φ_1 or constant Φ_2 are neutral. Such planes either avoid all charges or contain four charges that neutralize in pairs. We discuss a consequence of this for the conductance below. This property is presumably unstable under perturbations.

(4) Generically, one expects only $\pm$ charges. This is the case here. However, because of the symmetry of the network it is not possible to argue for this on the basis of genericity alone.

As we have explained in the previous sections, once the degeneracies are known, the charges can actually be computed analytically. To make analytic calculations for the table would require further guesswork for the eigenvectors for one point in the table for each gap index. That is, three pairs of eigenvectors would need to be guessed. We have contented ourselves by making this calculation for the first gap, and verified that the analytic result agrees with the numerical result. We have chosen point 2 and describe below the computation of its charge.

Two independent eigenvectors with eigenvalue 1 of point 2, of Table II, are

$$\begin{aligned} |\psi\rangle &= (z_3, -z_3, 1, -1, 0)\ , \\ |\varphi\rangle &= (2, 1+z_3, z_3^*, 1, 1)\ , \end{aligned} \tag{12.9}$$

where $z_3 \equiv \exp(2\pi i/3)$ is the cubic root of unity. $|\psi\rangle$ and $|\varphi\rangle$ are neither normalized nor orthogonal. For our purpose all that matters is that they are independent. Restricting the Hamiltonian to the degenerate subspace, using Eqs. (7.8), gives

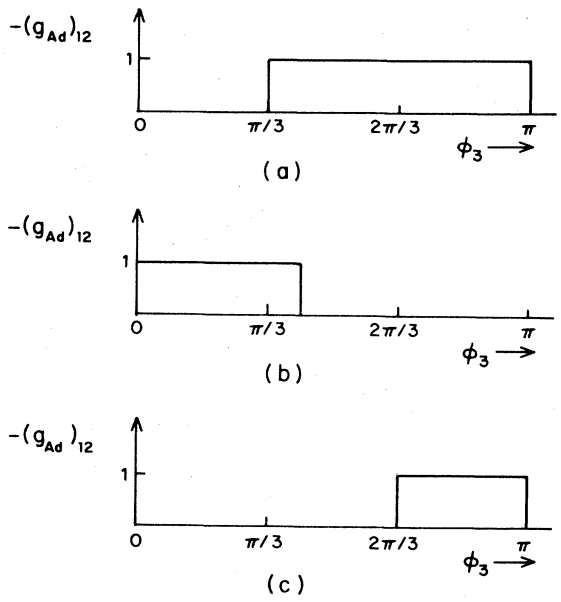

FIG. 21. The 1-2 conductances of the holes effect in the ground states for the tight-binding model of noninteracting (spinless) electrons: (a) the one-electron system; (b) the two-electron system, (c) the three-electron system. Since the graphs are periodic and antisymmetric, only half the period is shown. The four- and five-electron systems have vanishing conductances and are therefore not shown. The network is p-type, flux and μ stable.

$$d\epsilon_1=\frac{\sqrt{3}}{2}(d\Phi_1-d\Phi_2+d\Phi_3)\ ,$$
$$d\epsilon_2=\tfrac{1}{2}(-d\Phi_1+d\Phi_2+d\Phi_3)\ , \qquad (12.10)$$
$$d\epsilon_3=\frac{\sqrt{3}}{2}(d\Phi_2-d\Phi_3)\ .$$

The determinant of this map is $-\sin^2(2\pi/3)$, so the charge of point 2 is 1. From the neutrality of the cube we then learn that the change of point 1 is -1. This gives all the charges in the first gap.

From the table it follows that the average conductances [i.e., the periods of Eq. (8.10)] are as in Fig. 21. The three graphs correspond to the 1-2 conductances in (a) the one-electron ground state, (b) the two-electron ground state, and (c) the three-electron ground state. The four- and five-electron ground states have vanishing conductances. At most five electrons can be accommodated in the tight-binding Hilbert space for their network. That there are no charges associated with the five-electron ground state follows from general principles. However, that the four-electron ground state also has no charges is a special property of the holes graph and the tight-binding dynamics. We do not know the reason for that.

From the neutrality of the $\Phi_{1,2}$ sections of the torus, it follows that $[\langle g_{\rm Ad}\rangle]_{13}$ and $[\langle g_{\rm Ad}\rangle]_{23}$ vanish identically. This property is presumably unstable under perturbations.

Finally, we note that the conductances are flux stable, and μ stable in the sense of Sec. X.

With the holes graph we now associate the free-electron dynamics. The Alexander–de Gennes matrix $h_0(k,\Phi)$ corresponding to this dynamics, assuming a network with unit length links, is

$$\begin{bmatrix} 2\cos(k) & 0 & -e^{i\Phi_1} & 0 & -1 \\ 0 & 2\cos(k) & 0 & -e^{i\Phi_2} & -1 \\ -e^{-i\Phi_1} & 0 & 3\cos(k) & -e^{i\Phi_3} & -1 \\ 0 & -e^{-i\Phi_2} & -e^{-i\Phi_3} & 3\cos(k) & -1 \\ -1 & -1 & -1 & -1 & 4\cos(k) \end{bmatrix} . \qquad (12.11)$$

The eigenvalue equation is $\det[h_0(k,\Phi)]=0$, where

$$\begin{aligned}\det[h_0(k,\Phi)]=&\,144\cos^5(k)-124\cos^3(k)+4\cos^2(k)(-2\cos(\Phi_3)-3\cos(\Phi_2)-3\cos(\Phi_1))\\ &-2\cos(k)(2\cos(\Phi_3-\Phi_2)+2\cos(\Phi_1+\Phi_3)-9)\\ &+2(-\cos(\Phi_1-\Phi_2+\Phi_3)+\cos(\Phi_2)+\cos(\Phi_1))\ . \end{aligned} \qquad (12.12)$$

In contrast with the tight-binding network, which can accommodate only a finite number of electrons (five, in this case), the free-electron model can accommodate an arbitrarily large number of them. The spectrum and the conductances have a "trivial" dependence on the n quantum number of Eq. (4.32), so only the basic period, 5, associated with the quantum number j need be covered. Levels cross at those points in $[\cos(k),\Phi]$ that are simultaneous zeros of Eq. (12.14) and its derivative with respect to $\cos(k)$. The numerical results are summarized in Table III.

The free-electron Hamiltonian has flat bands along the symmetry lines of Eq. (12.4). Using this, the angles ϕ_j and $\cos(k)$ in Table III can be computed analytically. Reducing the matrix of Eq. (12.11) to the invariant subspace II of Eq. (12.7) gives two of the energy bands as solutions to a quadratic equation. The result is, again, four flat bands

$$\cos(k(\Phi,\Phi,0))=\frac{-1\pm\sqrt{7}}{6}\ ,$$
$$\cos(k(\Phi,\Phi,\pi))=\frac{1\pm\sqrt{7}}{6}\ . \qquad (12.13a)$$

From this, and the derivative of Eq. (12.12) with respect to $\cos(k)$, one derives analytic values for $\cos(\phi_{1,3})$ of Table III:

$$\cos(\phi_1)\equiv-\frac{7\sqrt{7}+1}{36}\ ,$$
$$\cos(\phi_3)\equiv\frac{-7\sqrt{7}+1}{36}\ . \qquad (12.13b)$$

Some further work gives

$$\cos(\phi_2)\equiv\frac{-31\sqrt{7}+164}{24(\sqrt{7}+13)}\ ,$$
$$\cos(\phi_4)\equiv\frac{31\sqrt{7}+164}{24(\sqrt{7}-13)}\ . \qquad (12.13c)$$

One can also compute the charges "by hand" when one does not have analytic expressions for crossing points and degenerate subspaces, provided one has approximate (i.e., numerical) vectors that span the degenerate subspaces. For example, for point 1 in Table III, a pair of degenerate vectors is

$$|\psi\rangle=(\alpha_1,\alpha_1,\alpha_2,\alpha_2,\alpha_3)\ ,$$
$$|\varphi\rangle=(-\alpha_4,\alpha_4,\alpha_5,-\alpha_5,0)\ , \qquad (12.14)$$
$$\alpha_1\sim0.3301,\quad \alpha_2\sim0.046+i0.138\ ,$$
$$\alpha_4\sim0.151-i0.234,\quad \alpha_5\sim0.338\ .$$

Using Eq. (7.8) one finds for the linearized map

$$\epsilon_2+i\epsilon_1=(e^{-i\phi_1}\alpha_1\alpha_5+e^{i\phi_1}\alpha_2^*\alpha_1)(-d\Phi_1+d\Phi_2) \\ -2\alpha_2^*\alpha_5 d\Phi_3 , \\ \epsilon_3=\mathrm{Im}(e^{i\phi_1}\alpha_1\alpha_2+\alpha_4^*\alpha_5)(d\Phi_1+d\Phi_2) . \tag{12.15}$$

The determinant of this map is negative, so the charge is $+1$. (Of course, with numerical values one finds a nonzero value for the determinant "with probability one." In numerical calculations the sign is not enough, and the actual numerical value has to be sufficiently far away from zero.) Charge neutrality then determines the charge of point 2, and the "π shift" of Eq. (10.9) that of points 8 and 9. These give half the entries in the table.

From the table one concludes that the corresponding graphs for the conductances are as in Fig. 22. The four graphs describe the 1-2 conductances in the ground state of the one-, two-, three-, and four-electron systems. In the five-electron system, the conductance vanishes in the ground state. For the next five electrons, the picture repeats itself up to reversal of signs and order, as discussed in Sec. X. With more electrons present, the picture repeats itself, with the number of electrons counted mod 10.

Comparing the results for the tight-binding and the de Gennes–Alexander realizations for this graph one finds similarities and differences. Many of the basic features are common: the conductances are flux stable; points of level crossing lie on the distinguished symmetry planes and lines; all charges are ± 1; and finally, planes with fixed Φ_1 or fixed Φ_2 are neutral, leading to the identical vanishing of the 1-3 and 2-3 conductances.

There are also differences, some expected, some not. One expected qualitative difference is that the free-electron model has the "π-shift" symmetry that is not shared by the (graph-theoretic) tight-binding model. Another (unexpected) qualitative difference is that there are no charges in the four-electron ground state in the tight-binding dynamics, but there are charges in the free-electron dynamics. There are also expected differences in details: the actual positions of crossings are distinct.

The tight-binding and the free-electron Hamiltonians are not close to each other in any sense, so the fact that their conductance graphs are distinct is not in conflict with anything. This suggests that an attempt to predict what would happen in actual settings may require a reasonably accurate modeling. Both models establish nontriviality. In fact, they do more, as they show that given a graph, nontriviality is not special to one dynamics. This suggests that more realistic and more complicated models corresponding to this graph also stand a good chance of being nontrivial.

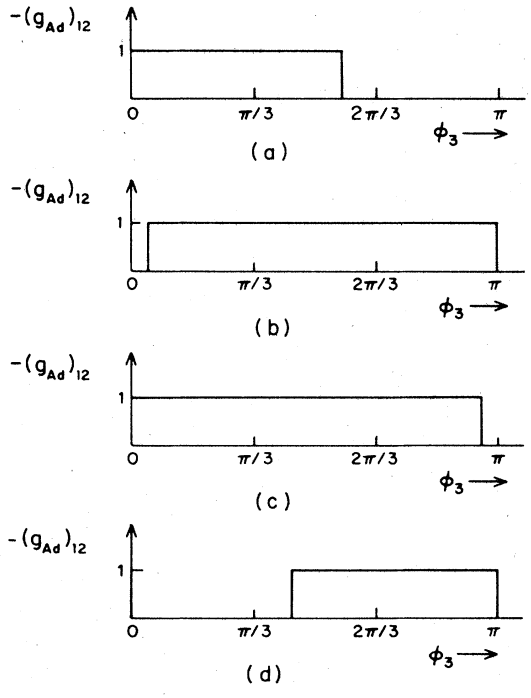

FIG. 22. The 1-2 conductances for free electrons on a network of thin wires associated with the holes effect graph: (a) The 1(mod 5)-electron systems; (b) the 2(mod 5)-electron systems; (c) the 3(mod 5)-electron systems; (d) the 4(mod 5)-electron systems. All graphs are for the ground-state conductances. The network is n-type (by definition) and is flux and μ stable.

XIII. THREE-FLUX NETWORKS OF EQUILATERAL TRIANGLES

In this section we collect results for a number of three-flux networks that correspond to the tight-binding Hamiltonians for various simple graphs. There are two reasons for this study. One is related to the question of stability of nontriviality, namely, that the graph of the holes effect considered in Sec. XII is not special. The second reason is a part of a larger program to try to gain insight into the Chern numbers that characterize various graphs and dynamics.

The simple graphs we consider are those that can be made with three equilateral triangles, 1, 2, and 3, carrying independent fluxes Φ_1, Φ_2, and Φ_3. Since, by general principles, disconnected networks are trivial, we consider only connected ones. There are six distinct planar graphs and three nonplanar ones. They are listed in Table IV. The planar graphs are shown in Fig. 23 and the nonplanar graphs in Fig. 24. The enumeration given in Table IV goes as follows. Since the network is connected, there is at least one triangle connected to the other two. Pick such a triangle and call it (tentatively) 2. Let $\#(i,j)$ be the number of common vertices of the ith and jth triangles. Clearly $\#(ij)<3$ if $i\neq j$, so

$$\#(1,2),\#(2.3)\in\{1,2\} .$$

TABLE IV. The nine distinct graphs that can be made with three equilateral triangles threaded by flux tubes. Six of the graphs are planar and three are not. Five have nontrivial topological conductances.

Name	Planar	$\{\#(1,2),\#(2,3),\#\}$	$\lvert V\rvert$	Trivial
windmill	Yes	1,1,1	7	Yes
Giza	Yes	1,1,2	7	Yes
gasket	Yes	1,1,3	6	No
wide kite	Yes	2,1,2	6	Yes
long kite	Yes	2,1,3	6	Yes
basket	No	2,1,4	5	No
tripod	No	2,2,2	5	Yes
holes effect	Yes	2,2,3	5	No
tetrahedron	No	2,2,4	4	No

Let 1 be the triangle such that $\#(1,2)\geq\#(3,2)$. This procedure may involve a choice for 2 if there are several triangles that connect the other two. In this case, we choose 2 so that $\#(1,2)$ is maximal.

The triplet $\{\#(1,3),\#(2,3),\#(1,2)\}$ determines a unique graph up to a possible two-fold ambiguity, which is removed by specifying $\lvert V\rvert$. A triplet that specifies a unique graph is

$$\{\#(2,3),\#(1,2),\#\}\ ,$$

where $\#$ is the number of vertices in the graph that belong to at least two triangles. The table is organized lexicographically in $\{\#(1,2)\#(2,3),\#\}$. The names are figments of our imagination.

Of the six planar networks, four are trivial in the sense that they do not have *isolated* crossing points, with nontrivial charges. They all have the property that the graphs are separable, in the graph-theoretic terminology, and one-particle reducible, in the Feynman diagram terminology. That is, the graphs are disconnected by cutting one vertex. In addition, the Wigner–von Neumann ansatz is not satisfied—the degeneracies lie on curves. Our numerical work suggests that these properties are stable under perturbations and are not a special property of equilateral triangles.

It therefore appears that the results proven at the end

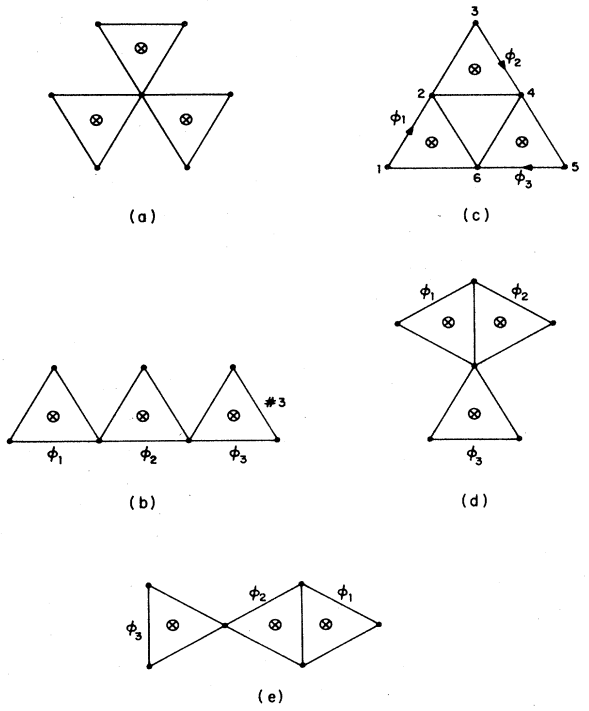

FIG. 23. The six planar graphs that can be made with three equilateral triangles: (a) the windmill; (b) the three pyramids of Giza; (c) the gasket; (d) the wide kite; (e) the long kite. The graph for the holes effect is shown in Fig. 20. We have numbered the fluxes and vertices only in those cases where such a numbering is important in the text.

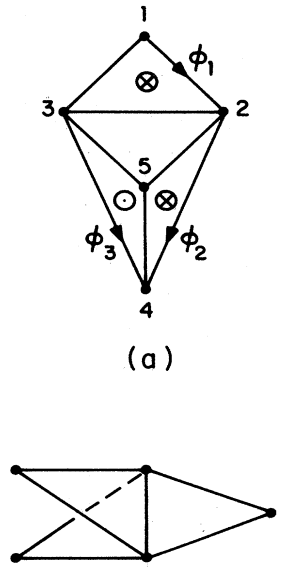

FIG. 24. Two of the three nonplanar graphs that can be made with three equilateral triangles; (a) the basket; (b) the tripod. The third, the tetrahedron, is shown in Fig. 14.

TABLE V. The charges for the tight-binding Hamiltonian for the gasket, Fig. 23(c). Only the charges in the half-cube Φ in $[0,\pi]$ are listed. There are identical charges at points with the coordinates reflected about zero.

$(\phi/\pi)(1,1,1)$	E	Gap	Charge	Multiplicity
$\frac{2}{3}$	1	1	1	2
1	$\frac{7-\sqrt{21}}{2}$	1	−2	1
0	$\frac{7-\sqrt{13}}{2}$	2	2	1
0.824	1.454	2	−1	2
1	2	3	0	1
0	$\frac{7+\sqrt{13}}{2}$	5	2	1
1	$\frac{7+\sqrt{21}}{2}$	5	−2	1

of Sec. VIII about disconnected graphs has a generalization to separable graphs. However, we do not know of a proof in general. Separability together with symmetry can be used to show that *some* periods vanish. For example, for the three pyramids of Giza, $\langle g_{AD}\rangle_{12}=\langle g_{AD}\rangle_{23}=0$ is a consequence of the following argument: $\langle g_{Ad}\rangle_{12}(\Phi_3)$ is antisymmetric in Φ_3 by the Onsager relation of Sec. IX. However, $\Phi_3\to-\Phi_3$ corresponds to permuting the two "free" vertices in triangle #3. This is implemented by a unitary operator. Unitaries leave the Chern number invariant, so $\langle g_{Ad}\rangle_{12}$ is both symmetric and antisymmetric in Φ_3 and hence zero identically. By a similar argument, $\langle g_{Ad}\rangle_{12}=0$ in the long and wide kites. For the windmill, the same argument gives $\langle g_{Ad}\rangle_{ij}=0$ for all pairs of loops i,j.

Of the nontrivial networks, the gasket and the tetrahedron have obvious symmetries; as a consequence a fair amount of analysis can be done "by hand."

The numerical procedure for analyzing these networks is the same as the one outlined in the previous section. Tables V, VI, and VII list the results for all nontrivial networks except for the holes graph, which was discussed in detail in the previous section. We have attempted to give analytic expressions in most cases.

Recall that tight-binding Hamiltonians can accommodate at most $|V|$ (spinless) electrons. The tables give the coordinates and the charges of level crossings corresponding to projections P_j with gap index j. The projection on the ground state of the one-electron system corresponds to gap index 1, the projection of the ground state of the two-electron system to gap index 2, etc. Since there are no charges in the $|V|$-electron ground state, all the tables list gap indices from 1 to $|V|-1$.

A. The gasket

The gasket looks like the first iteration in the Sierpinsky gasket (Mandelbrot, 1983), hence the name. The graph has C_3 symmetry. Among the nontrivial graphs, the gasket is unique in that the three flux-carrying triangles touch at vertices and have no common edge. All the other nontrivial graphs have at least one edge shared between the flux-carrying triangles.

As for all the other examples, there are no "accidental" level crossings, in the sense that all crossings lie on symmetry points in flux space. For the gasket, this is the line of equal fluxes (Φ,Φ,Φ). On this line, the tight-binding Hamiltonian corresponding to Fig. 23(c) can be chosen to be C_3 symmetric, for example, by putting the three fluxes on the edges (2,1), (4,3), and (6,5) in the figure. There are three two-dimensional, invariant vector subspaces of $\mathbb{C}^6$:

TABLE VI. The charges for the tight-binding Hamiltonian for the basket, Fig. 24(a). Only points in the half-cube with ϕ_3 in $[0,\pi]$ are listed. There are identical charges in the other half.

No.	ϕ/π	E	Gap	Charge	Multiplicity
1	(1.222,−0.517,0.517)	1.198	1	1	2
2	(1,1,1)	$\frac{7-\sqrt{17}}{2}$	1	−2	1
3	$(\frac{2}{3})(1,1,1)$	2	2	1	2
4	$(\frac{2}{3},1,1)$	2	2	−1	2
5	(0,0,0)	5	4	−2	1
6	(1,1,1)	$\frac{7+\sqrt{17}}{2}$	4	2	1

TABLE VII. The charges for the tetrahedron. This table applies both to the tight-binding and the free-electron model. Only the charges in the half-cube are listed.

No.	$(\Phi/\pi)(1,1,1)$	E	Gap	Charge	Multiplicity
1	1	2	1	−2	1
2	$\frac{1}{2}$	$3-\sqrt{3}$	1	1	2
3	$\frac{1}{2}$	$3+\sqrt{3}$	3	−1	2
4	0	4	3	2	1

$$\begin{aligned} &\text{I: } \mathbb{C}^2\times(1,1,1)\,, \\ &\text{II: } \mathbb{C}^2\times(1,z_3,z_3^*)\,, \\ &\text{III: } \mathbb{C}^2\times(1,z_3^*,z_3)\,. \end{aligned} \tag{13.1}$$

The six energy bands for this network, which for general position are given by the zeros of a polynomial of degree 6, split on the symmetry line to three quadratic equations, associated with the invariant subspaces. One finds

$$\begin{aligned} &E_{\rm I}(\Phi)=2(1\pm\cos(\Phi/2))\,, \\ &E_{\rm II,III}(\Phi)=\tfrac{7}{2}\pm\sqrt{\tfrac{17}{4}+2\cos(\Phi\pm 2\pi/3)}\,. \end{aligned} \tag{13.2}$$

The corresponding graphs of the energy bands are shown in Fig. 25. The crossing of the two bands in I occurs at $\Phi=\pi$ and $E=2$. The crossing of the bands in II and III occurs at $\Phi=\pi$ and $E=(7\pm\sqrt{21})/2$ and at $\Phi=0$ and $E=(7\pm\sqrt{13})/2$. Finally, there is a crossing between the lower band in I and the lower band in III at $\Phi=2\pi/3$ and $E=2$. There is one more crossing between the lower band in I and the lower band in II, the one associated with the second gap in the table, that gives a quartic equation in $\cos(\Phi/2)$. For this, only numerical values are given.

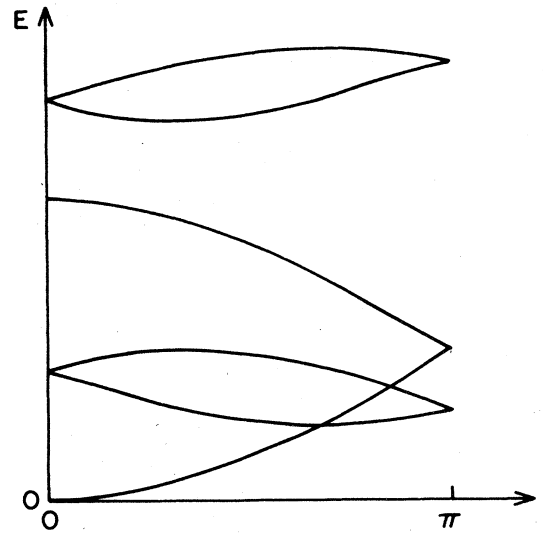

FIG. 25. The energy bands along the body diagonal in the flux spacecube, for the tight-binding model for the gasket. Only half the period is shown, since the bands are symmetric.

The charges for all nine crossing points are given in Table V. Because the degenerate subspaces are essentially identified by Eq. (13.1) one could, presumably, compute the charges analytically. We have not attempted to do so except for the zero charge at the third gap, which is computable almost by inspection: this gap closes when the two bands in I cross. The basis vectors for the degenerate subspace, $(0,1)\times(1,1,1)$ and $(1,0)\times(1,1,1)$, give a bipartition of the graph. The gauge fields do not link any two vertices in any one partition. This makes $d\epsilon_3(\Phi)$ in Eq. (7.8) vanish identically and implies zero degree, of course.

Some noteworthy features of Table V are as follows.

(1) The three-, four-, and six-electron ground states

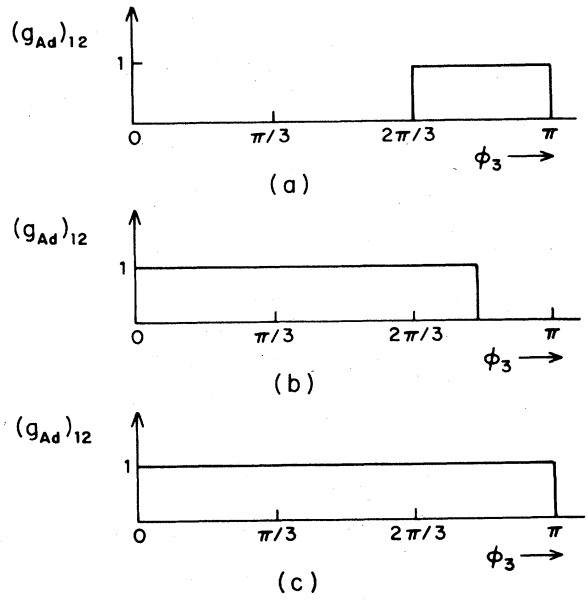

FIG. 26. The conductances of the gasket in the ground states of the tight-binding model: (a) the one-electron system; (b) the two-electron system; (c) the five-electron system. Only half the period is shown, as the graphs are antisymmetric. The three-, four-, and six-electron systems have trivial topological conductances at the ground state. The conductances are flux and μ stable.

have no charges. We do not know of a simple reason for that.

(2) In contrast with the holes effect, there are also multiple charges: 0, ± 1, ± 2. The appearance of 0 and ± 2 is an indicator of nongenericity. Multiple charges are expected to disintegrate to elementary charges under perturbations.

(3) The total charge for fixed gap label vanishes, as it should.

(4) Note that $(1,1,1)(2\pi/3)$ has an identical image charge under inversion, i.e., at $(1,1,1)(4\pi/3)$, while $\pi(1,1,1)$ is its own image under inversion.

The topological conductances of the network are shown in Fig. 26 and, like the holes effect, are flux and μ stable.

B. The basket

This is a nonplanar graph whose symmetry is not unlike that of the holes effect. The corresponding tight-binding model can accommodate at most five electrons. There are nine points of two-level crossings. The coordinates and charges are listed in Table VI. Note that projection on the three-electron ground state is free of charges.

Unlike the holes effect, which had nontrivial conductance associated with a single pair of loops, in the basket any pair leads to nontrivial conductances. The identical vanishing of the 2-3 conductance in the holes effect is not shared by the basket. Only a remnant of this is seen in the vanishing of the 2-3 conductance in the two-electron ground state by a miraculous cancellation, analogous to the one that occurred in the holes effect for all gap indices. The topological conductances in the ground states of the 1-5 electron systems are listed in Figs. 27 and 28. This network is flux stable but not μ stable. It is the only network among those we have considered that is μ unstable.

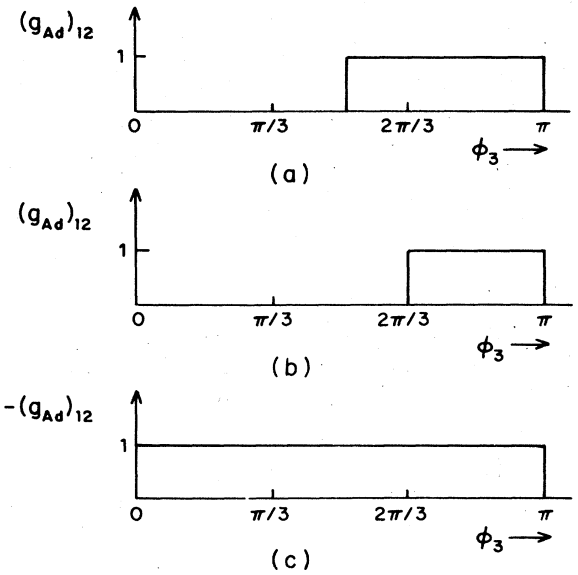

FIG. 27. The 1-2 conductances of the basket in the ground states of the tight-binding model: (a) the one-electron system; (b) the two-electron system; (c) the four-electron system. Only half the period is shown as the graphs are antisymmetric. The three- and five-electron systems have trivial topological conductances. This network is of mixed type: the four-electron system has opposite conductances to the one- and two-electron systems. The network is thus μ unstable. It is, however, flux stable.

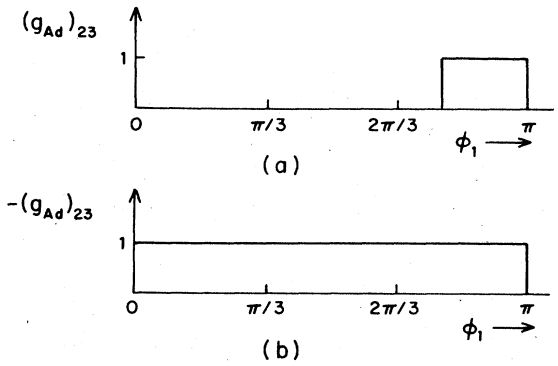

FIG. 28. The 2-3 conductances of the basket in the ground states of the tight-binding model: (a) the one-electron system; (b) the four-electron system. Only half the period is shown as the graphs are antisymmetric. The two-, three-, and five-electron systems have vanishing topological conductances. The conductance is flux stable but μ unstable.

C. The tetrahedron

Among the graphs in Table IV, the tetrahedron, Fig. 14, is noteworthy: it is the only regular graph; it is the graph with the least number of vertices; and it has a large (non-Abelian) symmetry group. A consequence of this is that the table for the charges can be computed analytically with relative ease. This is actually something we have realized with hindsight. Originally we studied the tetrahedron, as we did all other models, numerically. The analytic derivation presented below came later. There is, however, one bit of input from the numerical work that we shall need, namely, that there are no accidental degeneracies and charges. All the charges lie on the symmetry line of three equal fluxes.

Since the tetrahedron is a regular graph, its transport properties are the same in the tight-binding and the free-electron models. The energies are related by Eq. (4.37). For the sake of concreteness we use the tight-binding language.

The tight-binding Hamiltonian for the tetrahedral graph is

$$\begin{bmatrix} 3 & -e^{i\Phi_3} & -e^{-i\Phi_2} & -1 \\ -e^{-i\Phi_3} & 3 & -e^{i\Phi_1} & -1 \\ -e^{i\Phi_2} & -e^{-i\Phi_1} & 3 & -1 \\ -1 & -1 & -1 & 3 \end{bmatrix} . \tag{13.3}$$

The line of symmetry is

$$\Phi(1,1,1)\ , \tag{13.4}$$

corresponding to flux Φ through three of the faces of the tetrahedron and flux -3Φ through the fourth face. The corresponding Hamiltonian is C_3 invariant. This symmetry splits $\mathbb{C}^4$ into three invariant subspaces:

$$\begin{aligned} &\text{I: } (\alpha,\alpha,\alpha,\beta)\ , \\ &\text{II: } (\alpha,\alpha z_3,\alpha z_3^*,0)\ , \\ &\text{III: } (\alpha,\alpha z_3^*,\alpha z_3 0)\ . \end{aligned} \tag{13.5}$$

I is two (complex) dimensional, $\alpha,\beta\in\mathbb{C}$, and II and III are each one dimensional.

The energy bands on the line of symmetry can be computed analytically by reduction to invariant subspaces. This gives

$$\begin{aligned} E_{\rm I}(\Phi)&=3-\cos(\Phi)\pm\sqrt{3+\cos^2(\Phi)}\ , \\ E_{\rm II}(\Phi)&=3-2\cos(\Phi+2\pi/3)\ , \\ E_{\rm III}(\Phi)&=3-2\cos(\Phi-2\pi/3)\ . \end{aligned} \tag{13.6}$$

The bands are shown in Fig. 29.

The two bands in I never cross. Double crossings occur when one of the bands in I crosses one in II or III. This occurs at $\phi=\pm\pi/2$. Consider $\pi/2$. The lower branch of $E_{\rm I}$ crosses $E_{\rm II}$ at energy $3-\sqrt{3}$, and the upper branch of $E_{\rm I}$ crosses $E_{\rm III}$ at energy $3+\sqrt{3}$. There are also triple crossings at $\phi=0$ and $\phi=\pi$, by the general group-theoretic analysis of Sec. VII. This takes place at $E=4$ and $E=2$. This identifies the crossings and the degenerate subspaces.

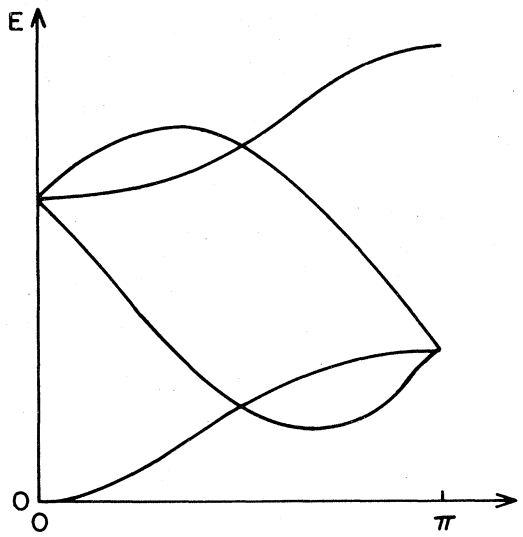

FIG. 29. The energy bands along the diagonal in flux space, for the tight-binding model for the tetrahedron. Since the bands are symmetric under reflection of Φ, only half the period is shown.

A remarkable thing about the tetrahedron is that it is enough to compute just one charge to get the full Table VII. For example, the charge of point 2 in the table determines that of point 1 by the overall neutrality. The "π shift" then determines the charges of points 3 and 4, so it remains to compute the charge of 2. Since this is a two-level crossing, the charge is a degree.

The degenerate subspace of point 2 is spanned by

$$(1,1,1,\sqrt{3})\times(1,z_3,z_3^*,0)\ . \tag{13.7}$$

One finds for the linearized map at $\phi=\pi/2$, from Eq. (7.8),

$$\begin{aligned} d\epsilon_1&=-d\Phi_1+\tfrac{1}{2}d\Phi_2+\tfrac{1}{2}d\Phi_3\ , \\ d\epsilon_2&=-\frac{\sqrt{3}}{2}d\Phi_2+\frac{\sqrt{3}}{2}d\Phi_3\ , \\ d\epsilon_3&=-\tfrac{3}{2}(d\Phi_1+d\Phi_2+d\Phi_3)\ . \end{aligned} \tag{13.8}$$

The associated determinant is negative, so the charge is $+1$.

In conclusion, we have seen several model Hamiltonians for several graphs made of three equilateral triangles, both planar and nonplanar, that have nontrivial Chern numbers. A common feature of the nontrivial bundles is simplicity: there are few charges in the j-electron ground state. There must be at least two in a nontrivial case (since the total charge is zero), and in all the networks the actual number is three. Another way of stating this is the following. All the conductances are flux stable in the sense of Sec. X. In fact, for most of the graphs the networks are also μ stable. The only exception is the basket, which changes type in the four-electron system.

Another simple feature common to the various graphs is that the degeneracies lie on distinguished symmetry planes and lines, and the eigenvalue equations on these lines often factorize, giving relatively simple expressions for the coordinates and energies of crossings. Finally, the charges of the degeneracies tend to be small, 0, 1, and 2. There are no charges larger than 3. This is even more remarkable when one considers the average conductances, which take only values 0, 1, and -1. None gives an average conductance of 2 or more. It is reasonable to speculate that the smallness of the integers is related to the small number of loops in the networks. However, we do not know how to relate the number of loops to Chern numbers.

XIV. CONCLUDING REMARKS AND OPEN QUESTIONS

In this work we have studied nondissipative quantum transport in multiply connected systems. Such transport is associated with an antisymmetric matrix of transport coefficients indexed by pairs of loops. The matrix is a function of, among other things, the fluxes threading the loops, and this dependence plays a key role in the analysis. We have focused on the topological aspects of the transport properties, and specifically on averages of the transport matrix that are quantized to be integers.

The resulting "topological conductance matrix" is an integer-valued function of some of the fluxes in the network. We have described some of its basic properties and have computed it for several networks. The situation is reminiscent of the integer quantum Hall effect, in which the Hall conductance is an integer-valued function of, say, the magnetic field acting on the Hall probe. There are two important differences, however. One is that, in the Hall effect, the integers characterize the crystal, while in networks they characterize the multiconnectivity of the graph. The second is that, in the Hall effect, the integer is directly measurable, while in networks, in general, the quantized transport arises only after averaging "by hand."

In this section we raise some of the questions that have not been adequately treated in the previous sections, in the hope that this will stimulate further work.

The most serious gap in the theoretical framework is that the self-inductance of the system has not been taken into account. The inductance matrix L_{ij}, with loop indices i and j, relates the flux change in loop i to the current change in other loops: $\delta\Phi_i = \sum L_{ij}\delta I_j$. By changing the flux in one loop to create an emf, the fluxes in the other loops change too. We have assumed that these fluxes are fixed. This is equivalent to looking at networks with no, or very small, inductances. We want to consider when this assumption is reasonable.

By dimensional arguments, the inductance L, in cgs, is of order l/c where l is a typical length scale and c the velocity of light. Typical currents are presumably on the order of the persistent currents, i.e., of order $c\partial E/\partial\Phi$. The energy scale is that of atomic units, $(e^4m/\hbar^2)$, and its dependence on Φ is like a dependence on boundary conditions and so scales like l^{-2}. Thus typical persistent currents are of the order $(c/\Phi_0)(e^4m/\hbar^2)(a_0/l)^2$, where $a_0 \equiv \hbar^2/me^2$ is the unit length in atomic units (Bohr radius). $\Phi_0 \equiv \hbar c/e$ is the unit flux. It follows that

$$\delta\Phi/\Phi_0 \sim (e^2/\hbar c)^2(a_0/l) . \tag{14.1}$$

In mesoscopic systems a_0/l is, of course, much smaller than unity and so is $e^2/\hbar c$, the fine-structure constant. This says that $\delta\Phi$ changes little due to typical currents. The fact that the change is proportional to the fine-structure constant is not surprising, for a change in the magnetic flux at one loop due to a change in the flux in another loop can be thought of as photon-photon scattering, mediated by the network. It is interesting, and less obvious, that the variations in the fluxes actually scale down with the size.

It is interesting and important to get an accurate handle on the conductances of networks, that goes beyond the order-of-magnitude calculation presented here. One reason is that one natural way to measure the currents is to measure the change of flux in the appropriate loop. One therefore does not want the inductance to be too small either, and so the smallness of the change in the flux is actually a mixed blessing.

There are many issues that the study of conductance in networks brings up that deserve further study, for example, the *unaveraged* conductance matrix in the adiabatic limit. With no averaging, the graph of the conductance is smooth, so that for the tetrahedron, a figure like Fig. 31 may replace Fig. 30. A detailed study of this for the graph in Secs. XII and XIII is of interest. Also of interest are corrections to adiabatic transport. Another set of problems is concerned with the study of networks with

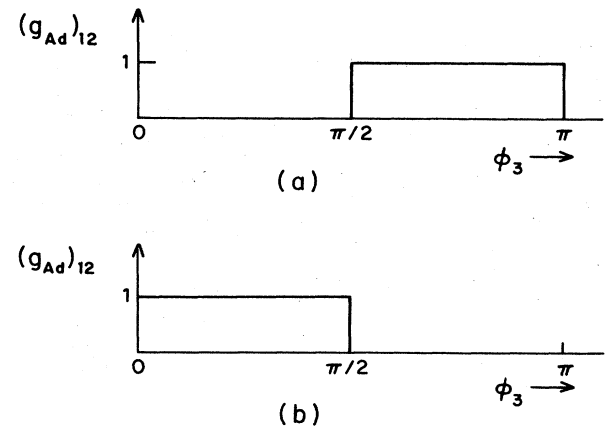

FIG. 30. The conductances of the tetrahedron in the tight-binding and free-electron models; (a) the one-electron ground state; (b) the three-electron ground state. Since the graphs are periodic and antisymmetric, only half a period is shown. The two- and four-electron ground states have vanishing topological conductances. The conductance is n-type, flux, and μ stable.

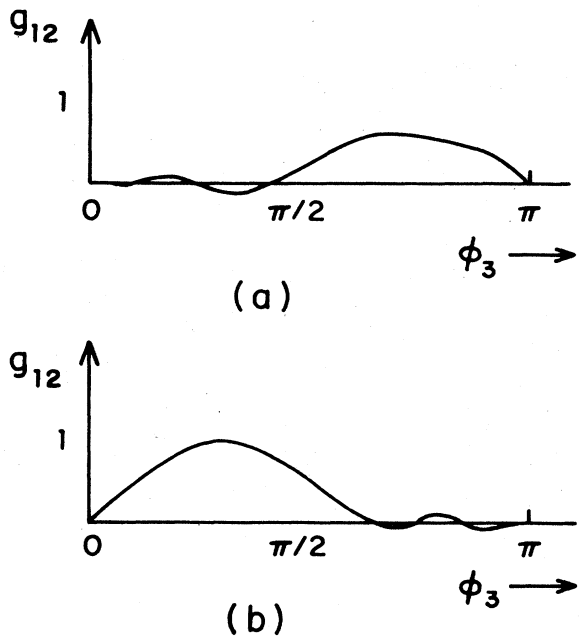

FIG. 31. Schematic graph of the unaveraged conductance of the tetrahedron network: (a) the one-electron system; (b) the three-electron system. Since the graphs are periodic and antisymmetric, only half a period is shown.

random potentials on the edges. There are at least two reasons why this is interesting. The first is that this is, of course, a natural mathematical and physical question. The second is that experience with the Hall effect suggests that randomness plays an important role *in stabilizing* the integrability of transport: the Hall conductance, even without averaging, and even at finite, but low, temperature, is a nontrivial integer. This is understood to be a consequence of random impurities, together with the macroscopy of the probe. It is therefore not inconceivable that random potentials may have some stabilizing effects in networks as well. If true, this may make mesoscopic networks candidates for nondissipating switching and computing devices.

An interesting set of questions concerns the qualitative and statistical theory of Chern numbers—understanding orders of magnitude of the charges, their distribution, etc. The study of graphs with many loops, with periodic, quasiperiodic, or hierarchical structures, etc. (Hofstadter, 1976; Rammal and Toulouse, 1982; Domany *et al.*, 1983) is completely open.

If the electron-hole concept is any guide, then one may expect that further and deeper understanding of the question of types, i.e., p-type versus n-type networks, is a useful pursuit. The related questions of flux stability and μ stability of the conductances (see Sec. X) also deserve further study.

Finally, an important subject we have not treated in any depth is the study of physical conditions. We have required coherence of the wave function over the entire network, and this may be difficult to achieve in practice. Coherence requires a large mean free path for inelastic processes. This favors temperatures so low that the temperature is small compared to the gaps in the energy levels. Further, the applied emf's have to be weak compared to this scale (so that the adiabatic theorem applies). Since energy gaps scale like $(\text{length})^{-2}$, this favors small networks. Networks of mesoscopic scale have energy gaps typically on the order of microvolts. This dictates temperatures in the milli-Kelvin range and emf in microvolts. The flux-sensitive effects in normal-metal rings (Büttiker, 1986a, 1986b) suggest that quantum coherence over mesoscopic networks is feasible today.

We want to conclude the discussion of mesoscopic systems with a remark that we owe to Y. Imry. Because mesoscopic networks are so small, it is not obvious how one can vary the fluxes in the loops independently. A way to do it is to fold the three triangles out of the plane, so that they become mutually perpendicular. For example, consider the network of Fig. 32, which is made of a corner of a cube. This network is a deformation of the tetrahedron and so very likely nontrivial. A magnetic field aligned with one of the normals will cause flux changes only in the corresponding loop. In this way the three fluxes can be modulated independently.

A different setting is that of superconducting networks. Since the superconducting wave function is coherent over macroscopic scales at temperatures of a few Kelvin, this may turn out to be a more favorable circumstance. (But it may be that, for some other reason, more stringent conditions on temperatures and scales need to be applied.) Here the wave function is associated with the superconducting order parameter in a Landau-type theory. This theory has all the relevant formal structure needed for the geometric interpretation of transport. The two main differences are that (a) the charge is that of Cooper pairs and (b) the theory is nonlinear and has ψ^4 interaction. These features do not affect the basic structure, which relies on minimal coupling and the definition of currents. Of course, the network has to have thin enough wires so that the fluxes inside the loops are not quantized and can be varied. In other words, the network could be realized as an array of Josephson junctions. Such arrays have been fabricated and have been studied before; see, for example, Webb *et al.* (1983) and Behrooz *et al.* (1986). However, the conductance matrix of such networks, with fluxes that can be independently modulated, has not been studied as yet. It appears that the physical conditions relevant to the quantum transport properties should be similar to those relevant to, say, tunneling phenomena in macroscopic superconductors. Substantial work has been done in this field of research, most notably by J. Clarke and collaborators [see Clarke (1987) and references therein]. We suggest that the study of nondissipative quantum transport be considered a part of these general programs.

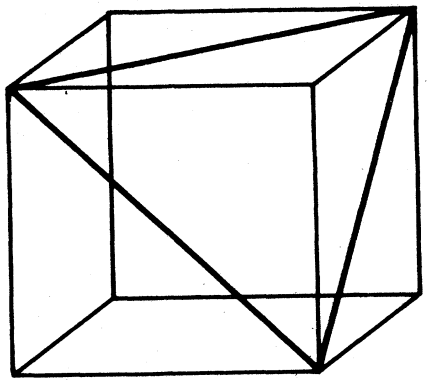

FIG. 32. A three-loop network made of the three corners of a cube. In this case, the fluxes through the mutually orthogonal triangles can be modulated independently with magnetic fields that are homogeneous on the scale of the network.

ACKNOWLEDGMENTS

This work was supported by the Israel Academy of Sciences, Minerva, and the US-Israel BSF Grant No. 84-00376 and NSF Grant No. DMS84-16049. J.E.A. acknowledges the support of the fund for the promotion of research at the Technion, and thanks M. Cross, D. Politzer, B. Simon, E. Stone, R. Vogt, and D. Wales for the hospitality extended to him at Caltech. We are indebted to M. Cross, S. Fishman, F. Gesztesy, Y. Imry, F. Kuchar, H. Kunz, B. Shapiro, S. Shtrikman, B. Simon,

and J. Zak for useful discussions and comments. We thank Professor J. Goldberg for help with the transmission of files between Caltech and the Technion, and P. Weichman for a critical reading of the manuscript. This work grew out of a research program one of us (J.E.A.) has with R. Seiler, to whom is due a special acknowledgment. Parts of Secs. II, V, VI, VIII, and IX borrow from this common project. Finally we want to express our indebtedness to A. Libchaber, who, during a visit to the Technion first suggested to us that networks are like the Hall effect with no Hall probes.

REFERENCES

Aharonov, Y., and D. Bohm, 1959, "Significance of electromagnetic potentials in the quantum theory," Phys. Rev. **115**, 485.

Aharonov, Y., and D. Bohm, 1961, "Further considerations on electromagnetic potentials in the quantum theory," Phys. Rev. **123**, 1511.

Albeverio, S., F. Gesztesy, H. Holden, and R. Hoegh-Krohn, 1988, *Solvable Models in Quantum Mechanics* (Springer, New York).

Alden Mead, C., 1987, "Molecular Kramers degeneracy and non-Abelian adiabatic phase factor," Phys. Rev. Lett. **59**, 161.

Alden Mead, C., and D. G. Truhlar, 1979, "On the determination of Born-Oppenheimer nuclear motion wave function including complications due to conical intersections are identical nuclei," J. Chem. Phys. **70**, 2284.

Alexander, S., 1983, "Superconductivity of networks: A percolation approach to the effect of disorder," Phys. Rev. B **27**, 1541.

Alt'shuler, B. L., 1985, "Fluctuations in the extrinsic conductivity of disordered conductors," Pis'ma Zh. Eksp. Teor. Fiz. **41**, 530 [JETP Lett. **41**, 648 (1985)].

Alt'shuler, B. L., A. G. Aronov, and B. Z. Spivak, 1981, "The Aharonov-Bohm effect in disordered conductors," Pis'ma Zh. Eksp. Teor. Fiz. **33**, 101 [JETP Lett. **33**, 94 (1981)].

Anderson, P. W., D. J. Thouless, E. Abrahams, and D. S. Fisher, 1980, "New method for a scaling theory of localization," Phys. Rev. B **22**, 3519.

Arnol'd, V. I., 1978, *Mathematical Methods of Classical Mechanics,* Graduate Texts in Mathematics No. 60 (Springer, New York).

Avron, J. E., and R. Seiler, 1985, "Quantization of the Hall conductance for general multiparticle Schrödinger Hamiltonians," Phys. Rev. Lett. **54**, 259.

Avron, J. E., R. Seiler, and B. Simon, 1983, "Homotopy and quantization in condensed matter physics," Phys. Rev. Lett. **51**, 51.

Avron, J. E., R. Seiler, and L. Yaffe, 1987, "Adiabatic theorems and applications to the quantum Hall effect," Commun. Math. Phys. **110**, 33.

Avron, J. E., and B. Simon, 1978, "Analytic properties of band functions," Ann. Phys. (N.Y.) **110**, 85.

Avron, J. E., and L. G. Yaffe, 1986, "A diophantine equation for the Hall conductance of interacting electrons on a torus," Phys. Rev. Lett. **56**, 2085.

Avron, Y., R. Seiler, and B. Shapiro, 1986, "Generic properties of quantum Hall Hamiltonians for finite systems," Nucl. Phys. B **265** [FS15], 364.

Behrooz, A., M. J. Burns, H. Deckman, D. Lavine, B. Whitehead, and P. M. Chaikin, 1986, "Flux quantization on quasicrystalline networks," Phys. Rev. Lett. **57**, 368.

Bellissard, J., 1986a, "Ordinary quantum Hall effect and noncommutative cohomology," Lecture delivered at Bad Schandau (unpublished).

Bellissard, J., 1986b, "K-Theory of C^*-algebras in solid state physics, in *Statistical Mechanics and Field Theory: Mathematical Aspects,* edited by T. C. Dorlas, N. M. Hugenholtz, and M. Winnik, Lecture Notes in Physics No. 257 (Springer, Berlin/New York), p. 99.

Benoit, A. D., S. Washburn, C. P. Umbach, R. B. Laibowitz, and R. A. Webb, 1986, "Asymmetry in the magnetoconductance of metal wires and loops," Phys. Rev. Lett. **57**, 1765.

Berry, M. V., 1983, "Semiclassical mechanics of regular and irregular motion" in *Comportement Chaotique des Systemes Deterministes,* edited by G. Iooss, R. H. Helleman, and R. Stora (North-Holland, Amsterdam).

Berry, M. V., 1984, "Quantal phase factors accompanying adiabatic changes," Proc. R. Soc. London, Ser. A **392**, 45.

Berry, M. V., 1987, "Interpreting the anholonomy of coiled light," Nature (London) **326**, 277.

Berry, M. V., and M. Wilkinson, 1984, "Diabolical points in the spectra of triangles," Proc. R. Soc. London, Ser. A **392**, 15.

Biggs, N., 1974, *Algebraic Graph Theory,* Cambridge Tracts in Mathematics No. 67 (Cambridge University, London/New York).

Born, M., and R. Oppenheimer, 1927, "Zur Quantentheorie der Moleküle," Ann. Phys. (Leipzig) **84**, 457.

Büttiker, M., 1986a, "Flux sensitive effects in normal metal loops," Ann. N.Y. Acad. Sci. **480**, 114.

Büttiker, M., 1986b, "Four terminal phase coherent conductance," Phys. Rev. Lett. **57**, 1761.

Büttiker, M., Y. Imry, and R. Landauer, 1983, "Josephson behavior in small normal one-dimensional rings," Phys. Lett. A **96**, 365.

Büttiker, M., Y. Imry, R. Landauer, and S. Pinhas, 1985, "Generalized many-channel conductance formula with application to small rings," Phys. Rev. B **31**, 6207.

Byers, N. B., and C. N. Yang, 1961, "Theoretical consideration concerning quantized magnetic flux in superconducting cylinders," Phys. Rev. Lett. **7**, 46.

Chandrasekhar, V., M. J. Rooks, S. Wind, and D. E. Prober, 1985, "Observation of Aharonov-Bohm electron interference effects with periods h/e and $h/2e$ in individual micron size normal-metal rings," Phys. Rev. Lett. **55**, 1610.

Chern, S.-s., 1979, *Complex Manifolds without Potential Theory, Second Edition* (Springer, New York).

Choquet-Bruhat, Y., C. DeWitt-Morette, and M. Dillard-Bleick, 1982, *Analysis, Manifolds, and Physics, Revised Edition* (North-Holland, Amsterdam/New York/Oxford).

Clarke, J., 1987, "Quantum phenomena in superconductors, in *Proceedings of the 18th International Conference on Low Temperature Physics* (Jpn. J. Appl. Phys. **26**, 1771).

Combes, J. M., P. Duclos, and R. Seiler, 1981, "The Born-Oppenheimer Approximation," in *Rigorous Atomic and Molecular Physics,* edited by G. Velo and A. Wightman (Plenum, New York/London), p. 185.

Connes, A., 1969, "Noncommutative differential geometry," Pub. IHES **62**, 43.

Dana, I., Y. Avron, and J. Zak, 1985, "Quantised Hall conductance in a perfect crystal," J. Phys. C **18**, L679.

de Gennes, P. G., 1981, "Champ critique d'une boucle supraconductrice ramifiee," C. R. Acad. Sci., Ser. B **292**, 9; 279.

Domany, E., S. Alexander, D. Bensimon, and L. Kadanoff, 1983, "Solutions to the Schrödinger equation on some fractal lattices," Phys. Rev. B **28**, 3110.

Dubrovin, B. A., A. T. Fomenko, and S. P. Novikov, 1984, *Modern Geometry—Methods and Applications,* Graduate Texts in Mathematics Nos. 93 and 104 (Springer, New York).

Dubrovin, B. A., and S. P. Novikov, 1980, "Ground states of a two-dimensional electron in a periodic magnetic field," Zh. Eksp. Teor. Fiz. **79**, 1006 [Sov. Phys. JETP **52**, 511 (1980)].

Dyson, F., 1964, "Statistical theory of energy levels of complex systems," J. Math. Phys. **2**, 140.

Exner, P., and P. Šeba, 1987, "Free quantum motion on a branching graph," JINR Reports Nos. E2-87-213 and E2-87-214.

Flanders, H., 1963, *Differential Forms, with Applications to the Physical Sciences* (Academic, New York).

Friedland, S., J. W. Robbin, and J. H. Sylvester, 1984, "On the crossing rule," Commun. Pure Appl. Math. **37**, 19.

Gefen, Y., Y. Imry, and M. Azbel, 1984, "Quantum oscillations and the Bohm-Aharonov effect for parallel resistors," Phys. Rev. Lett. **52**, 129.

Gefen, Y., and D. J. Thouless, 1987, "Zener transition and energy dissipation in small driven systems," Phys. Rev. Lett. **59**, 1752.

Haldane, F. D. M., 1986, "Path dependence of the geometric rotation of polarization in optical fibers," Opt. Lett. **11**, 730.

Hall, E. H., 1879, "On a new action of the magnet on electric currents," Am. J. Math. **2**, 287.

Herring, C., 1937, "Effects of time reversal symmetry on energy bands of crystals," Phys. Rev. **52**, 361.

Herzberg, G., and H. C. Longuet-Higgins, 1963, "Intersection of potential energy surfaces in polyatomic molecules," Discuss. Faraday Soc. **35**, 77.

Hofstadter, D. R., 1976, "Energy levels and wave functions of Bloch electrons in rational and irrational magnetic fields," Phys. Rev. B **14**, 2239.

Imry, Y., 1986, "Physics of mesoscopic systems," in *Directions in Condensed Matter Physics,* edited by G. Grinstein and G. Mazenko (World Scientific, Singapore/Philadelphia).

Johnson, R., and J. Moser, 1982, Commun. Math. Phys. **84**, 403.

Kato, T., 1950, "On the adiabatic theorem of quantum mechanics," J. Phys. Soc. Jpn. **5**, 435.

Kato, T., 1966, *Perturbation Theory of Linear Operators* (Springer, Berlin).

Klein, M., and R. Seiler, 1988, private communication.

Kohmoto, M., 1985, "Topological invariant and the quantization of the Hall conductance," Ann. Phys. (N.Y.) **160**, 343.

Kuchar, F., R. Meisels, K. Y. Lim, P. Pichler, G. Weimann, and W. Schlapp, 1987, "Hall conductivity at microwave and submillimeter frequencies in the quantum Hall effect regime," EPS Condensed Matter Conference, Pisa Physica Scripta **T19**, 79.

Kugler, M., and M. Shtrikman, "Berry's phase, local frames and classical analogues," Weizmann Institute preprint.

Kunz, H., 1986, "Quantized currents and topological invariants for electrons in incommensurate potentials," Phys. Rev. Lett. **57**, 1095.

Kunz, H., 1987, "The quantum Hall effect for electrons in a random potential," Commun. Math. Phys. **112**, 121.

Landau, L. D., and E. M. Lifshitz, 1977, *Quantum Mechanics, 3rd Revised Edition* (Pergamon, Oxford/New York).

Landau, L. D., E. M. Lifshitz, and L. P. Pitaevskii, 1984, *Electrodynamics of Continuous Media, Second Edition* (Pergamon, Oxford/New York).

Laughlin, R. B., 1981, "Quantized Hall conductivity in two dimensions," Phys. Rev. B **23**, 5632.

Longuet-Higgins, H. C., 1975, "The intersection of potential energy surfaces of polyatomic molecules," Proc. R. Soc. London, Ser. A **344**, 147.

Lyskova, A. S., 1985, "Topological characteristics of the spectrum of the Schrödinger operator in a magnetic field and in a weak potential," Teor. Mat. Fiz. **65**, 368 [Theor. Math. Phys. (USSR) **65**, 1218 (1986)].

Mandelbrot, B., 1983, *The Fractal Geometry of Nature* (Freeman, San Francisco).

Mittra, R., and S. W. Lee, 1977, *Analytical Techniques in the Theory of Guided Waves* (Macmillan, New York).

Niu, Q., and D. J. Thouless, 1984, "Quantum adiabatic charge transport in the presence of substrate disorder and many body interaction," J. Phys. A **17**, 2453.

Niu, Q., and D. J. Thouless, 1987, "Quantum Hall effect with realistic boundary conditions," Phys. Rev. B **35**, 2188.

Niu, Q., D. J. Thouless, and Y. S. Wu, 1985, "Quantized Hall conductance as a topological invariant," Phys. Rev. B **31**, 3372.

Novikov, S. P. 1981, Dok. Akad. Nauk SSSR **257**, 538.

Onsager, L., 1931, "Reciprocal relations in irreversible processes. II," Phys. Rev. **38**, 2265.

Patterson, E. M., 1969, *Topology* (Oliver and Boyd, Edinburgh).

Platt, J. R., K. Ruedenberg, C. W. Scherr, N. S. Ham, H. Labhart, and W. Lichten, 1964, *Free-electron Theory of Conjugated Molecules: A Source Book* (Wiley, New York).

Porter, C. E., 1965, Ed., *Statistical Theories of Spectra: Fluctuations* (Academic, New York/London).

Prange, R. E., and S. T. Girvin, 1987, Eds., *The Quantum Hall Effect* (Springer, New York).

Rammal, R., and G. Toulouse, 1982, "Spectrum of the Schrödinger equation on a self-similar structure," Phys. Rev. Lett. **49**, 1194.

Ramo, S., J. R. Whinnery, and T. van Duzer, 1984, *Fields and Waves in Communication Electronics,* 2nd ed. (Wiley, New York).

Reed, M., and B. Simon, 1972–1978, *Methods of Modern Mathematical Physics,* Vols. I–IV (Academic, New York/San Francisco/London).

Rellich, F., 1969, *Perturbation Theory of Eigenvalue Problems* (Gordon and Breach, New York).

Ruedenberg, K., and C. W. Scherr, 1953, "Free-electron network model for conjugated systems. I. Theory," J. Chem. Phys. **21**, 1565.

Shapiro, B., 1983, "Quantum conduction on a Caley tree," Phys. Rev. Lett. **50**, 747.

Sharvin, D. Yu., and Yu. V. Sharvin, 1981, "Magnetic flux quantization in cylindrical films of normal metals," Pis'ma Zh. Eksp. Teor. Fiz. **34**, 285 [JETP Lett. **34**, 272 (1981)].

Simon, B., 1983, "Holonomy, the quantum adiabatic theorem and Berry's phase," Phys. Rev. Lett. **51**, 2167.

Tao, R., and F. D. M. Haldane, 1986, "Impurity effect, degeneracy and topological invariance in the quantum Hall effect," Phys. Rev. B **33**, 3844.

Thouless, D. J., 1983, "Quantization of particle transport," Phys. Rev. B **27**, 6083.

Thouless, D. J., M. Kohmoto, M. P. Nightingale, and M. den Nijs, 1982, "Quantized Hall conductance in a two-dimensional periodic potential," Phys. Rev. Lett. **49**, 405.

Thouless, D. J., and Q. Niu, 1984, "Nonlinear corrections to the quantization of Hall conductance," Phys. Rev. B **30**, 3561.

Umbach, C. P., S. Washburn, R. B. Laibowitz, and R. A. Webb, 1984, "Magnetoresistance of small quasi one-dimensional normal-metal rings and lines," Phys. Rev. B **30**, 4048.

von Klitzing, K., G. Dorda, and M. Pepper, 1980, "New method for high-accuracy determination of the fine-structure constant based on quantized Hall resistance," Phys. Rev. Lett. **45**, 494.

von Neumann, J., and E. Wigner, 1929, "Über das Verhalten von Eigenwerten bei Adiabatischen Prozessen," Phys. Z. **30**, 467.

Webb, R., A. R. F. Voss, G. Grinstein, and P. M. Horn, 1983, "Magnetic field behavior of Josephson junction array: Two dimensional flux transport on a periodic substrate," Phys. Rev. Lett. **51**, 690.

Webb, R. A., S. Washburn, C. P. Umbach, and R. B. Laibowitz, 1985 "Observation of the h/e Aharonov-Bohm oscillations in normal-metal rings," Phys. Rev. Lett. **54**, 2696.

Wilczeck, F., and A. Zee, 1984, "Appearance of gauge structure in simple dynamical systems," Phys. Rev. Lett. **52**, 2111.

Wilson, K., 1974, "Confinement of quarks," Phys. Rev. D **10**, 2445.

Wilson, R. J., 1972, *Introduction to Graph Theory* (Oliver and Boyd, Edinburgh).

Witten, E., 1986, "Noncommutative geometry and string field theory," Nucl. Phys. **268**, 253.

Yurke, B., and J. S. Denker, 1984, "Quantum network theory," Phys. Rev. A **29**, 1419.